P-13-43

Äspö Task Force on modelling of groundwater flow and transport of solutes

Task 7 – The numerical modelling of pump tests at the Olkiluoto site

Urban Svensson, CFE AB

October 2015

Svensk Kärnbränslehantering AB
Swedish Nuclear Fuel
and Waste Management Co

Box 250, SE-101 24 Stockholm
Phone +46 8 459 84 00

ISSN 1651-4416
SKB P-13-43
ID 1413966
October 2015

Äspö Task Force on modelling of groundwater flow and transport of solutes

Task 7 – The numerical modelling of pump tests at the Olkiluoto site

Urban Svensson, CFE AB

Abstract

Task 7 aims to provide a bridge between the information derived from site characterisation (SC) and performance assessment (PA). Task 7 has a particular focus: how information from the new flow-logging tools (so-called POSIVA Flow Log) can be used to maximum benefit, to reduce key uncertainties for the PA.

The overall strategy of Task 7 is to progress from the large scale (Olkiluoto site-scale with focus on fracture zones) to the much smaller scale, that of the engineered barrier. At each scale, specific goals will be defined within the context of the overall Task 7 goal, and modelling tasks will be defined to support those goals.

The aim and scope of Task 7 above is the one stated in the Task description (Vidstrand et al. 2012). However, different modelling groups and supporting organizations have focused on different aspects. The specific objective for the work reported here can be stated as: “Develop groundwater modelling techniques to simulate the effect of boreholes and open shafts on a range of spatial scales”.

The main achievements of the work reported can be summarized as follows:

- Task 7 has provided an opportunity to develop methods to simulate boreholes, in the code DarcyTools. Methods to analyze pumped, open and packed-off boreholes are now available in DarcyTools.
- The PFL data on flow along boreholes has provided a new, challenging way to test simulation models. Such tests have been carried out.
- The final Task ABC model illustrates a novel way to set up models; all scales from the heterogeneity of fractures to the regional scale are handled simultaneously. The unstructured grid technique made this development possible.
- Hopefully, all the simulations reported have contributed to the understanding of the hydrogeology of the Olkiluoto site.

Sammanfattning

Task 7 syftar till att bygga en bro mellan information erhållen från SC (Site Characterisation) och PA (Performance Assessment). Speciellt ska utvärderas hur information från Posiva Flow Log (PFL) kan utnyttjas.

Strategin är att börja med en studie av den regionala skalan och sedan successivt gå ner till skalan för ingenjörsbarriärerna, dvs m-skalan. Olika modelleringsuppgifter definieras för hela spektrat av skalor.

Olika modelleringsgrupper och organisationer har emellertid lite olika fokus när det gäller modelleringsutvecklingen. I denna rapport kan fokus säjas vara ”utveckla modelleringsteknik för att simulera borrhål och ventilationsschakt i olika rumsliga skalor”.

De huvudsakliga resultaten som uppnåtts är:

- Metoder för att simulera borrhål har utvecklats och är nu en del av koden DarcyTools.
- Flöden längs borrhål har simulerats och jämförts med mätningar från Posiva Flow Log.
- En modelluppsättning som integrerar alla skalor i en och samma modell har presenterats och använts för att simulera pumptester.
- Förhoppningsvis har simuleringsresultaten bidragit till ökad kunskap om de hydrogeologiska förhållandena i Olkiluoto.

Contents

1 Introduction and objectives

1.1 Background

The Äspö Task Force provides a platform for interaction in the area of conceptual and numerical modelling of groundwater flow and solute transport in fractured rock. The work of the Task Force is conducted within well-defined tasks focused of specific issues and have been usually related to specific experiments at the Äspö Hard Rock Laboratory (HRL).

Task 7 aims to provide a bridge between the information derived from site characterisation (SC) and performance assessment (PA). Task 7 has a particular focus: how information from the new flow-logging tools (so-called POSIVA Flow Log) can be used to maximum benefit, to reduce key uncertainties for the PA.

The overall strategy of Task 7 is to progress from the large scale (Olkiluoto site-scale with focus on fracture zones) to the much smaller scale, that of the engineered barrier. At each scale, specific goals will be defined within the context of the overall Task 7 goal, and modelling tasks will be defined to support those goals.

Task 7A considered a region of approximately 10 km^2 in the vicinity of borehole KR24 at the Olkiluoto site in Finland. KR24 was used for a long-term pumping test.

Task 7B considered a localized near-field scale (50 m×50 m×50 m) volume within an approximately 500 by 500 m^2 region surrounding a group of boreholes KR14–18. The local volume also includes a ventilation shaft, which provides unique geologic and hydrogeologic characterization access to fracture traces where they intersect the shaft.

Task 7C focused on three single fractures. The single fractures specification is based on single fracture characteristics from the characterisation of three ventilation shafts at the Onkalo of the Olkiluoto site in Finland.

1.2 Scope and objectives of Task 7

The aim and scope of Task 7 above is the one stated in the Task description (Vidstrand et al. 2012). However, different modelling groups and supporting organizations have focused on different aspects. The specific objective for the work reported here can be stated as:

- Develop groundwater modelling techniques to simulate the effect of boreholes and open shafts on a range of spatial scales. Regarding the scope, all simulations will consider the Olkiluoto site. First the large scale (about 10 km^2) is considered and then progressively smaller scales. For all scales comparisons with field data are carried out and evaluated.

2 Task specifications

2.1 Task 7A – Regional scale

Task 7A will consider an approximately 10 km^2 region surrounding borehole KR24. KR24 was used for a long-term pumping test. The test setup included pumping from two borehole sections. The lower part of KR24 was partially isolated by a by-pass packer (throttle valve) so that the drawdown in the deep section could be controlled.

The main aim of Task 7A is to simulate the effect of the long-term pumping test in KR24. Drawdowns as well as flow along boreholes are requested as deliveries.

2.2 Task 7B – Block scale

The scope of Task 7B is to simulate the performance of the groundwater system and response to different interference pumping in the presence of open and sealed-off boreholes, by building and testing the sensitivity of numerical groundwater flow models of the KR 14–18 region. An important aspect of the data from the site is the use of the Posiva Flow Log to measure flow in/out of the boreholes during "undisturbed" and pumped conditions and the possibility to compare this kind of "flow response" data to "pressure response" data in the same boreholes.

The main delivery of this task is a comparison between the measured and simulated draw downs in the KR14–18 pump test.

2.3 Task 7C – Single-fracture scale

The intention of Task 7C is to develop a near-field single fracture scale model incorporating essential micro structural information in order to assess flow pattern on a section of a shaft wall and assess the transport characteristics by F-factor predictions and also assess the flow distribution on a large scale within a fracture. The task is not about addressing effects of shaft wall EDZ and unsaturated conditions, nor effects due to the grouting of investigation boreholes.

Data concerning pump tests on the metre scale are available as well as inflow distribution to an excavated shaft. These data will be utilized in the development of a micro structural model, which is the main outcome of Task 7C.

2.4 Task 7ABC – Combining the scales

As a final task it was suggested that the micro structural model, developed in Task 7C, should be implemented in the Task 7B set-up and the effect on the comparison with field data should be evaluated. As the Task 7B set-up was built on, and included, Task 7A this means that a single set-up covering all three tasks should result.

This model was developed and the pump test KR14–18 was revisited. A number of realizations of the heterogeneous fractures revealed some interesting effects.

3 Task 7A

3.1 Introduction

3.1.1 Background

Site investigations are to a large extent based on the information gathered from drilled boreholes. The core gives valuable information about the rock properties and the fracture system. If several boreholes are drilled interference tests of various kinds may give further information about both the hydraulic and transport properties.

Boreholes can be of various kinds; they can be open or packed off into sections. We may further distinguish between pumped boreholes, or borehole sections, and observation boreholes. A pumped borehole will get a certain drawdown that generates an inflow to the borehole. If a steady state is reached the pumping rate is then equal to this inflow. A borehole, or a borehole section, which is not pumped, has both inflows and outflows along the borehole. For a packed off section one can assume that these are equal in magnitude. For all the kind of boreholes discussed a certain flow along the borehole will develop.

The Äspö Task Force has decided to address the question how boreholes can be analyzed by and implemented in numerical simulations model. The exercise is called Task 7. In particular, a long term pumping test at the Olkiluoto site in Finland should be analyzed. Another, related question is how boreholes may contribute to the general circulation at the site. It is further expected that the modelling exercises will provide information about the groundwater system in general, the hydro structural model, advective travel times, etc.

3.1.2 Objectives

The present chapter concerns Task 7A and has the following objectives:

- Describe the numerical model set-up (which is based on the code DarcyTools). In particular the implementation of boreholes.
- Deliver results in form of the provided “Performance Measures”.
- Provide views on the groundwater system at Olkiluoto and the effects of boreholes.

3.1.3 Outline

In the next section the site and input data will be briefly described. This section is largely based on the provided documents describing the task. Next results are shown. Some results are also delivered in form of spread sheets, which are not part of the report. Finally some discussions and conclusions are given. Appendix A gives some details about the implementation of boreholes in the numerical model.

3.2 Site and data

The site is described in the background documents for Task 7 (Vidstrand et al. 2012). From these we quote the following text and figures.

Geographical settings

Spent fuel from the Finnish nuclear power reactors is planned to be disposed of in a KBS-3 type repository to be constructed at a depth between 400 and 600 m in the crystalline bedrock at the Olkiluoto site.

Olkiluoto is an island of the size of about 10 km^2, separated from the mainland by a narrow strait, on the coast of the Baltic Sea. The repository for spent fuel will be constructed in the central part of the island (Figure 3-1). Olkiluoto Island has a continental climate with some local marine influence. In the spring, temperature is significantly lower on the island than inland. Correspondingly, the warm sea equalises the temperature differences between day and night in the fall, so that frosts are rare. The winter is usually temperate. The mean temperature at Olkiluoto in the period of 1992 to 2001 was 5.8°C. The snow thickness is usually less than 20 cm and water equivalent of snow is below 40 mm. The amount of snow varies during winter with temperature fluctuating around 0°C.

The site investigations will culminate in the construction of the ONKALO underground rock characterization facility. This construction work started in July 2004 and is expected to complete in 2010. The investigations in the ONKALO are an essential support for the application of the construction license for the repository. The application of the construction license is to be submitted to the authorities by the end of 2012 (Figure 3-2).

The investigations in ONKALO will aim at further characterization of bedrock properties and to find the most suitable locations for the first deposition tunnels and holes for spent fuel canisters (Posiva 2003b). Tests and demonstrations of repository technologies will also be carried out in ONKALO. The underground parts of ONKALO consist of a system of exploratory tunnels accessed by a tunnel and a ventilation shaft. The ventilation shaft is to be located in the place of borehole KR24. The main characterization level will be located at a depth of about 400 m and the lower characterization level at a depth of about 500 m. Demonstrations and tests of repository technologies will mainly be carried out on the main level. The total underground volume of ONKALO will be approximately 330,000 m^3 with the combined length of tunnels and shaft of about 8,500 m.

According to current plans, the operation of the facility would commence after 2020.

Borehole KR24 pumping test

The construction of the underground facilities at Olkiluoto will affect the water table, hydraulic head in the vicinity of the access tunnel and shafts, and also the groundwater circulation at depth in general. To predict the effects and to characterize hydraulic connections on the scale of 100 m to 1 km, a long-term pumping test was carried out in the 550 m deep, vertical borehole KR24 from 25 March to 2 June 2004.

After this general introduction to the site we will continue with some details of direct relevance to the set-up of the numerical model.

- The potential recharge, i.e. precipitation minus evapotranspiration, is estimated to 100–150 mm/year.
- The salinity gradient is weak down to a depth of 400–500 mbsl. The salinity of the Baltic Sea around Olkiluoto is 6 g/l.
- The bedrock can be divided into an upper part, about 80 m thick, of high conductivity and a lower part which is dominated by a few (of the order 20) large scale fracture zones. The fracture zones are listed in Table 3-1, where also some properties are given.
- A number of boreholes have been drilled at the site, as is illustrated in Figure 3-1. The boreholes that will be considered in this study are given in Table 3-2. The borehole KR24 is of special interest as this is the pumped borehole in the pump test. KR24 can be seen in Figure 3-1 and is located where the ventilation shaft is shown in Figure 3-2.

This brief introduction to the site and the data is only intended to give some background to the numerical simulations to be presented. A final illustration of the fracture zones and boreholes is given by Figure 3-3. One of the objectives of this study is to evaluate how boreholes may influence the groundwater circulation: this figure quite nicely illustrates that this concern is relevant.

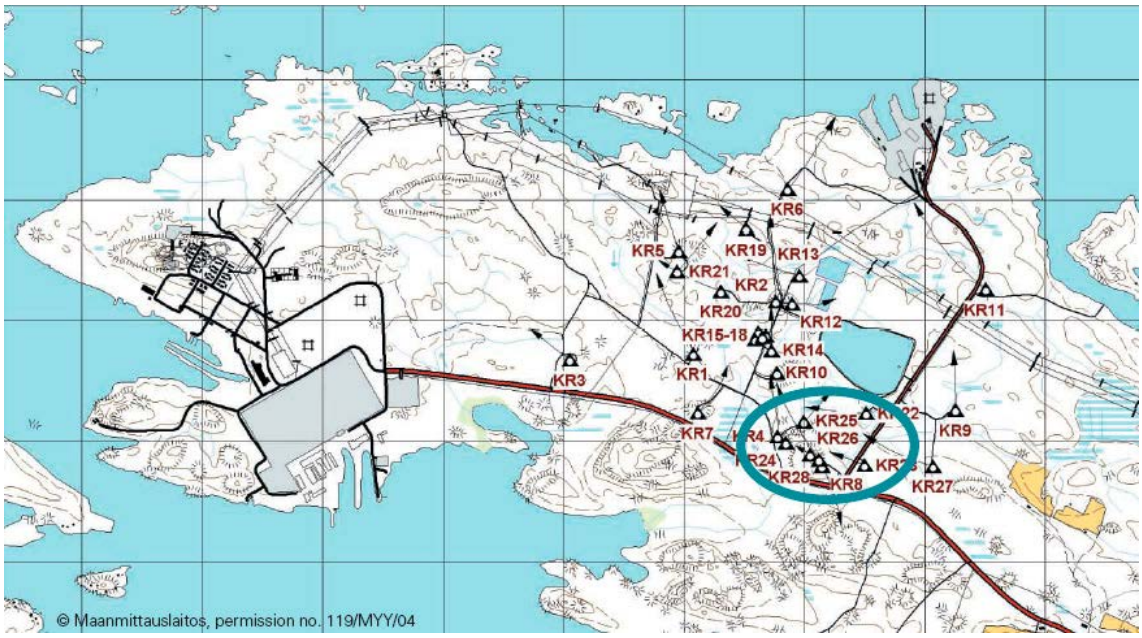

Figure 3-1. *Olkiluoto Island and the location of the ONKALO (thick oval). The repository for spent nuclear fuel will be constructed in the north west of the ONKALO.*

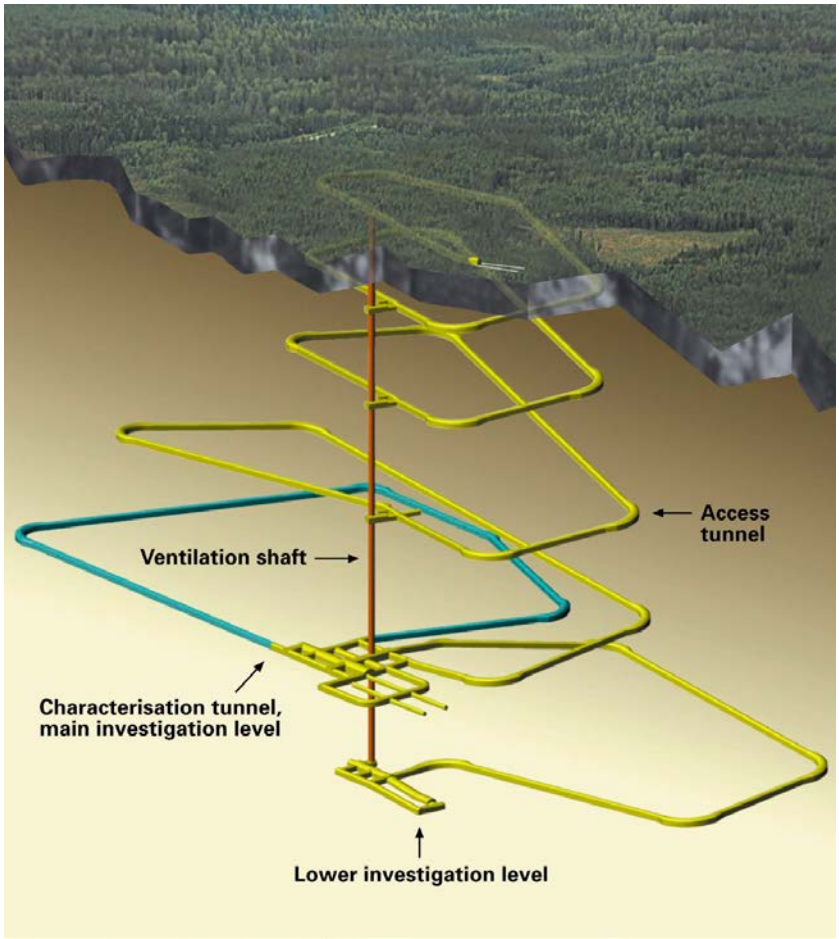

Figure 3-2. *The ONKALO rock characterization facility. The construction of ONKALO started in July 2004 and is planned to last until about 2010.*

Table 3-1. Major fracture zones that are included in the numerical model.

Fracture zone Name	Transmissivity (log) Geometric mean (m^2/s)	Standard deviation Log(T)	Storativity (–)	Transport Aperture (by Dows law)*	Fracture width (mm)	Geological width (mean/range) (m)
HZ001	–7.9	2.1	2.5×10^{-08}	7.0×10^{-06}	1–20	5 / 1–20
HZ002	–6.0	0.6	2.0×10^{-06}	6.3×10^{-05}	1–20	5 / 1–10
HZ003	–6.2	1.3	1.3×10^{-06}	5.0×10^{-05}	1–20	5 / 1–10
HZ004	–6.8	0.7	3.2×10^{-07}	2.5×10^{-05}	1–20	25/10–40
HZ19A	–5.8	1.6	3.2×10^{-06}	7.9×10^{-05}	1–20	5 / 1–15
HZ008	–5.0	–	1.6×10^{-05}	2.0×10^{-04}	1–20	2 / 1–5
HZ19C	–5.5	1.3	6.3×10^{-06}	1.1×10^{-04}	1–20	4 / 1–10
HZ20A	–5.1	0.7	1.6×10^{-05}	1.8×10^{-04}	1–20	5 / 1–15
HZ20AE	–6.0	1.2	2.0×10^{-06}	6.3×10^{-05}	1–20	5 / 1–10
HZ20B_ALT	–5.5	0.9	6.3×10^{-06}	1.1×10^{-04}	1–20	8 / 1–20
HZ21	–7.8	1.8	3.2×10^{-08}	7.9×10^{-06}	1–20	11 / 3–25
HZ21B	–6.1	0.9	1.6×10^{-06}	5.6×10^{-05}	1–20	7 / 1–10
BFZ099	–7.8	1.8	3.2×10^{-08}	$7{,}9\times10^{-06}$	1–20	8 / 1–25

Table 3-2. Boreholes included in the numerical model.

Borehole	Comments
KR24	The pumped borehole. Packed off into two sections.
KR06	Casing depth guessed to 40 metres.
KR08	
KR09	
KR12	
KR14	
KR22	
KR23	Packed off into seven sections.
KR25	Packed off into eight sections.
KR28	

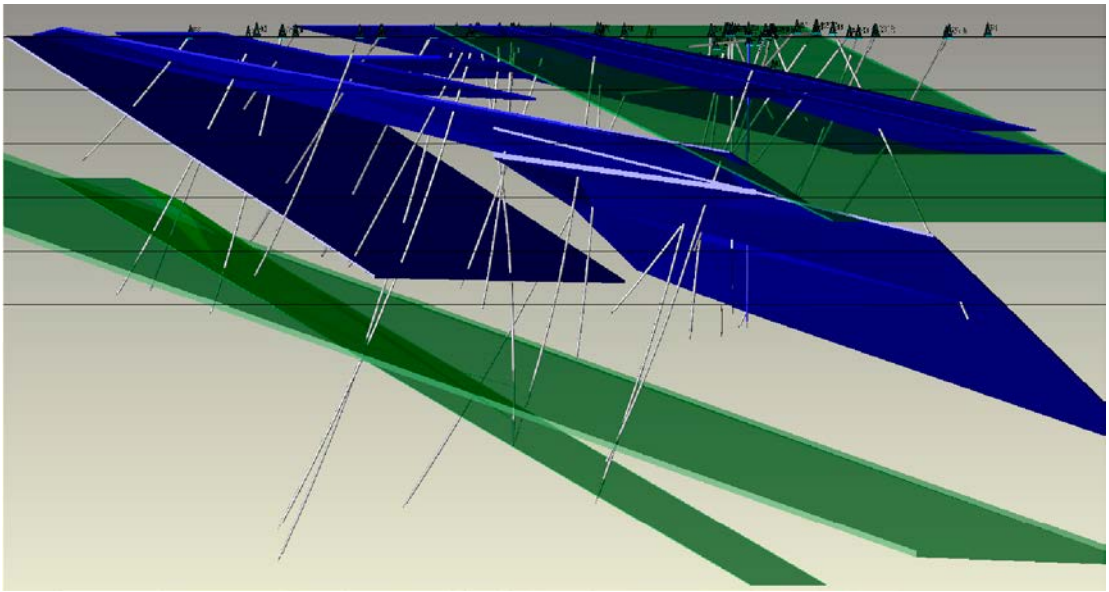

Figure 3-3. *Illustration of the zones and boreholes, without masking zones HZ004 and HZ008.*

3.3 Numerical model

3.3.1 Introduction

The code DarcyTools (Svensson et al. 2010) will be used for the simulations. It is outside the scope of this report to describe this code, but a few features of specific relevance to the present application will be listed.

- An adaptive Cartesian grid will be used. Geometrical features like topography, fracture zones, boreholes, etc can be read in as CAD files and the computational grid adapts itself to these, following a set of rules and conditions.
- New ways to represent boreholes have been evaluated in this project, see Appendix A. Both the numerical resolution of the borehole and the mass conservation condition (for example inflows equal outflows for a packed off section) have been studied.
- Discrete fracture networks (DFN) have been generated and implemented in the model. A novel feature is that the DFN can be associated to subvolumes of the domain.
- DarcyTools has a built in method to handle a free groundwater table; this feature will be used.

These are some problem specific features that are employed in this study. Regarding equations we may state that the mass conservation and the Darcy equations form the foundation, while buoyancy effects are not considered; the salinity equation is hence not solved.

3.3.2 Computational grid

The grid on the top boundary is shown in Figure 3-4. The model domain is defined by a set of boundary lineaments. A cell size of 16 m is used on the top boundary. The grid follows the topography, which was used as an input to the grid generation.

A vertical east-west section that goes through borehole KR24 is shown in Figure 3-5. There are several things to note in this figure. The grid is continues close to ground (top 80 metres) while at deeper levels the grid cells in “the good rock” have been removed. The grid cells at depth thus illustrate the fracture zones. However, boreholes are also explicitly represented in the grid. In the vicinity of KR24 fracture zones are resolved by a cell size of 8 m, while the boreholes are resolved by cells of the size 0.06 m. A detail of the grid at the crossing between KR24 and fracture zone HZ20B_ALT is shown in Figure 3-6. In this figure the resolution of the borehole can be seen. It is also seen that a local grid resolves the crossing point. The reason for this grid is a local DFN that intends to increase the contact between KR24 and the fracture zone; more comments on this will follow.

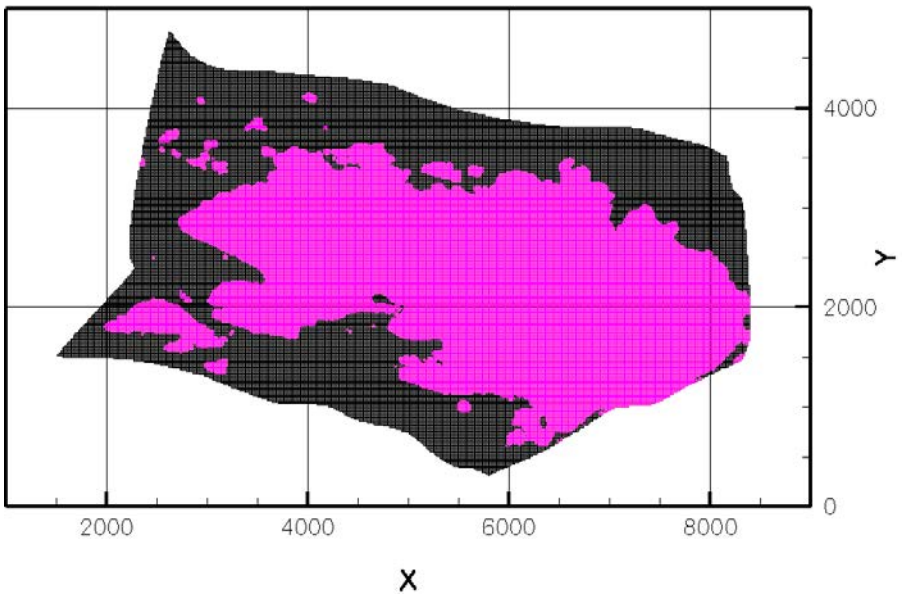

Figure 3-4. *Computational grid at the top boundary.*

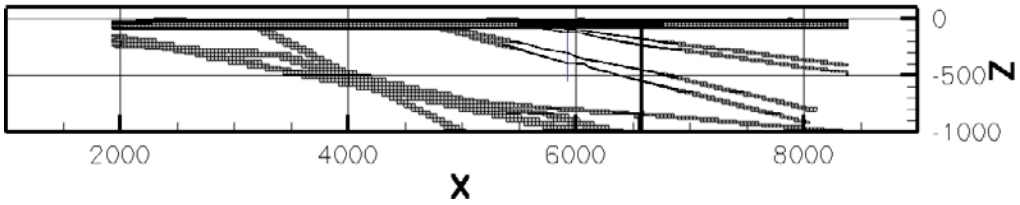

Figure 3-5. *Computational grid in a west-east vertical section through borehole KR24.*

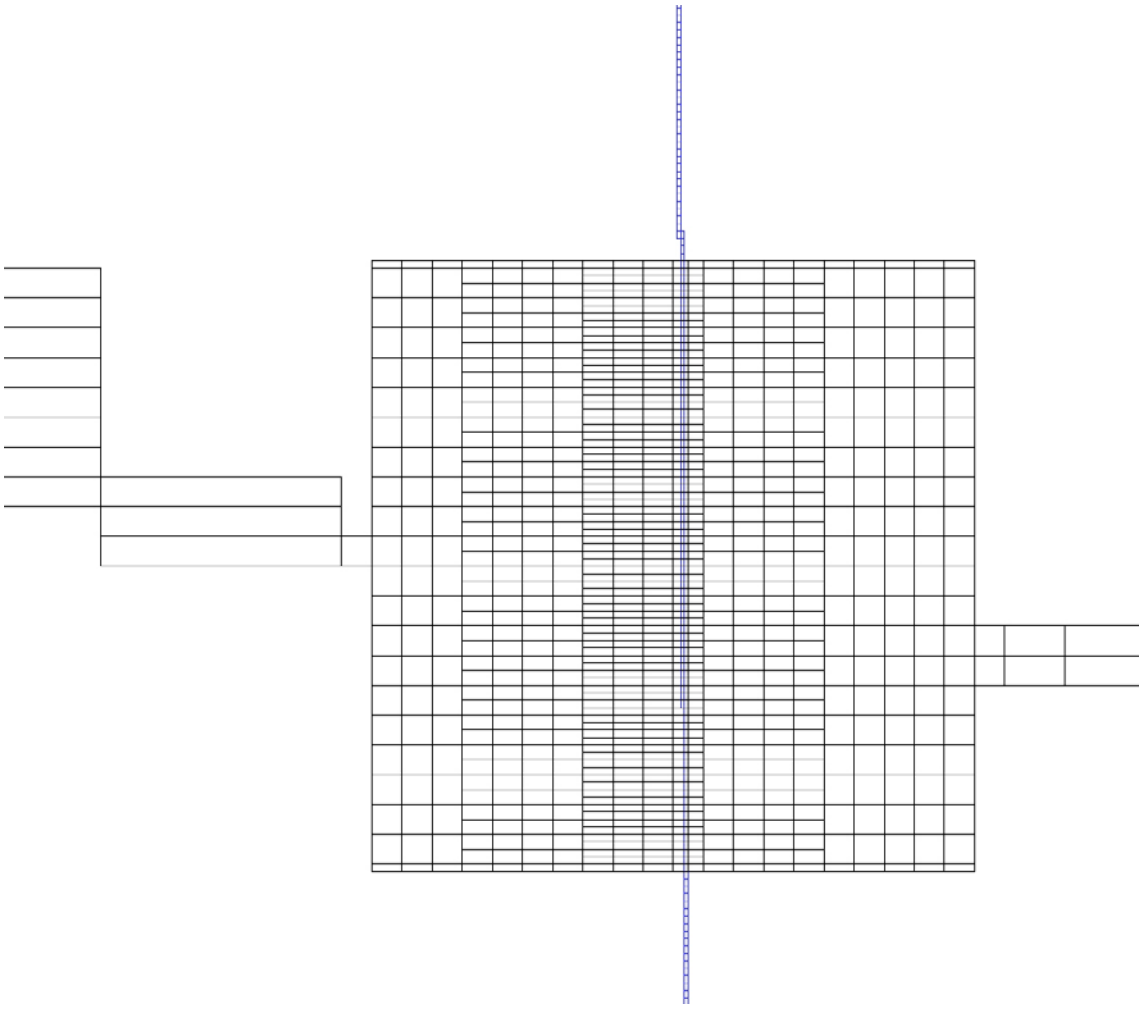

Figure 3-6. *Computational grid at the crossing between borehole KR24 and fracture zone HZ20B_ALT.*

3.3.3 Boundary condition

The following points summarize the boundary conditions employed.

- At the lateral boundaries a hydrostatic pressure distribution is prescribed.
- The bottom boundary condition is of the zero flux type.
- At the top boundary pressure is prescribed below sea level, with an account of the water depth, while a free groundwater table is simulated above the sea level. The net recharge was set to 100 mm/year.

3.4 Results

3.4.1 Introduction

The number of simulation cases requested in the task description is quite extensive, as can be seen in Table 3-3. The cases labelled "Forward" are intended to be based on the provided data while the cases labelled "Inverse" should represent the result after calibration. However, due to time constraints, a somewhat modified approach to calibration was adopted in this work, details below.

In addition to the cases in Table 3-3 a so called Reference case should be carried out. The basic data provided should be used and the upper boundary condition should be a specified head (topographic elevation). Cases SS01 and SS02a in Table 3-3 should be simulated using these conditions.

The task description also specifies the requested output from the simulations, so called Performance Measures (PM). These include heads and draw downs but also inflows/outflows along boreholes. The PM-data will be given in supplied spread sheets, for further compilation and analyzes by the task organisers. Some of these data will be repeated here.

3.4.2 Calibration

The calibration strategy is based on two features of the KR24 pump test that are believed to be essential. Firstly, one should try to get the draw downs in the upper and lower section of KR24 right (the pump rates in the two sections are specified). Secondly, it is expected that the near ground layer (roughly the upper 80 metres) is essential as a hydraulic connection between KR24 and other boreholes. Based on these concepts it was decided that the following points should define the calibration procedure:

- Apply a high conductivity near ground that decays exponentially:
  $K(z) = K_{top}e^{-depth/2}$. Use K_{top} to get a realistic groundwater table.
- For the upper 80 metres a DFN was generated according to the task description. Add a background conductivity, K80, to this layer. Use K80 to get the right drawdown in the upper section of KR24.
- Below 80 mbsl KR24 is only crossed by a few major fracture zones. The specified pump rate in this section will for this reason generate too large drawdown. Specify a local DFN at the fracture crossings, using the volumes around the crossings shown in Figure 3-6. Use the transmissivity of the fractures of the DFN to reduce the drawdown in the lower section of KR24.

Test simulations showed that the three calibration points were quite independent, which made the task easier. The outcome of the calibration can be summarized as:

- If Ktop is put to 10^{-3} m/s a realistic groundwater table results, see Figure 3-7. It should be pointed out that some representation of streams is required if further details of the groundwater table should be captured. In Figure 3-7 an illustration of "wet areas" is also given. An area is regarded as wet if the water table is closer to ground than 0.5 m.
- If K80 is put to 9×10^{-8} m/s, the drawdown in the upper section of KR24 will be around 18 metres, which is in agreement with the recorded drawdown.
- A local DFN around the crossings between KR24 and fracture zones does reduce the drawdown. However, it was not possible to achieve the recorded drawdown of 1.2 m. Using a transmissivity of 10^{-6} m^2/s for the 5 metres long fractures in the network, a typical drawdown of 5 metres was obtained. Increasing the transmissivity further produced only small effects. This result indicates that KR24 is in contact with more fractures or that fracture zones in contact are more transmissive than given by the input data.

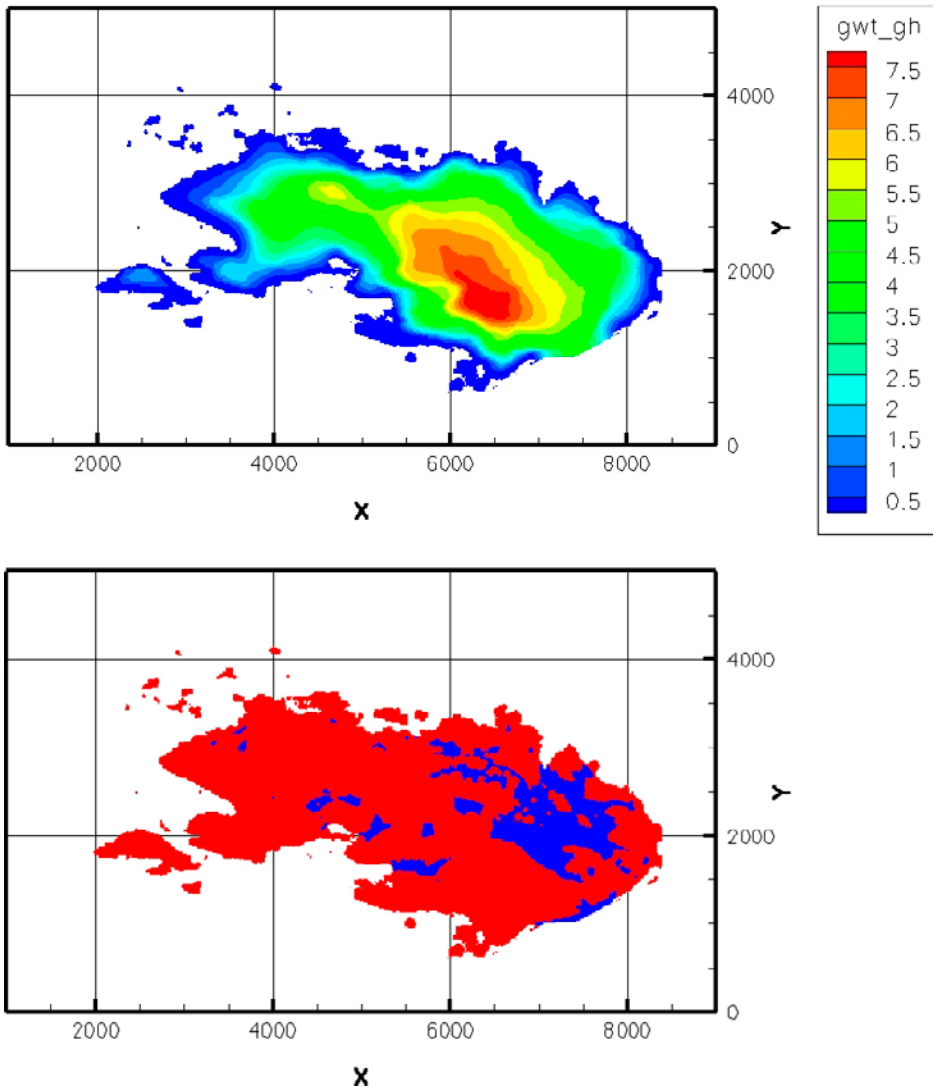

Figure 3-7. *Groundwater table for virgin conditions (top) and "wet areas" (blue).*

3.4.3 Steady state cases

Four steady state cases are listed in Table 3-3, the first two without pumping while SS3 and SS4 concern pumping in KR24. Heads in boreholes and borehole sections for these four cases are summarized in Table 3-4. As we have not introduced the positions of all boreholes, neither the positions of the crossings with fracture zones, it is not possible to give detailed explanations of the data. However, some main effects can be identified:

- For KR24 a comparison between SS2 and SS4 shows that the drawdown in the upper section is 18 metres (5.5 + 12.5) while the lower section gets a drawdown of 5.4 metres.
- KR25 is a borehole that is located fairly close to KR24 and it is hence not surprising that we get a drawdown of more than 1.0 metre. KR09 is located some 600 metres away from KR24 and the drawdown is accordingly much smaller, about 0.2 metres.

For the SS1 and SS3 cases it should be noted that the head values are picked where the boreholes, or sections, are located but there is of course no flow along the boreholes in these cases (except for KR24 in case SS3).

A brief comparison with measured draw downs shows that the simulated draw downs are in general agreement with measurements. The exception is the drawdown in the lower section of KR24, as discussed above.

Table 3-3. Requested simulation cases.

Name	Task	Description	Forward/Inverse	Boreholes
SS01	7A1	Steady state flow conditions without pumping	Forward	No boreholes
SS02a	7A1	Steady state flow conditions with open boreholes	Forward	Boreholes are open and free to cross-flow.
SS02b	7A1	Steady state flow conditions with open boreholes	Inverse	Boreholes are open and free to cross-flow.
SS02c	7A1	Steady state flow conditions without pumping	Based on SS02b final set-up	No boreholes
SS03	7A1	Steady states flow with extraction from KR24	Forward	KR24 only
SS04a	7A1	Steady states flow with extraction from KR24	Forward	KR24 + monitoring boreholes
SS04b	7A1	Steady states flow with extraction from KR24	Inverse	KR24 + monitoring boreholes
TR01	7A1	Transient simulation of KR24 test	Forward	KR24 only
TR02a	7A1	Transient simulation of KR24 test	Forward	KR24 + monitoring boreholes
TR02b	7A1	Transient simulation of KR24 test	Inverse	KR24 + monitoring boreholes
PA01	7A2	Transport pathway simulation from KR24 to discharge under PA relevant boundary conditions*.		No boreholes (particles start from position along KR24)

Table 3-4. Simulated heads in boreholes and borehole sections for steady state cases.

Borehole	Section	SS1	SS2	SS3	SS4	Ref SS1	Ref SS2
KR24	Upper	6.8–6.9	5.5	–12.4	–12.5	9.5–10.2	7.7
	Lower	2.2–6.8	5.5	–0.9	0.1	3.1–8.2	7.7
KR04	Entire	1.0–7.0	5.9	1.1–5.4	4.4	2.5–9.0	7.9
KR08	Entire	2.0–7.0	5.9	1.0–7.0	5.4	2.9–12.2	9.0
KR09	65–75	6.3	5.0	6.2	4.8	5.8	5.2
	140–150	5.1	5.0	5.0	4.8	5.6	5.2
	565–575	1.9	5.0	1.5	4.8	2.7	5.2
KR12	40–50	6.1	4.9	6.0	4.7	7.5	6.3
KR14	10–40	6.7	6.0	6.6	5.8	8.4	7.7
	40–60	6.7	6.0	6.6	5.8	8.4	7.7
	70–90	6.7	6.0	6.6	5.8	8.4	7.7
KR22	90–120	6.8–7.1	5.9	6.2–7.0	5.3	7.7–8.3	7.3
	140–150	5.7	5.9	4.9–5.2	5.3	6.8	7.3
	385–395	2.4	5.9	1.4	5.3	3.6	7.3
KR23	150–155	6.0	5.8	5.3	5.1	7.5	7.3
KR25	90–100	7.0	6.9	6.2–6.7	6.6	9.0	9.1
	120–130	6.0	6.1	4.7–4.8	5.1	7.5	7.7
	345–355	2.4	4.5	1.5	3.4	3.5	6.1
	405–410	2.1	4.0	1.3	3.9	3.1	5.6

We will now continue with some more results for the steady state conditions, starting with some large scale effects. The drawdown at 50 mbsl is illustrated in Figure 3-8. As can be seen quite a large area is affected and it is likely that draw downs in observation holes are partly due to the connections in the upper 80 metres. The drawdown in Figure 3-8 was calculated as the head difference in SS2 and SS4.

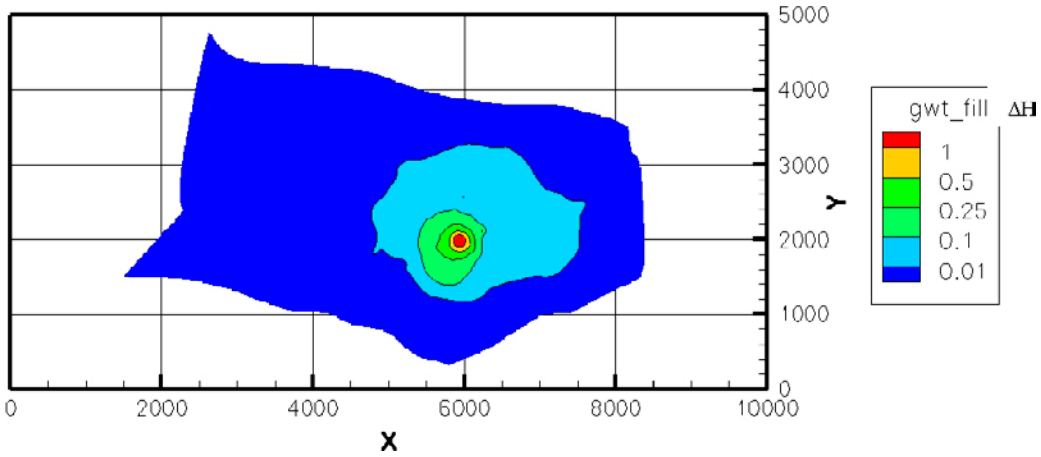

Figure 3-8. *Drawdown at 50 mbsl, based on cases SS2 and SS4.*

Next we study some details at borehole scale, which is the novel feature of the simulations presented. A local DFN was generated in the contacts between KR24 and fracture zones. In Figure 3-9 we can study the inflow to KR24 at such a crossing, based on case SS4. The inflow is not at a point, but distributed over a distance; a feature often seen from field measurements. As we are resolving the boreholes explicitly it is possible to obtain the flow along boreholes. In Figure 3-10 the flow along four boreholes are shown. Once again we use case SS4 and the net flow in KR24 is hence 18 l/min, while the other boreholes should have a zero net flow. A typical feature of these distributions is that the inflow is very irregular for the 80 upper metres, while a more discrete pattern is found below this level. This is clearly seen in Figure 3-11 where the inflows to the four boreholes are shown. This is of course due to the assumed conductivity distributions with only a few large scale features below 80 mbsl.

In Table 3-4 also the results for the Reference cases are included. The general impression is that the heads are too high. This is not surprising as a groundwater table that everywhere follows the topography is “the highest possible”. A specified head also implies an infinite source of water at this boundary. We hence conclude that this boundary condition is not the most realistic.

3.4.4 Transient cases

The Performance Measures specify that heads and flow distribution along boreholes should be evaluated by simulating the pump test in a transient mode, see Table 3-3. Conditions at two times (28 and 1,708 hours after start of the pumping) are requested in form of the above mentioned spread sheets. Here we will be more selective and only point to some interesting features. One may however question the transient simulations as these are expected to be sensitive to the specific storativity field used. Very little information is available about this field. Furthermore, in the present model set-up the rock in between the fracture zones below 80 metres depth is not considered at all. In the view of the present writer, the storativity effect is to a large extent due to the stagnant water in these volumes. However, the transient simulations were carried out using a constant specific storativity of 10^{-6} m^{-1}.

In Table 3-5 the heads at the two specific times are listed, this for case TR02. A comparison with Table 3-4 shows that the heads are very close to the steady state values after 1,708 hours. In the deepest section of KR25 one may note that without pumping the head is 4.0 m, after 28 hours of pumping it is 3.8 m, after 1,708 hours of pumping it is 3.0 m while the steady state value with pumping is 2.9 m.

The transient development of the heads in two boreholes is illustrated in Figure 3-12, where also the measured development is included. A fair agreement is found.

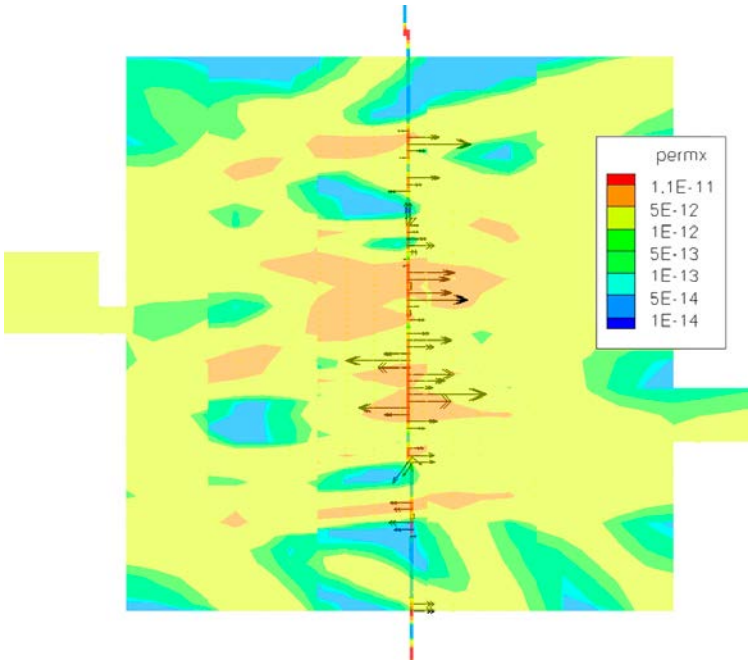

Figure 3-9. *Inflow vectors at the crossing between KR24 and HZ20B_ALT. The background field is the horizontal permeability.*

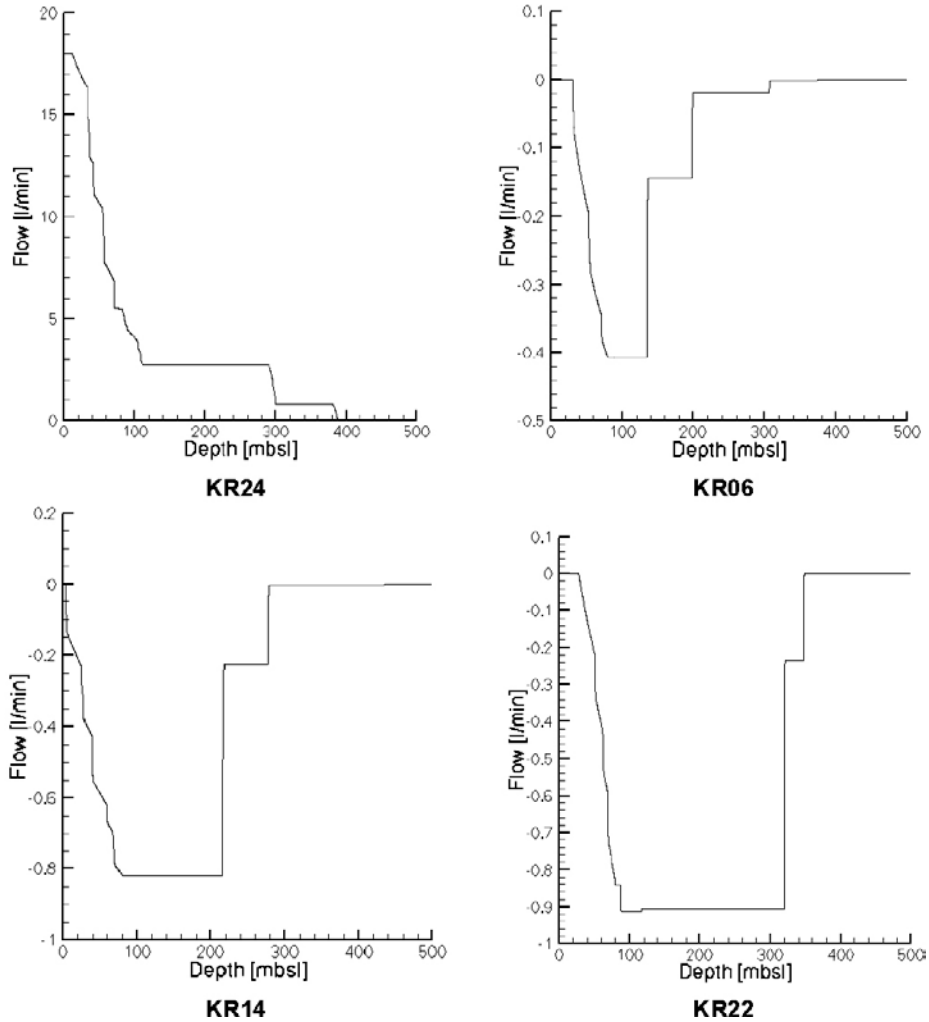

Figure 3-10. *Flow along four boreholes.*

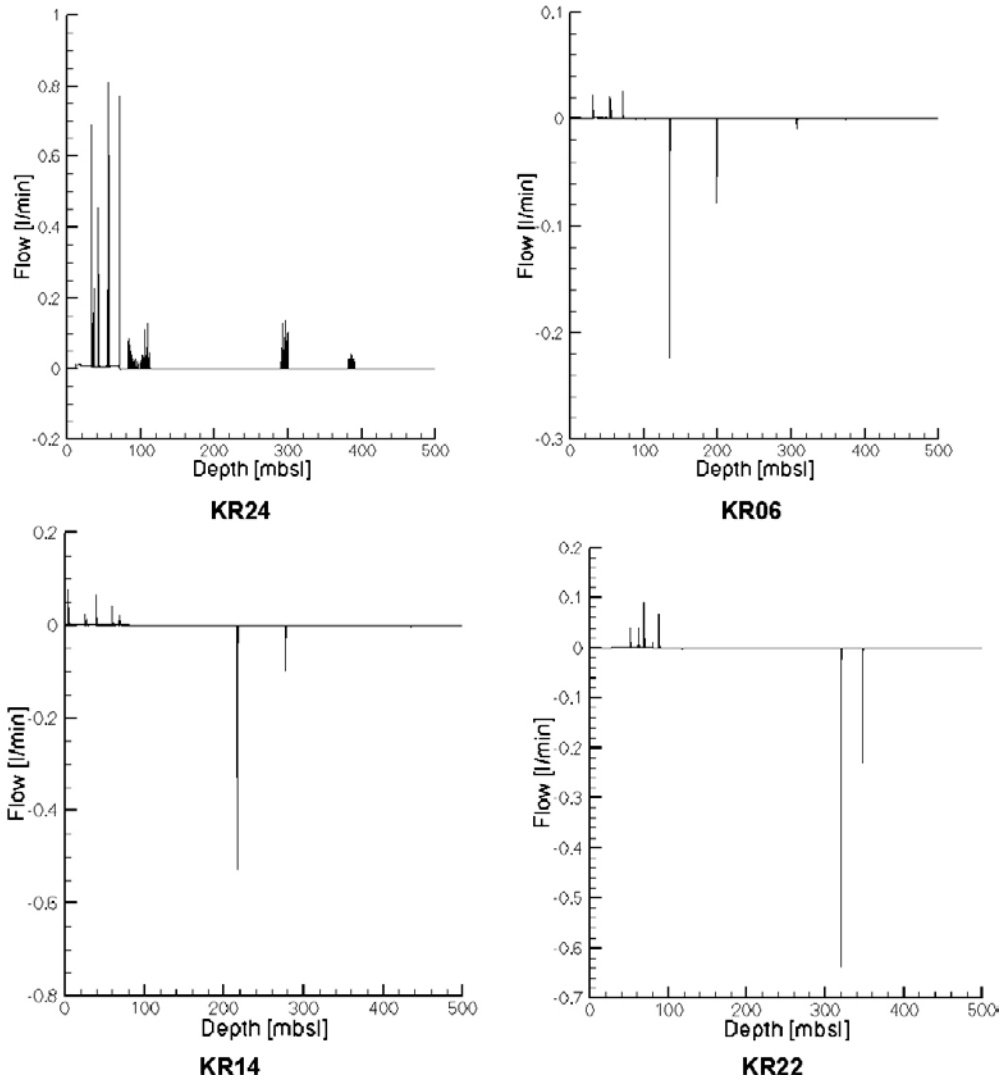

Figure 3-11. *Inflows to four boreholes.*

Table 3-5. Heads in boreholes and borehole sections for case TR02.

		Time	
Borehole	**Section**	**28 hours**	**1,708 hours**
KR24	Upper	–12.3	–12.5
	Lower	0.7	0.1
KR04	Entire	4.8	4.5
KR08	Entire	5.7	5.4
KR09	65–75	5.0	4.8
	140–150	5.0	4.8
	565–575	5.0	4.8

		Time	
Borehole	**Section**	**28 hours**	**1,708 hours**
KR12	40–50	4.9	4.7
KR14	10–40	5.9	5.8
	40–60	5.9	5.8
	70–90	5.9	5.8
KR22	90–120	5.6	5.3
	140–150	5.6	5.3
	385–395	5.6	5.3
KR23	150–155	5.3–5.7	5.0–5.4
KR25	90–100	6.8	6.6
	120–130	5.4	5.1
	345–355	4.0	3.5
	405–410	3.8	3.0

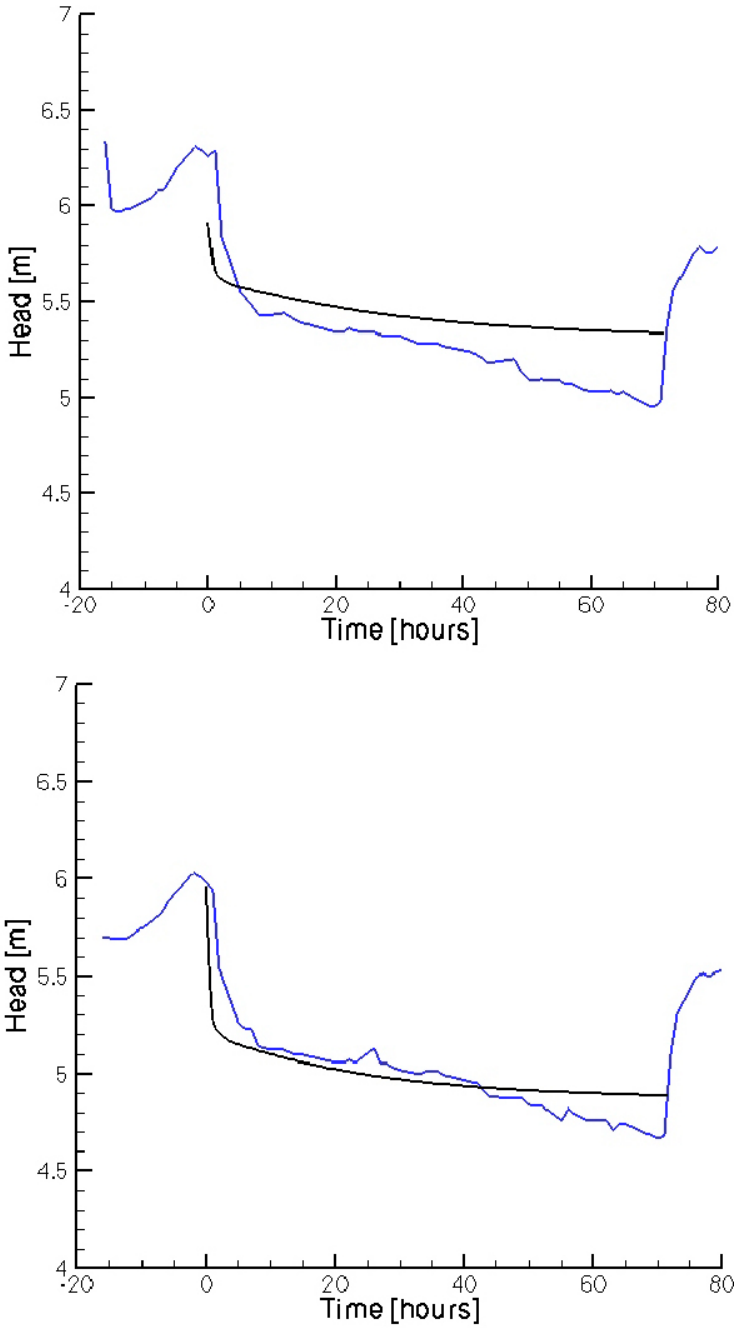

Figure 3-12. *Transient heads in boreholes KR22 (top) and KR28. Black lines show simulated heads, while blue represent measurements.*

3.4.5 Transport pathways

The final case listed in Table 3-3 concerns transport pathways under Performance Assessment (PA) conditions. No boreholes should be present and we hence base the simulations on case SS1. Particles are to be released at positions where KR24 crosses some deep fracture zones (HZ19C, HZ20AL and HZ20B_ALT) and the time to reach the ground or the domain boundaries should be recorded.

The result of the simulation is shown in Figure 3-13. All particles moved south, and most end up beneath the Baltic Sea. Considering that the island generates a higher than ambient pressure due to the groundwater table, it is not surprising to find this result. However the pressure gradient below the Baltic Sea will decrease with distance from the shore which means that the particles will move slower and slower. The total integration time in the simulation was set to 100 years; most of this time was spent below the Baltic Sea.

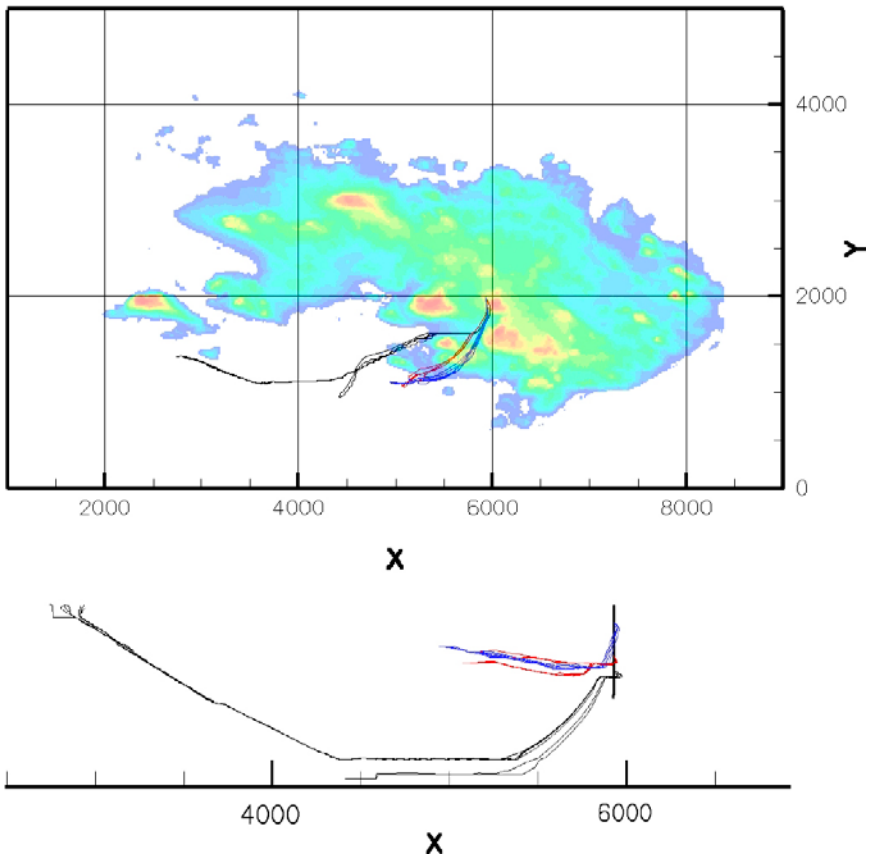

Figure 3-13. *Transport pathways from three positions along KR24. Horizontal view (top) and a west-east view close to KR24.*

3.5 Discussion

This task is devoted to various aspects of boreholes. In the discussion we will bring up two such topics, one is the large scale effect of boreholes the other one concerns the details of the Posiva Flow Log.

It has been questioned if a large number of boreholes may affect the general groundwater circulation at a site like Olkiluoto. During the simulations carried out for the Performance Measures some additional information that may bring some light on this topic was compiled. The flow through two squares (1,200×1,200 m) centred at KR24 and at depths 0 mbsl and 100 mbsl was calculated. The up and down going flux components were separated. The result can be studied in Table 3-6. First we note that the net vertical flux at 0 mbsl is about 20 mm/year, which reduces to about 1 mm/year at a depth of 100 mbsl. In the background material to the task it is stated that "the most likely deep groundwater recharge to the bedrock during natural conditions is approximately 5–20 mm/year". Regarding the effect of boreholes on the general circulation, one may note that the presence of boreholes increases the downward flow at 0 mbsl, while the effect is the opposite at 100 mbsl. One can only speculate in the reason for this.

Next we turn our attention to the Posiva Flow Log. In the task descriptions it was suggested that the bypass resistance, due to the packer that separates the upper and lower sections of KR24, should be explicitly included in the numerical model. This has not been done in the present study, as it was not considered necessary. A brief analysis of the bypass was however carried out. Under natural conditions (i.e. no pumping) the field data indicate a head difference of 0.2 m between the upper and lower section of KR24. A laminar pipe flow analysis shows that about 0.7 l/min may flow through the 1 m long and 4 mm diameter bypass tube. This flux was prescribed in the numerical mode as a sink in the upper section and a source in the lower. This resulted in a head difference of about 0.4 m, which shows that the numerical model can simulate the effect of the Posiva Flow log also for natural conditions. For pumped conditions a pipe flow analysis shows that the flux will be about 5–6 l/min. For pumped conditions the flow will be turbulent as the Reynolds number is above 20,000.

Table 3-6. Vertical flux (in mm/year) at two depths through a horizontal surface (1,200×1,200 m) centred around KR24.

Case	Depth			
	0 mbsl		100 mbsl	
	↑	↓	↑	↓
SS1	4.0	21.0	0.007	0.83
SS2	3.7	21.9	0.011	0.73
SS3	3.5	23.3	0.005	1.22
SS4	3.3	23.9	0.005	1.04

3.6 Concluding remarks

This is the first subtask of Task 7 and it is not yet the time to make firm claims about the modelling results. One should perhaps also point out that most modelling groups in Task 7 will not have the time to develop a fully fledged site model; some shortcuts will be needed. In the present work we have chosen to be fairly brief in the calibration process and the comparisons with field data have been done in a qualitative way. A more ambitious site model development should certainly be more thorough on these two topics.

The main achievements that can be reported are:

- A numerical model of the Olkiluoto site and the pumping test in KR24 has been set up and tested. All simulation results seem plausible, although detailed comparisons with field data are lacking.
- Methods to simulate pumped, open and packed off boreholes have been developed, tested and applied.

4 Task 7B

4.1 Introduction

4.1.1 Background

Site investigations are to a large extent based on the information gathered from drilled boreholes. The core gives valuable information about the rock properties and the fracture system. If several boreholes are drilled interference tests of various kinds may give further information about both the hydraulic and transport properties.

Boreholes can be of various kinds; they can be open or packed off into sections. We may further distinguish between pumped boreholes, or borehole sections, and observation boreholes. A pumped borehole will get a certain drawdown that generates an inflow to the borehole. If a steady state is reached the pumping rate is then equal to this inflow. A borehole, or a borehole section, which is not pumped, has both inflows and outflows along the borehole. For a packed off section one can assume that these are equal in magnitude. For all the kind of boreholes discussed a certain flow along the borehole will develop.

The Äspö Task Force has decided to address the question how boreholes can be analyzed by and implemented in numerical simulations model. The exercise is called Task 7. In particular, pump tests at the Olkiluoto site in Finland should be analyzed. Another, related, question is how boreholes may contribute to the general circulation at the site. It is further expected that the modeling exercises will provide information about the groundwater system in general, the hydro structural model, advective travel times, etc.

4.1.2 Objectives

The present chapter concerns Task 7B and has the following objectives:

- Describe the numerical model set-up (which is based on the code DarcyTools). In particular the implementation of boreholes.
- Deliver results in form of the provided “Performance Measures”. The results should concern the pump test in boreholes KR14–KR18.
- Provide views on the groundwater system at Olkiluoto and the effects of boreholes.

4.1.3 Outline

In the next section the site and input data will be briefly described. This section is largely based on the provided documents describing the task. Next results are shown. Some results are also delivered in form of spread sheets, which are not part of the report. Finally some discussions and conclusions are given.

4.2 Site and data

The site is described in the background documents for Task 7 (Vidstrand et al. 2012). From these we quote the following text and figures.

Geographical settings

Spent fuel from the Finnish nuclear power reactors is planned to be disposed of in a KBS-3 type repository to be constructed at a depth between 400 and 600 m in the crystalline bedrock at the Olkiluoto site.

Olkiluoto is an island of the size of about 10 km^2, separated from the mainland by a narrow strait, on the coast of the Baltic Sea. The repository for spent fuel will be constructed in the central part of the island (Figure 3-1) Olkiluoto Island has a continental climate with some local marine influence. In the spring, temperature is significantly lower on the island than inland. Correspondingly, the warm sea equalises the temperature differences between day and night in the fall, so that frosts are rare. The winter is usually temperate. The mean temperature at Olkiluoto in the period of 1992 to 2001 was 5.8°C. The snow thickness is usually less than 20 cm and water equivalent of snow is below 40 mm. The amount of snow varies during winter with temperature fluctuating around 0°C.

The site investigations will culminate in the construction of the ONKALO underground rock characterization facility. This construction work started in July 2004 and is expected to complete in 2010. The investigations in the ONKALO are an essential support for the application of the construction license for the repository. The application of the construction license is to be submitted to the authorities by the end of 2012.

The investigations in ONKALO will aim at further characterization of bedrock properties and to find the most suitable locations for the first deposition tunnels and holes for spent fuel canisters (Posiva 2003b). Tests and demonstrations of repository technologies will also be carried out in ONKALO. The underground parts of ONKALO consist of a system of exploratory tunnels accessed by a tunnel and a ventilation shaft. The ventilation shaft is to be located in the place of borehole KR24. The main characterization level will be located at a depth of about 400 m and the lower characterization level at a depth of about 500 m. Demonstrations and tests of repository technologies will mainly be carried out on the main level. The total underground volume of ONKALO will be approximately 330,000 m^3 with the combined length of tunnels and shaft of about 8,500 m.

The KR14–KR18 pump tests

Two sets of test have been carried out in these boreholes.

- In 2001 to 2002 a test in open boreholes was carried out. The test can be described as “a cross hole interference test in the scale of 10–100 m, where several boreholes were pumped one at the time”.
- In 2004 the same boreholes were used but now with a multi-packer system installed.

After this general introduction to the site we will continue with some details of direct relevance to the set-up of the numerical model.

- The potential recharge, i.e. precipitation minus evapotranspiration, is estimated to 100–150 mm/year.
- The salinity gradient is weak down to a depth of 400–500 mbsl. The salinity of the Baltic Sea around Olkiluoto is 6 g/l.
- The bedrock can be divided into an upper part, about 80 m thick, of high conductivity and a lower part which is dominated by a few (of the order 20) large scale fracture zones. The fracture zones are listed in Table 3-1, where also some properties are given.
- A number of boreholes have been drilled at the site, as is illustrated in Figure 3-1. The boreholes that will be considered in this study are shown in Figure 4-1.

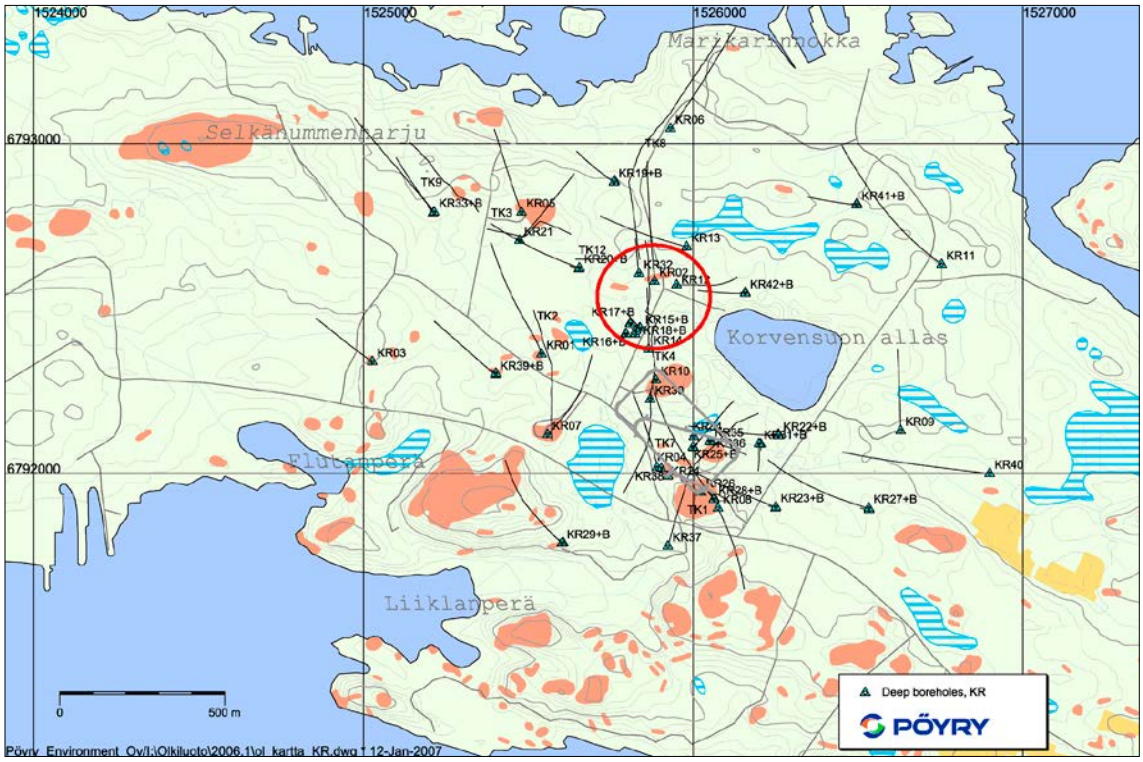

Figure 4-1. *Location (red circle) of boreholes KR14 to KR18.*

4.3 Numerical model

4.3.1 Introduction

The code DarcyTools (Svensson et al. 2010) will be used for the simulations. It is outside the scope of this report to describe this code, but a few features of specific relevance to the present application will be listed.

- An adaptive Cartesian grid will be used. Geometrical features like topography, fracture zones, boreholes, etc can be read in as CAD files and the computational grid adapts itself to these, following a set of rules and conditions.
- New ways to represent boreholes have been evaluated in this project, see Appendix A. Both the numerical resolution of the borehole and the mass conservation condition (for example inflows equal outflows for a packed off section) have been studied.
- Discrete fracture networks (DFN) have been generated and implemented in the model. A novel feature is that the DFN can be associated to sub volumes of the domain.
- DarcyTools has a built in method to handle a free groundwater table; this feature will be used.

These are some problem specific features that are employed in this study. Regarding equations we may state that the mass conservation and the Darcy equations form the foundation, while buoyancy effects are not considered; the salinity equation is hence not solved.

4.3.2 Computational grid

The grid on the top boundary is shown in Figure 4-2. A cell size of 16 m is used on the top boundary. The grid follows the topography, which was used as an input to the grid generation. Around the boreholes KR14 to KR18 a successively smaller cell size is used, as can be seen in Figure 4-2 and Figure 4-3. At the 100 m scale a cell size of 1.0 metre is used, while the boreholes are resolved with a cell size of 0.0625 metre.

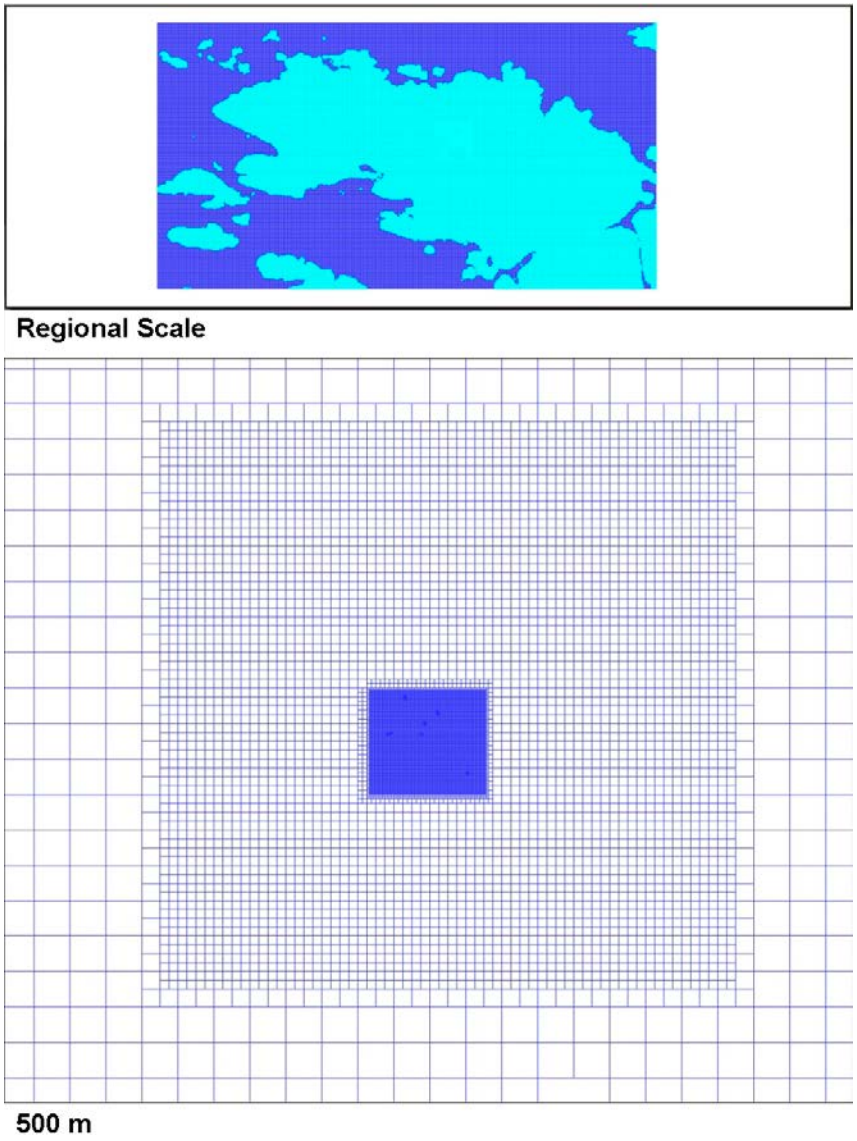

Figure 4-2. *Computational grid. Regional scale (top) and around the pumptest area.*

A vertical east-west section that goes through the pump test volume is shown in Figure 4-4. There are several things to note in this figure. The grid is continues close to ground (top 80 metres) while at deeper levels the grid cells in "the good rock" have been removed. The grid cells at depth thus illustrate the fracture zones.

4.3.3 Boundary condition

The following points summarize the boundary conditions employed.

- At the lateral boundaries a hydrostatic pressure distribution is prescribed.
- The bottom boundary condition is of the zero flux type.
- At the top boundary pressure is prescribed below sea level, with an account of the water depth, while a free groundwater table is simulated above the sea level. The net recharge was set to 100 mm/year.

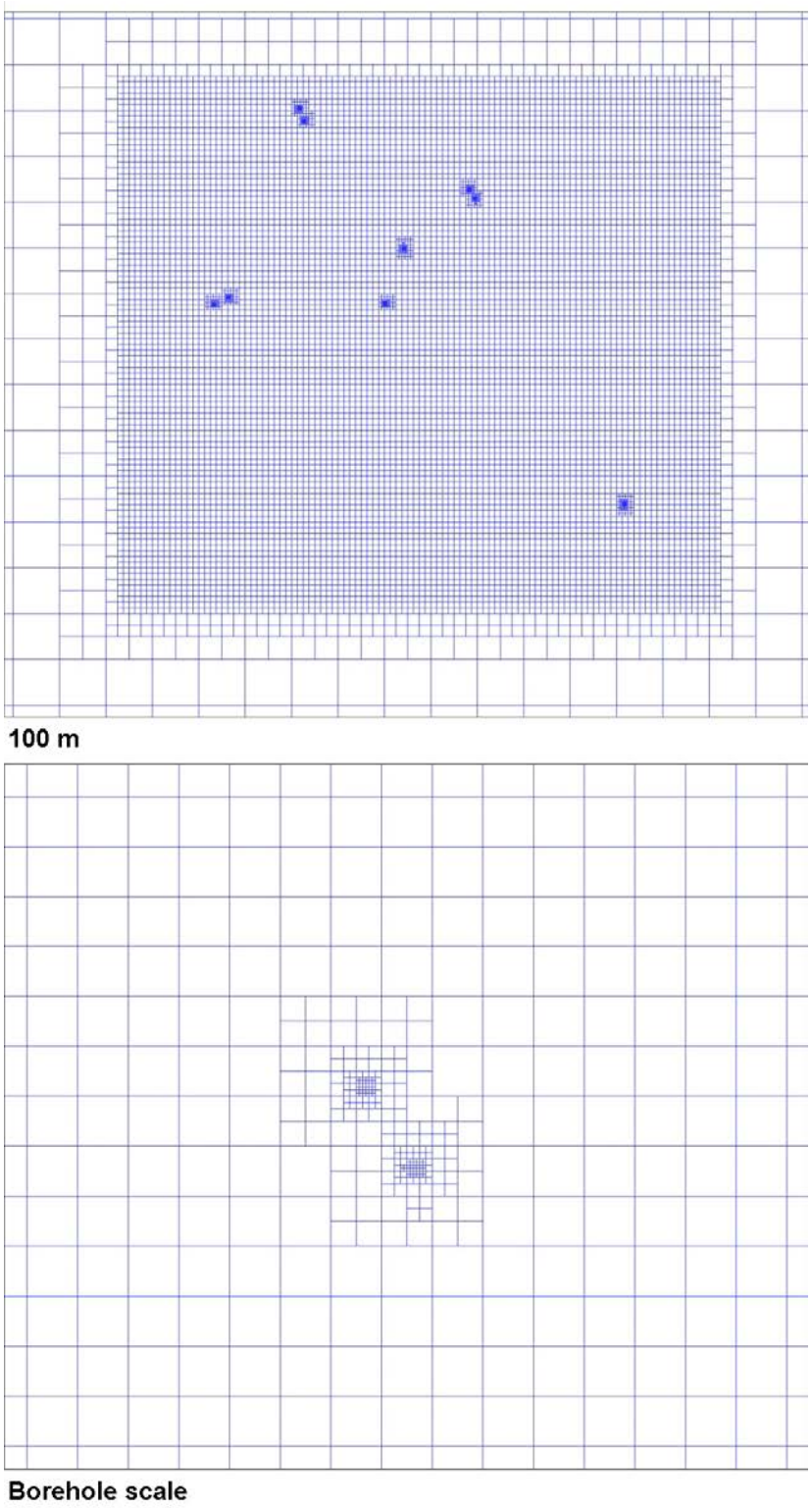

Figure 4-3. *Grid around boreholes.*

4.3.4 Summary of concepts

In Task 7B1 a request for a summary of concepts was formulated. A response to this request was given at a project meeting in Oxford, UK 2008-05-13. The PowerPoint presentation from this meeting is included as Appendix C.

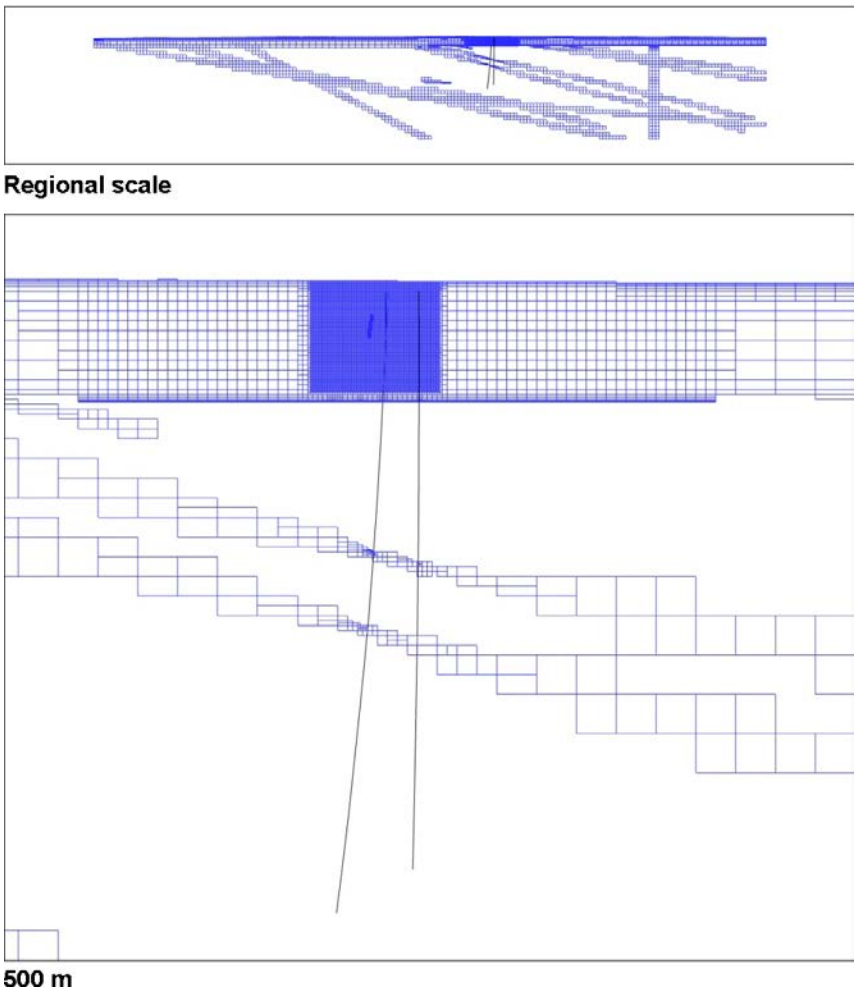

Figure 4-4. *Vertical sections.*

4.4 Results

4.4.1 Introduction

The number of simulation cases requested in the task description is quite extensive, as can be seen in Table 4-1. The cases labeled “Forward” are intended to be based on the provided data while the cases labeled “Inverse” should represent the result after calibration. However, due to time constraints, a somewhat modified approach to calibration was adopted in this work, details below.

During the project a New Structural Model (NSM) was introduced. The first set of simulations was hence first calculated with the Old Structural Model (OSM) and later updated. For the relatively small site where the pump tests were performed the difference between the NSM and the OSM is minor; the main change is that boreholes KR14 and KR15A are not in contact with any zones at depth (say deeper than 200–300 metres) in the NSM. In the present project the NSM was considered by simply eliminating these deep contacts.

However; some interesting effects were noted in the change of structural model and for this reason both models will be included in the presentation of results.

The task description also specifies the requested output from the simulations, so called Performance Measures (PM). These include heads and draw downs but also inflows/outflows along boreholes. The PM-data will be given in supplied spread sheets, for further compilation and analyzes by the task organizers. Some of these data will be repeated here.

4.4.2 Calibration

The calibration strategy is based on the following guidelines:

- The calibration carried out in Task 7A is kept with respect to large scale features (lakes, wetlands, etc).
- The interference test with open boreholes is used for a calibration of the local site.
- The pump tests with packed off boreholes are simulated in a forward manner i.e. no calibration is performed. This seems logical as the rock volume in questions is the same as for the open borehole tests (KR14–KR18).

The main calibration effort in this project thus concerns the pump test in open boreholes.

Table 4-1. Simulations suggested in the task description.

Name	Description	Boreholes	Purpose
SS20a	"Natural conditions"	No boreholes	Forward
SS21	"Natural conditions"	Boreholes are open and free to cross-flow	Calibration
SS22	"Natural conditions"	Boreholes are packed-off	Calibration
SS20b	"Natural conditions"	No boreholes	Based on calibrated models after SS21 & SS22
PA20c	"PA conditions"**	No boreholes	Forward
SS23a	Pumping in KR14	Boreholes are open and free to cross-flow	Forward (followed by …)
SS23b	Pumping in KR14	Boreholes are open and free to cross-flow	Calibration
SS24a	Pumping in KR14	Boreholes are packed-off	Forward (followed by …)
SS24b	Pumping in KR14	Boreholes are packed-off	Calibration
SS25a	Pumping in KR18	Boreholes are open and free to cross-flow	Forward (followed by …)
SS25b	Pumping in KR18	Boreholes are open and free to cross-flow	Calibration
SS26a	Pumping in KR18	Boreholes are packed-off	Forward (followed by …)
SS26b	Pumping in KR18	Boreholes are packed-off	Calibration
TS27***	Pumping in KR15	Boreholes are open and free to cross-flow	Forward
TS28***	Pumping in KR14	Boreholes are open and free to cross-flow except for one isolated flowing structures in other boreholes*	Forward
PA29	"PA conditions"**	No boreholes	Forward

* Tested flowing structures are to be specified at the planned work-shop for task 7B.

** The Boundary Conditions specified is defined below.

*** These test could first be done as steady-state and reported in a similar manner as the proposed SS simulations. Transient simulations could be done if times available or if the modeling groups prefer.

The pump test in open boreholes.

The pump test, see Figure 4-5, was carried out in 2001/2002 and is described in Koskinen and Rouhiainen (2007). The drawdown pattern is really puzzling and indicates hydraulic connections that need to be understood.

Note:

- Pumping 25 l/min in KR14 causes the same drawdown as pumping 5–7 l/min in A-holes.
- Pumping in A-holes causes a uniform drawdown in A-holes, but a lower drawdown in B-holes and KR14.
- The effect of pumping in A-holes is the same, irrespective of which hole is pumped.
- The response in KR17B is generally lower.

Suggested conceptual model.

The introduction of two horizontal sheet joints, see Figure 4-6, may explain the observed draw downs, qualitatively. One may also expect that the upper sheet joint has a higher transmissivity, as pumping in KR14 with 25 l/min does not cause any large draw downs.

- Casing depths are important, especially for KR14.
- Due to the lower sheet joint a uniform response is achieved.
- Due to the upper sheet joint a weak response in KR14 is expected when pumping in A-holes.
- Pumping 25 l/min in KR14 causes a weak effect in A-holes due to the upper sheet joint.
- KR17B is not connected.

More about the sheet joints

- Have been found in boreholes at the site.
- During a pump test we expect an outflow from nearby boreholes if the boreholes are well connected. From measurements we estimate the depths to 20 and 50 mbsl.
- Transmissivities in the range $10^{-5} \rightarrow 10^{-4}$ m^2/s can be expected.
- Hence, we introduce a rectangular sheet joint at 50 mbsl and a triangular (in order to exclude KR17B) sheet joint at 20 mbsl. Transmissivities from a calibration.

Sheet joints have been found at the Forsmark site; perhaps the existence of sheet joints in the upper part of the rock is the rule and not the exception?

Pumped borehole (l/min)	Drawdowns (m)								
	KR14	KR15 A, B		KR16 A, B		KR17 A, B		KR18 A, B	
KR14 (25)	6.0	3.4	4.4	3.0	3.0	3.0	0.2	3.0	5.6
KR15 A (6.7)	1.0	10.0	2.0	3.5	2.4	3.0	1.0	3.2	1.3
KR16 A (5.9)	0.9	3.3	1.0	10.0	1.7	3.4	0.4	3.7	0.9
KR17 A (7.7)	1.0	3.5	2.0	3.9	1.5	11.0	0.2	3.7	0.9
KR18 A (5.3)	0.8	3.5	0.9	3.5	1.5	3.2	0.2	10.0	0.8

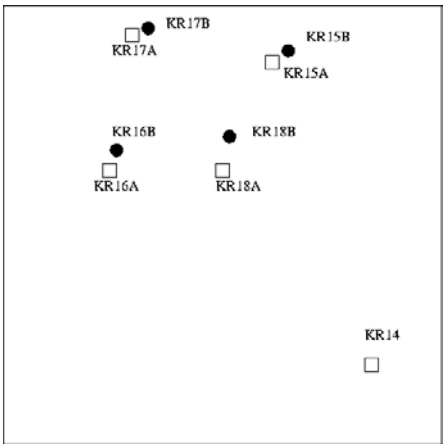

Figure 4-5. *The measured draw downs (top) and position of boreholes. In the table the left column gives the pumped borehole.*

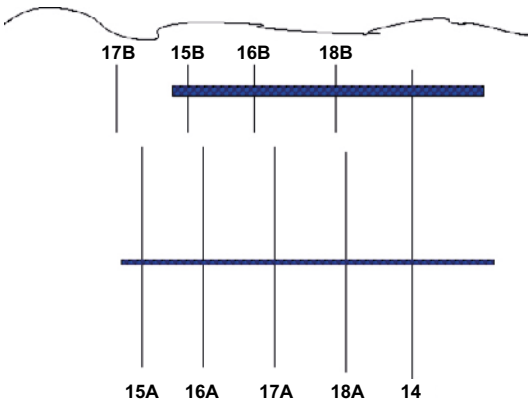

Figure 4-6. *Two horizontal sheet joints.*

Background fracture network (DFN).

- Power law intensity and length distribution.

$$n = \frac{\alpha}{a-1}\left(l_{\min}^{-a+1} - l_{\max}^{a+1}\right)$$

$l_{\min} = 5,\ l_{\max} = 100,\ a = 3.6$ and $\alpha = 0.2$

- Transmissivity law: $T = 10^{-5}\ (l/100)^2$.
- Sub horizontal.
- The network is generated down to 60 mbsl (fracture centres) and may hence reach down to about 80 mbsl.

The power law parameters are explained in and found from Task 6F2 (Svensson 2006a). Also the *T-l* relation is discussed in this report.

Calibration strategy and conditions

The strategy suggested in the Task Description (forward, calibrate, new pump tests,.....) not considered the best approach. Instead we should look for a way to satisfy the following conditions simultaneously:

- The groundwater table should be correct (lakes, wetlands, etc). In the area of the pump test a level of 6–7 m is expected.
- The DFN should show the right frequency of HPF (High Permeability Features), i.e. number of fractures per 100 m with a T-value greater than 10^{-6}, 10^{-7}, etc m^2/s. Different realisations should be tested.
- The interference test should be used to find the transmissivities of the two sheet joints.

If the two sheet joints provide a solution to the puzzling pump tests, it is realized that it is not possible to consider one test after the other as a calibration strategy.

Calibration procedure and results

In order to meet all conditions simultaneously it is important to find the interdependency between different conditions. The following procedure was adopted.

- The surface hydrology part was kept from Task 7A as it produces the right water table.
- The DFN parameters were briefly evaluated and it was found that the “standard values” produce the right HPF statistics. Different realisations did not produce a big difference and the choice of the realisation could be left as a “fine tuning”.
- The transmissivity of the lower sheet joint was evaluated by simulate pumping in KR15A and KR18A. A $T = 10^{-5}$ m^2/s was found to work. The pump test in KR14 was used to evaluate the upper sheet joint: $T = 2.2\times10^{-4}$ m^2/s is a good value. See Table 4-2.

The final part of the procedure is to evaluate three realisations of the DFN and choose one. From Table 4-2 we find that the draw downs are not very sensitive and that realization three is the best one.

The results for “No pumping” are not very sensitive to DFN realisations see Table 4-3. We choose number three as the best and all the following results are based on this realisation. The heads for “no pumping” are needed as a reference for draw downs but are also of interest as a validation; the levels are in general agreement with field data. Regarding the HPF result one should note that it is more important to get the condition $T > 10^{-6}$ m^2/s right than the $T > 10^{-7}$ m^2/s condition.

Results, the complete interference test.

The agreement is very good, see Table 4-4, and needs no further comments. The pump tests KR16A and KR17A were not part of the calibration and are in this sense “forward predictions”.

Table 4-2. Results , the interference test. The draw downs due to pumping in KR14, KR15A and KR18A are shown for three realisations of the DFN. It is clear that the result is not very sensitive to the DFN realisation used. As a simple measure of the realisation the draw downs were summed up; other, and perhaps better, measures could be used.

Borehole KR14 pumped (25 l/min)	Measured ΔH	Simulated ΔH		
		Real .1	Real .2	Real .3
KR14	6.0	6.3	6.6	6.7
KR15A	3.4	3.4	3.4	3.1
KR15B	4.4	4.6	4.8	4.0
KR16A	3.0	3.6	3.8	3.7
KR16B	3.0	4.5	4.7	4.8
KR17A	3.0	3.6	3.7	3.5
KR17B	0.2	2.7	2.8	2.6
KR18A	3.0	3.8	3.9	3.7
KR18B	5.6	4.7	4.9	5.0
	31.6	37.2	38.6	37.1
Borehole R15A pumped (6.7l/min)	**Measured ΔH**	**Simulated ΔH**		
		Real .1	**Real .2**	**Real .3**
KR14	1.0	0.9	0.9	0.9
KR15A	10.0	6.6	8.4	8.6
KR15B	2.0	0.9	0.8	0.8
KR16A	3.5	2.6	2.6	2.6
KR16B	2.4	0.9	0.7	0.7
KR17A	3.0	3.0	3.1	3.1
KR17B	1.0	0.5	0.5	0.4
KR18A	3.2	3.1	3.3	3.3
KR18B	1.3	0.9	0.8	0.7
	27.4	19.4	21.1	21.1
Borehole KR18A pumped (5.3 l/min)	**Measured ΔH**	**Simulated ΔH**		
		Real .1	**Real .2**	**Real .3**
KR14	0.8	0.8	0.8	0.8
KR15A	3.5	2.4	2.6	2.7
KR15B	0.9	0.8	0.7	0.7
KR16A	3.5	3.2	4.0	3.9
KR16B	1.5	0.8	0.7	0.7
KR17A	3.2	3.3	4.0	4.1
KR17B	0.2	0.5	0.5	0.3
KR18A	10.0	7.5	11.1	10.2
KR18B	0.8	0.8	0.7	0.7
	24.4	20.1	25.1	24.1

Table 4-3. Results, the interference test. The heads for no pumping (used as a reference for drawdowns) and the HPF statistics for three realisations.

Borehole	Heads for "no pumping"		
	Real. 1	Real. 2	Real. 3
KR14	6.4	6.3	6.3
KR15A	5.6	5.4	5.4
KR15B	6.5	6.5	6.5
KR16A	6.2	6.3	6.3
KR16B	6.5	6.5	6.5
KR17A	6.2	6.2	6.2
KR17B	6.6	6.6	6.7
KR18A	6.2	6.1	6.2
KR18B	6.5	6.5	6.5

Number of fractures per 100 m	Measured	Calculated		
		Real. 1	Real. 2	Real. 3
$T > 10^{-6}$ m^2/s	6	8.2	6.5	6.3
$T > 10^{-7}$ m^2/s	20	11.1	10.0	10.1

Table 4-4. Measured and simulated draw downs. Black indicates measured draw downs, red simulated.

	KR14	KR15 A, B		KR16 A, B		KR17 A, B		KR18 A, B	
KR14	6.0 6.7	3.4 3.1	4.4 4.0	3.0 3.7	3.0 4.8	3.0 3.5	0.2 2.6	3.0 3.7	5.6 5.0
KR15 A	1.0 0.9	10.0 8.6	2.0 0.8	3.5 2.6	2.4 0.7	3.0 3.1	1.0 0.4	3.2 3.3	1.3 0.7
KR16 A	0.9 0.9	3.3 2.4	1.0 0.8	10.0 13.7	1.7 0.8	3.4 4.5	0.4 0.5	3.7 4.3	0.9 0.8
KR17 A	1.0 1.1	3.5 3.5	2.0 1.0	3.9 5.9	1.5 0.9	11.0 17.5	0.2 0.6	3.7 5.9	0.9 1.0
KR18 A	0.8 0.8	3.5 2.7	0.9 0.7	3.5 3.9	1.5 0.7	3.2 4.1	0.2 0.3	10.0 10.2	0.8 0.7

4.4.3 The new structural model

The new structural model calls for a re-calibration of the open borehole pump test.

Re-calibration of interference test

After a few tests the following modification was adopted:

$$T = 1.0\times10^{-5}\left(\frac{l}{100}\right)^2 \text{ was replaced by } T = 1.5\times10^{-5}\left(\frac{l}{100}\right)^2$$

for the stochastic fracture network.

The pump test is now well simulated using the new structural model, see Table 4-5.

Both structural models were tested in simulations of flow along boreholes, see Table 4-6.

Discussion

- The draw downs are well predicted after the update.
- Flow along boreholes for “No pumping” changes dramatically, see Table 4-6. For KR14 and KR15A the flow is reduced as expected. However for other boreholes the flow is also significantly reduced and is now smaller than the measured values. A suggestion is that this is due to the uniform head that results from the update, see Table 4-7.

Perhaps we need to resolve the topography better in order to create head differences on the decimetre scale.

Table 4-5. The re-calibrated interference test. Black indicates measured draw downs, red simulated.

	KR14	KR15 A, B		KR16 A, B		KR17 A, B		KR18 A, B	
KR14	6.0 6.8	3.4 4.0	4.4 4.9	3.0 3.9	3.0 4.7	3.0 3.7	0.2 2.5	3.0 3.9	5.6 4.9
KR15 A	1.0 1.0	10.0 14.3	2.0 1.0	3.5 3.8	2.4 0.9	3.0 4.5	1.0 0.5	3.2 5.0	1.3 0.9
KR16 A	0.9 0.9	3.3 3.3	1.0 0.8	10.0 13.5	1.7 0.8	3.4 4.3	0.4 0.5	3.7 4.3	0.9 0.8
KR17 A	1.0 1.1	3.5 5.2	2.0 1.0	3.9 5.6	1.5 1.0	11.0 16.5	0.2 0.6	3.7 6.0	0.9 1.0
KR18 A	0.8 0.8	3.5 3.9	0.9 0.7	3.5 3.8	1.5 0.7	3.2 4.1	0.2 0.4	10.0 10.0	0.8 0.7

Table 4-6. Results, flow along boreholes. Measured (black), simulated before update (red) and simulated after update (blue).

	No pumping				KR14 pumping				KR18 pumping			
Borehole	**Max inflow l/h**		**Max outflow l/h**		**Max inflow l/h**		**Max outflow l/h**		**Max inflow l/h**		**Max outflow l/h**	
KR14	3		2		784		–		13		21	
	60	1	55	2	960	960	–		114	54	60	50
KR15A	3		3		13		14		15		13	
	30	0.1	35	0.1	7	1	10	1	20	4	16	6
KR15B	3		3		16		15		12		11	
	1	0.2	1	0.1	15	13	30	30	7	12	9	12
KR16A	1		0.5		2		1		2		1	
	0.6	0.04	0.9	0.05	0.3	3	0.4	2	4	5	9	9
KR16B	1		0.8		3		4		4		2	
	2	0.4	3	0.4	27	23	40	39	6	4	6	7
KR17A	4		5		8		6		12		17	
	0.6	0.2	0.4	0.2	4	2	2	3	7	4	4	7
KR17B	–		–		–		–		–		–	
	0.6	0.02	0.5	0.02	8	7	7	6	2	1	2	0.8
KR18A	0.2		0.6		2		3		238		–	
	0.4	0.04	0.4	0.04	2	1	2	1	288	288	–	
KR18B	3		3		21		33		2		3	
	3	0.2	3	0.2	31	27	31	27	7	4	7	4

Table 4-7. Heads for “no pumping” before and after the update of structural model.

	KR14	KR15A	KR15B	KR16A	KR16B	KR17A	KR17B	KR18A	KR18B
Before update	6.3	5.4	6.5	6.3	6.5	6.2	6.7	6.2	6.5
After update	6.91	6.89	6.91	6.90	6.92	6.88	6.87	6.89	6.91

The large scale results.

It was earlier stated that the results from Task 7A ought to ensure that lakes and wetlands are well predicted. Figure 4-7 shows that a realistic ground water table is predicted also after the calibration studies carried out in Task 7B.

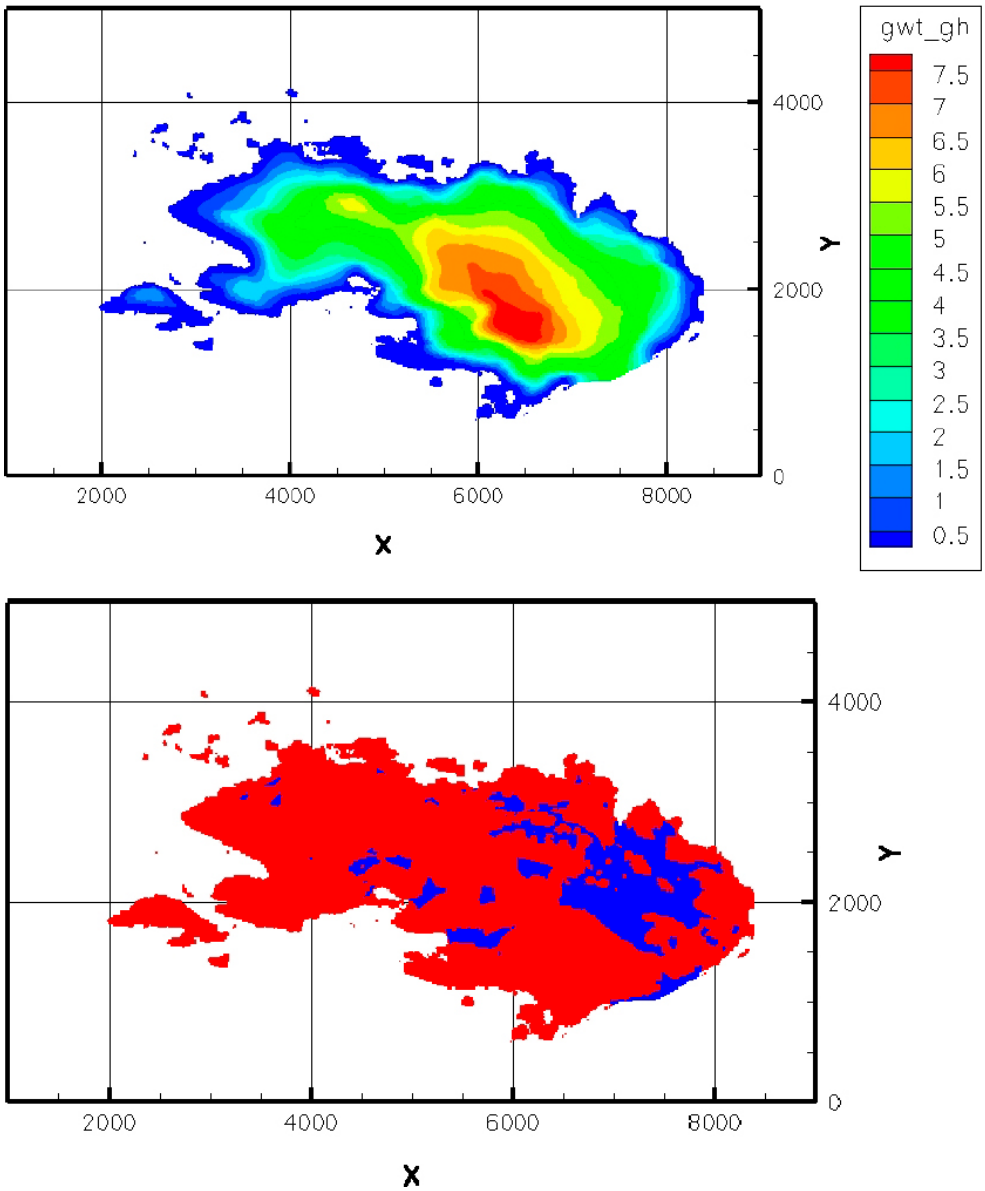

Figure 4-7. *Groundwater table for virgin conditions (top) and “wet areas” (blue).*

4.4.4 The pump test with packed off sections

As mentioned earlier this pump test is carried out as a forward simulation, i.e. we do not include any calibration phase.

The positions of the packers were given in the Task Description and are here included as Table 4-8. Also the casing depth is given for each borehole.

Table 4-8. Packed-off intervals and observations during pressure response tests in 2004 (note: some observations have been continued after tests as a part of long-term monitoring)

Drillhole	Note	Code of obs. Interval (GWMS)	Sec. up	Sec. down	Observations
KR14	casing 0–9.52 m	L3	9.52	46	13.10 – 14.12. 2004
KR14		L2	47.5	52.5	
KR14		L1	53.5	514.1	
Drillhole	**Note**	**Code of obs. Interval (HTU)**	**Sec. up**	**Sec. down**	**Observations**
KR14		L3	9.52	46.5	28.9. – 11.10. 2004
		L2	47.5	52.5	
		L1	53.5	514.1	
Drillhole	**Note**	**Code of obs. Interval (GWMS)**	**Sec. up**	**Sec. down**	**Observations**
KR15	casing 0–39.98 m	L6	40	50	8.9. – 31.12. 2004
KR15		L5	51	65	
KR15		L4	66	75	
KR15		L3	116	145	
KR15		L2	241	245	
KR15		L1	446	460	
Drillhole	**Note**	**Code of obs. Interval (GWMS)**	**Sec. up**	**Sec. down**	**Observations**
KR15B	casing 0–4.48 m	L2	4.5	28.7	8.9. – 31.12. 2004
KR15B		L1	29.7	45	
Drillhole	**Note**	**Code of obs. Interval (GWMS)**	**Sec. up**	**Sec. down**	**Observations**
KR16	casing 0–40.23 m	L6	40	52	10.9. – 14.12. 2004
KR16		L5	53	62	
KR16		L4	63	82	
KR16		L3	83	112	
KR16		L2	113	142	
KR16		L1	143	170.2	
Drillhole	**Note**	**Code of obs. Interval (GWMS)**	**Sec. up**	**Sec. down**	**Observations**
KR16B		L3	4.5	25	10.9. – 14.12. 2004
KR16B	casing 0–4.48 m	L2	26	35	
KR16B		L1	36	45	
Drillhole	**Note**	**Code of obs. Interval (GWMS)**	**Sec. up**	**Sec. down**	**Observations**
KR17	casing 0–39.92 m	L6	40	51	9.9. – 9.11. 2004
KR17		L5	52	66	
KR17		L4	67	71	
KR17		L3	82	96	
KR17		L2	97	111	
KR17		L1	122	157.13	
Drillhole	**Note**	**Code of obs. Interval (GWMS)**	**Sec. up**	**Sec. down**	**Observations**
KR17B	casing 0–4.1 m	L2	4.1	30.3	9.9. – 22.11. 2004
KR17B		L1	31.3	45	
Drillhole	**Note**	**Code of obs. Interval (GWMS)**	**Sec. up**	**Sec. down**	
KR18	casing 0–39.81 m	L5	40	53	10.9. – 27.9. 2004 + 11.11. – 31.12. 2004
KR18		L4	54	58	
KR18		L3	59	63	
KR18		L2	74	83	
KR18		L1	89	125.49	
Drillhole	**Note**	**Code of obs. Interval (GWMS)**	**Sec. up**	**Sec. down**	
KR18B	casing 0–6.51 m	L2	6.51	22.7	10.9. – 31.12. 2004
KR18B		L1	23.7	45	

Two pump tests were simulated in this set-up; pumping 25 l/min in KR14 and pumping 5.3 l/min in KR18. First the natural, or undisturbed, pressure in each section was calculated and after that the pumped condition was calculated. All results are summarized in Table 4-9, where also the measured draw downs are found. A fair agreement between measured and simulated draw downs is found.

Table 4-9. Pump test with packed off sections.

	Pumping KR14				Pumping KR18				Comments
			ΔH				ΔH		
Bh	P_{NAT}	P	Simulated	Measured	P_{NAT}	P	Simulated	Measured	
KR14 L3	6.9	0.3	6.6	6.8	6.91	6.13	0.8	0.6	
L2					6.92	5.48	1.4	0.7	
L1					6.92	5.05	1.9	2.8	
KR15 L6	6.90	2.88	4.0	5.6	6.89	4.05	2.8	0.9	
A L5	6.90	3.04	3.9	3.5	6.89	2.12	4.8	3.6	
L4	6.86	3.52	3.3	3.4	6.82	3.11	3.7	3.5	
L3	–	–	–	1.5	–	–	–	0.3	
L2		–	–	–	–	–	–	–	
L1		–	–	–	–	–	–	–	
KR15 L2	6.91	3.6	3.3	4.7	6.90	6.31	0.6	0.6	
B L1	6.90	2.87	4.0	5.7	6.89	4.12	2.8	0.9	
KR16 L6	6.91	3.05	3.9	3.2	6.86	3.53	3.3	3.3	
A L5	6.91	3.11	3.8	3.2	6.90	2.12	4.8	3.7	
L4	6.90	4.06	2.8	2.4	6.89	3.75	3.1	3.9	
L3	6.81	4.02	2.8	2.1	6.89	3.93	3.0	2.2	
L2	–	–	–	0.9	–	–	–	0.5	
L1	–	–	–	0.5	–	–	–	0.3	
KR16 L3	6.94	4.40	2.5	–	6.94	6.50	0.4	–	No measurement
B L2	6.92	2.35	4.6	3.3	6.91	6.14	0.8	1.0	
L1	6.91	3.9	3.9	3.3	6.85	3.54	3.3	3.1	
KR17 L6	6.86	3.57	3.3	3.2	6.85	3.74	3.1	3.4	
A L5	6.88	3.30	3.6	3.2	6.88	2.10	4.8	3.4	
L4	6.86	3.60	3.3	3.3	6.85	2.75	4.1	3.0	
L3	6.85	3.89	3.0	1.3	6.84	3.33	3.5	1.2	
L2	6.84	3.96	2.9	1.3	6.84	3.45	3.4	1.2	
L1		–	–	0.4	–	–	–	–	
KR17 L2	6.88	4.53	2.4	1.7	6.87	6.42	0.5	0.5	
B L1	6.86	3.8	3.1	3.3	6.85	4.82	2.0	2.8	
KR18 L5	6.91	2.96	4.0	3.2	6.89	–3.72	10.6	8.1	
A L4	6.90	3.08	3.8	3.4	–	–	–	–	
L3	6.90	3.09	3.8	3.4	–	–	–	–	
L2	6.88	3.58	3.3	2.5	–	–	–	–	
L1	6.88	3.68	3.2	2.7	–	–	–	–	
KR18 L2	6.95	6.27	0.7	5.4	6.95	6.80	0.2	0.7	
B L1	6.91	2.15	4.8	6.1	6.91	6.10	0.8	0.8	

4.4.5 Transport pathways

The final case listed in Table 4-1 concerns transport pathways under Performance Assessment (PA) conditions. No boreholes should be present and we hence base the simulations on case SS20b. Particles are to be released in a rectangular area at a depth of 100 mbsl. However, in the present model we do not have a continuous grid at this depth and it is hence not possible to use this location. Instead particles were released in an area with down-going flow at a depth of 10 mbls. The area is a rectangle at *x*: 5,815–5,830 m and *y*: 2,405–2,420 m.

The result of the simulation is shown in Figure 4-8. All particles moved north, and most end up beneath the Baltic Sea. Considering that the island generates a higher than ambient pressure due to the groundwater table, it is not surprising to find this result. However the pressure gradient below the Baltic Sea will decrease with distance from the shore which means that the particles will move slower and slower.

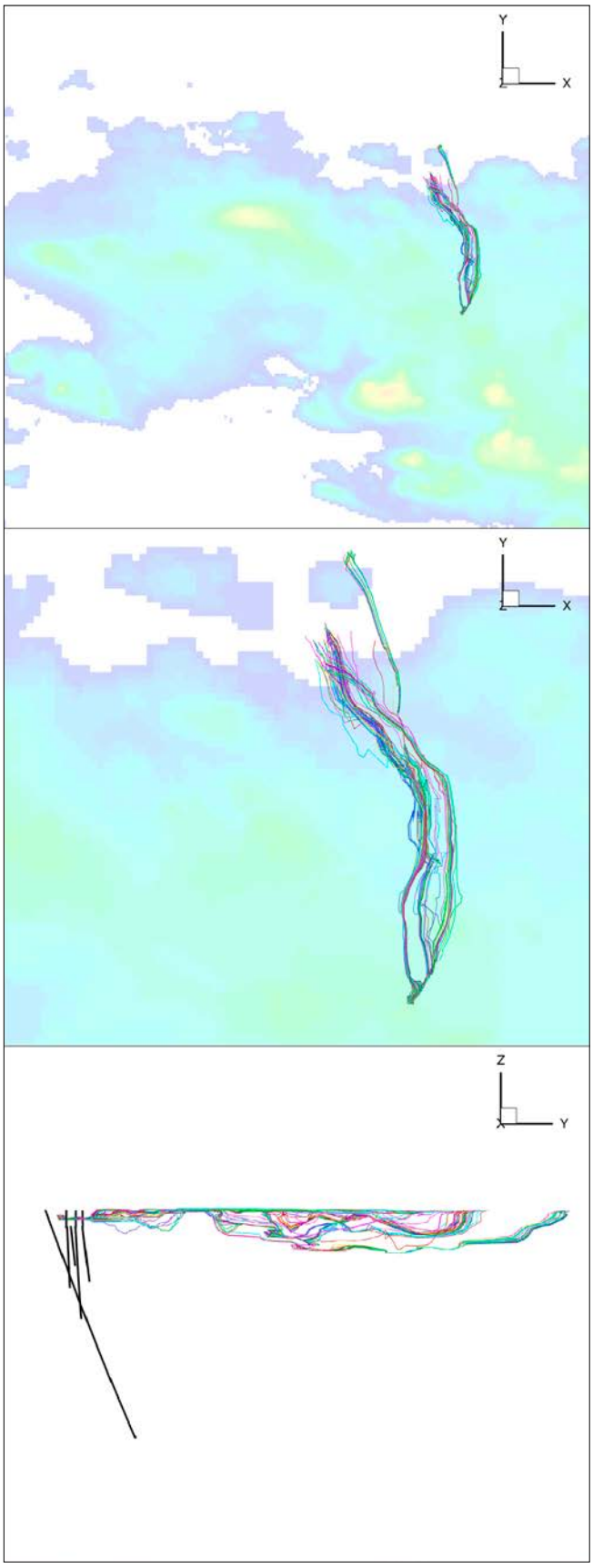

Figure 4-8. *Trajectories. Large scale horizontal view (top) enlargement (middle) and a vertical south-north section.*

4.4.6 Some additional results

In this section some results concerning flow along and across boreholes will be presented.

In Table 4-6 above the maximum inflow and outflow to boreholes were given. The reason for presenting results that way was that comparisons with field measurements could be carried out. In Figures 4-9 to 4-11 the flow along boreholes is presented in a somewhat different manner; now all inflows/outflows with position along the borehole can be studied. The three figures represent "No pumping", "Pumping in KR14" and "Pumping in KR18", all for open boreholes and the new structural model. When studying these figures one should note that the curve should start at zero and end at zero when the borehole is not pumped. For pumped boreholes (KR14 and KR18) the total flow along the borehole is equal to the pump rate (25 and 5.2 l/min, respectively).

Next we show some very preliminary results concerning flow across boreholes, see Table 4-10 and Figure 4-12. Only results for natural conditions (no boreholes) and the two sheet joints are discussed. It is hence assumed that the flow across a certain cross-sectional area is the same whether the borehole is present or not. The results were obtained using the old structural model and may hence be somewhat modified if the new structural model is used. The flow pattern in Figure 4-12 indicates that random fractures are crossing the sheet joint.

The flow pattern in Figure 4-12 is somewhat explained by the visualization of the fracture network shown in Figure 4-13.

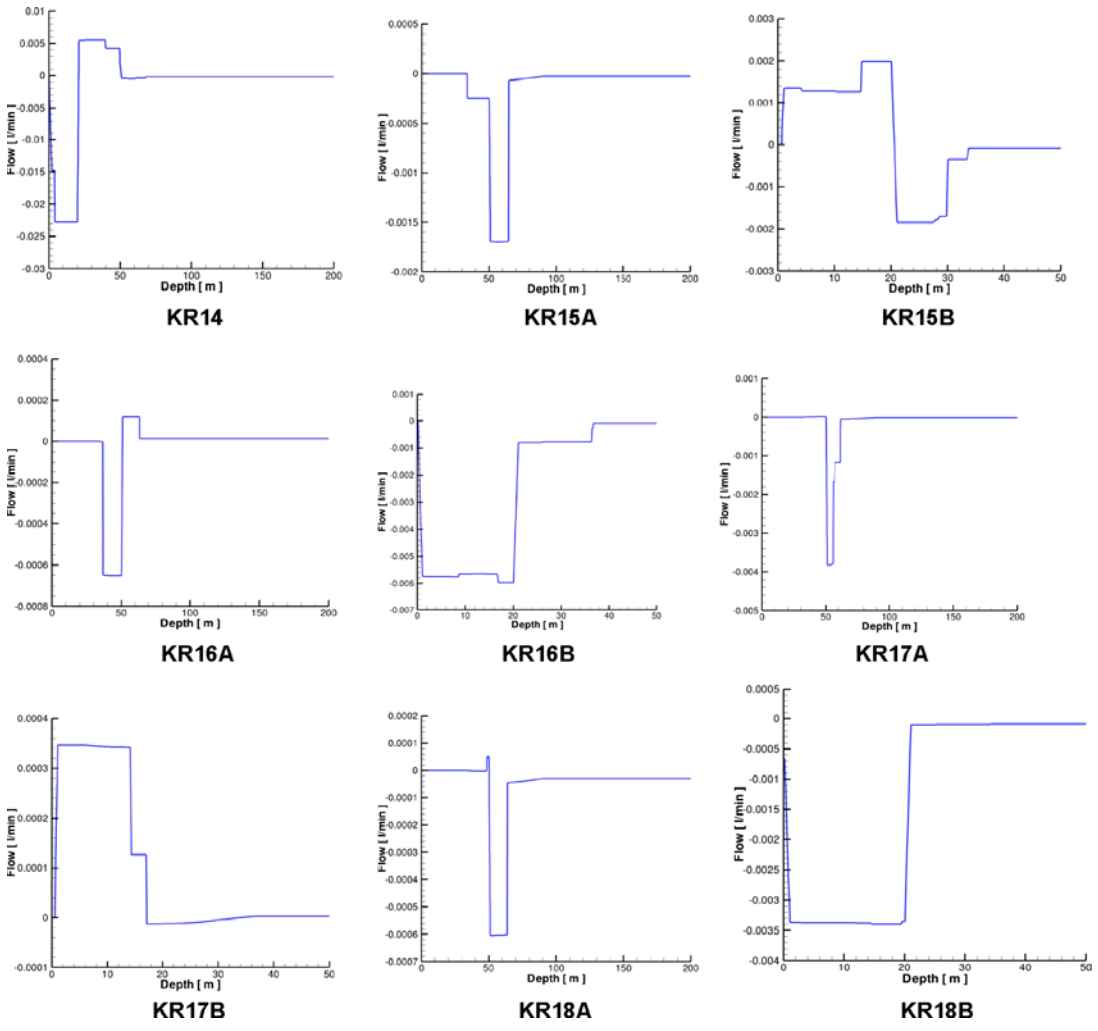

Figure 4-9. *Flow along boreholes. No pumping.*

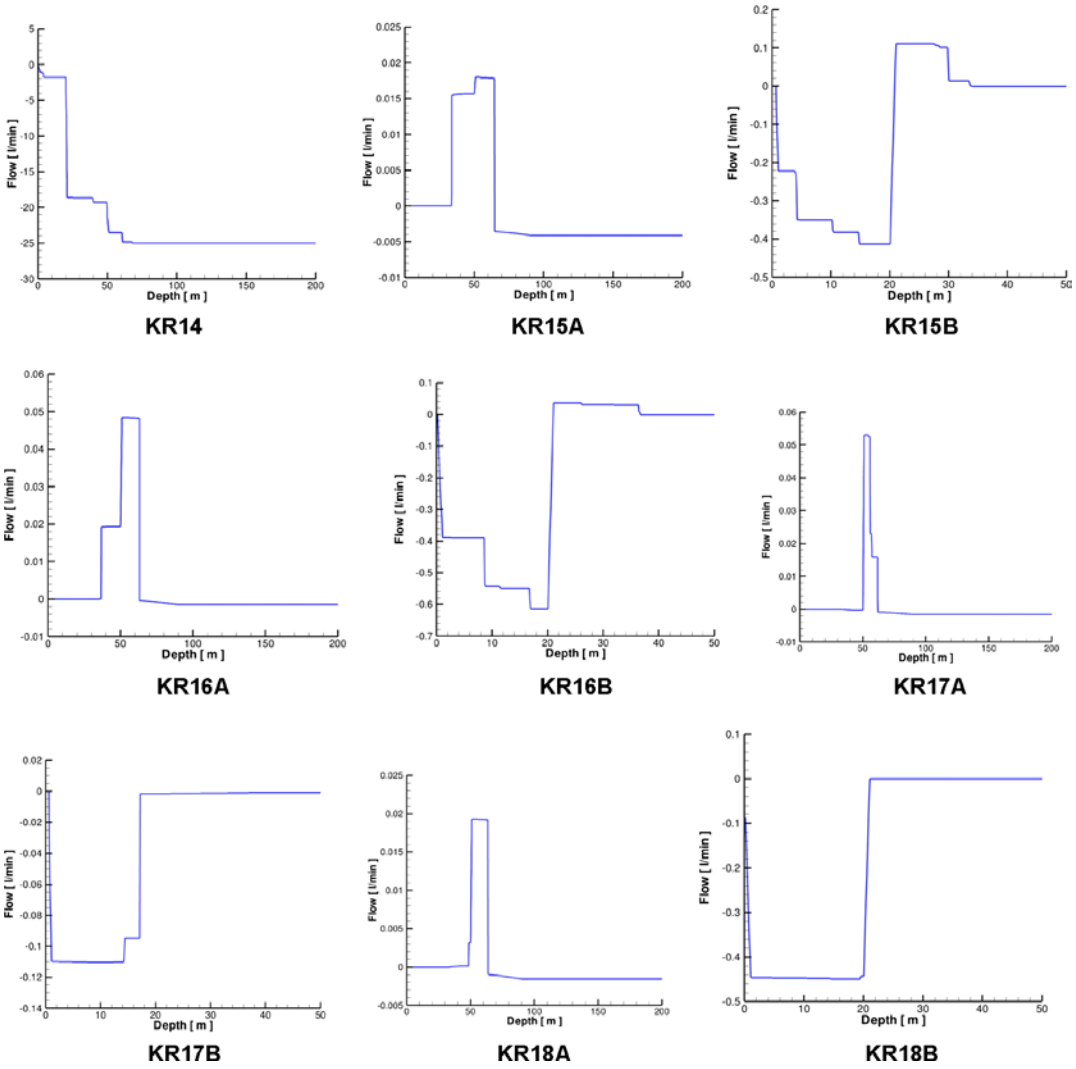

Figure 4-10. *Flow along boreholes. Pumping in KR14.*

Table 4-10. Flow across boreholes.

Borehole	Flux [l/min]
KR14	2.0×10^{-5}
KR15A	2.8×10^{-5}
KR16A	1.4×10^{-5}
KR17A	2.8×10^{-5}
KR18A	4.3×10^{-5}

Sheet joint at 50 mbsl

Borehole	Flux [l/min]
KR14	1.1×10^{-4}
KR15B	2.3×10^{-4}
KR16B	2.8×10^{-4}
KR17B	0
KR18B	2.1×10^{-4}

Sheet joint at 20 mbsl.

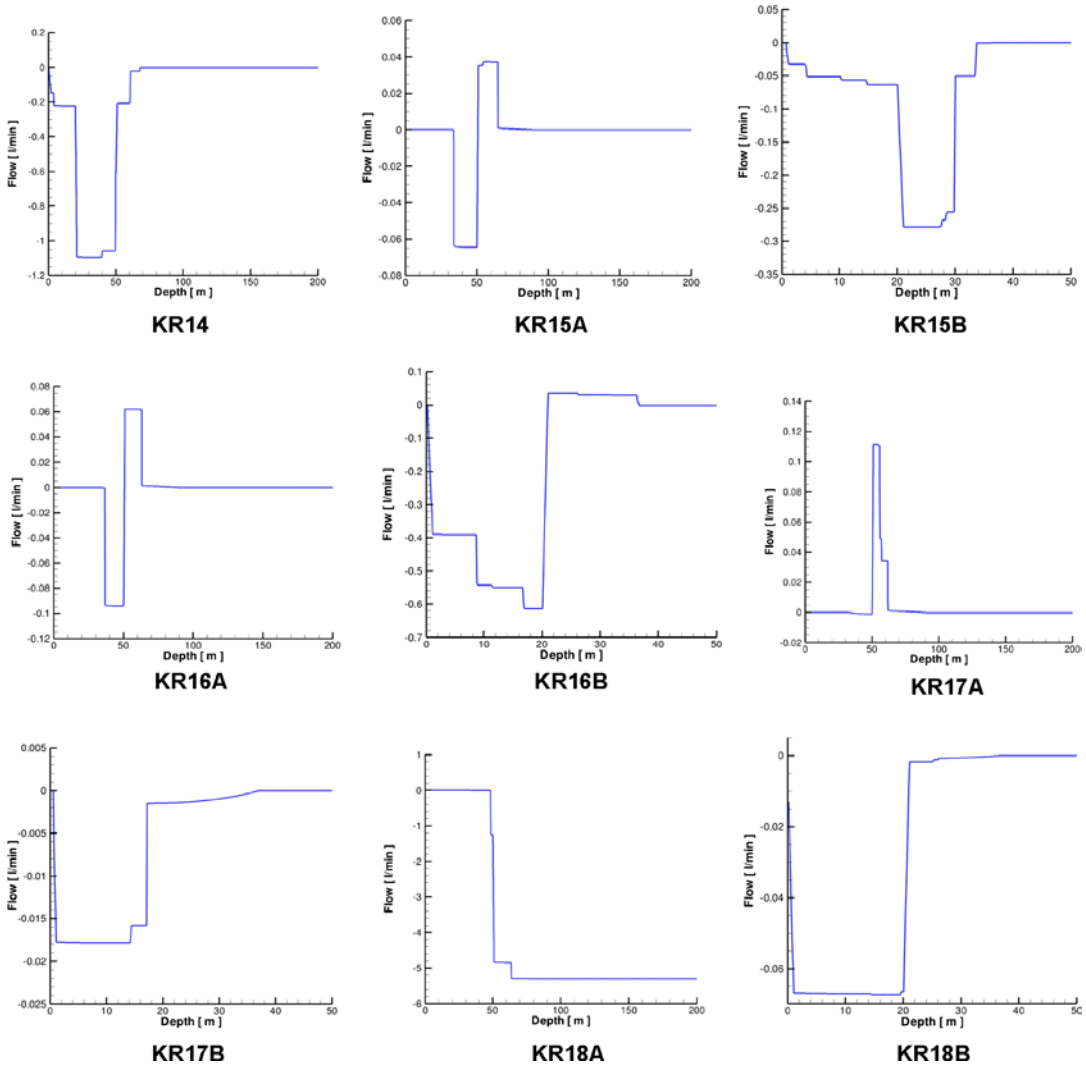

Figure 4-11. *Flow along boreholes. Pumping in KR18.*

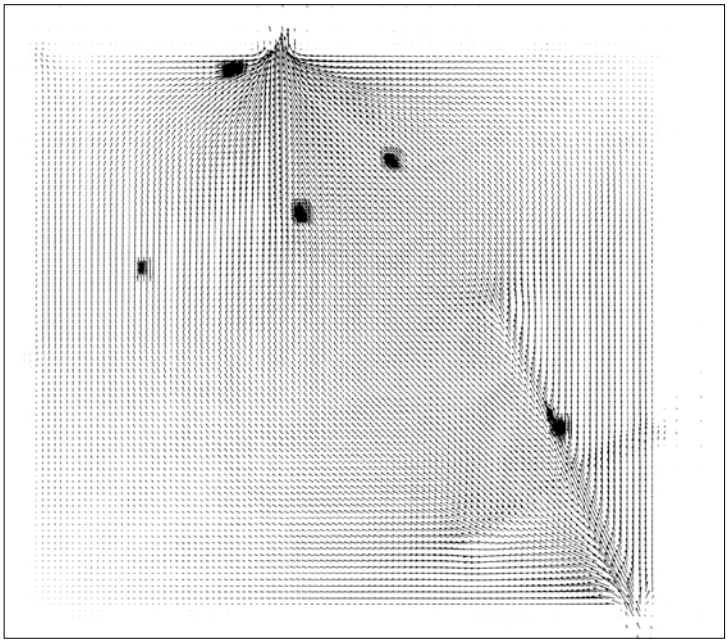

Figure 4-12. *Flow across the sheet joint at 50 mbsl.*

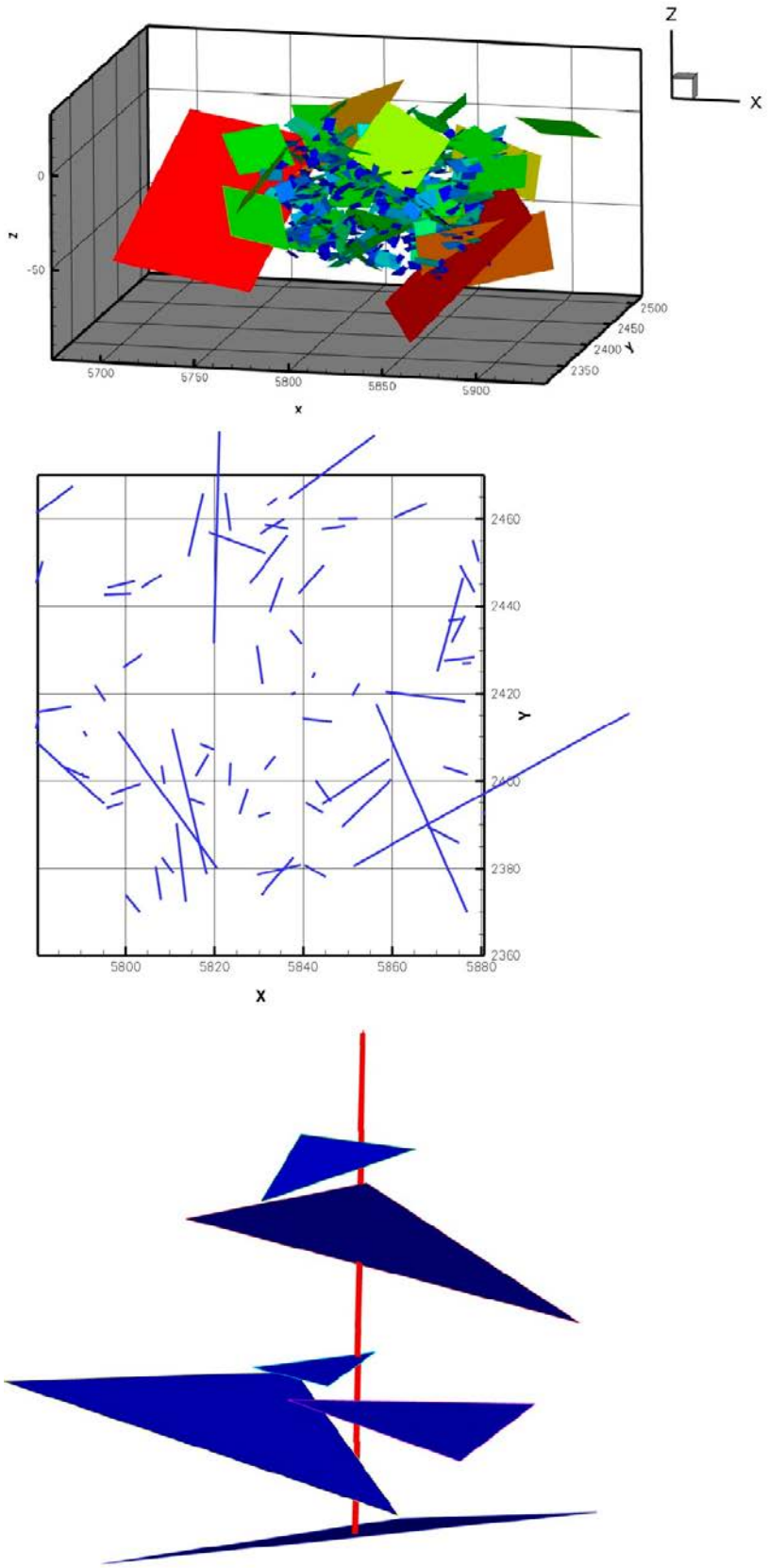

Figure 4-13. *Visualization of the fracture network. A 3D (top), 2D (middle) and 1D (bottom) view of the random part of the fracture network. The 2D view is at 50 metres depth and hence at the lower sheet joint.*

4.5 Discussion

The following points are brought up:

- In the task description it is suggested that the work should be developed by a series of “Forward” and “Calibration” exercises, considering one pump test at the time. This strategy has not been followed in this report. Instead a conceptual idea (the two sheet joints) was developed and introduced. It seems that this method has been successful and good results for both the open and pack-off pump tests have been obtained.
- A new structural model was introduced during the course of the work. It is interesting to note that good draw downs could be obtained for both models, while the flow along boreholes was very different. The comparison with measured flow along boreholes is hence valuable when testing the structural models.

4.6 Concluding remarks

- Good simulations of the pump tests in KR14 to KR18 have been achieved.
- Flow along boreholes provides a new and interesting way of comparing simulations with field data.

5 Task 7C

5.1 Introduction

5.1.1 Background

Task 7 progresses from large scale to smaller; in Task 7C the computational domain is a ventilation shaft and we are hence considering the metre scale.

Three single fractures of low transmissivity have been characterized by various methods and pump tests. The available data will be used to develop a micro structural model, which can be implemented in a numerical simulation model.

The three fractures were selected because they represent a class of low transmissivity fractures which are important for performance assessment, yet have only limited characterization using conventional hydrogeologic test methods. The Task 7C fractures are estimated to have transmissivity values of approximately 1×10^{-9}, 1×10^{-10}, and 1×10^{-11} m^2/s.

5.1.2 Objectives

The objectives of Task 7C are:

- To use PFL to characterise and analyse procedures to quantitatively describe low transmissive fractures.
- And to demonstrate procedures of characterisation of flow in fractures of transmissivity less than 1×10^{-9} m^2/s.

5.1.3 Outline

The first step was to evaluate different ways to generate heterogeneous fractures; this work is found in Appendix D.

After a decision about the appropriate way to generate a heterogeneous fracture, the model was tested by applying it to single hole pump tests in three shafts called KU1, KU2 and KU3.

The final step was to study the inflow distribution to one of the shafts (KU2).

5.2 Site and data

The three shafts (KU1, KU2 and KU3) are located in the ramp area of the tunnel, see Figure 5-1. Pump tests were carried out as single hole pump tests before excavation; draw downs and flow rates are summarized in Figure 5-2. These data will be used to evaluate a micro structural model

After the excavation the inflow distributions due to fractures that cross shaft KU2 were measured. Here we will focus on the inflow due to Fracture one, see Figure 5-3. As one can expect that the number of inflow spots is related to the correlation length of the fracture heterogeneity, we will use these data to evaluate this aspect of the micro structural model.

5.3 Numerical model

5.3.1 Introduction

The computational domain is a circle with radius 15 m. In this domain a single heterogeneous fracture is first generated. In a second step a discrete fracture network, with fracture lengths in the interval 0.1 → 30 m, is generated and all fractures in contact with the single fracture are kept and allowed to modify the local properties of the single fracture. Fracture crossings will hence form conductive paths.

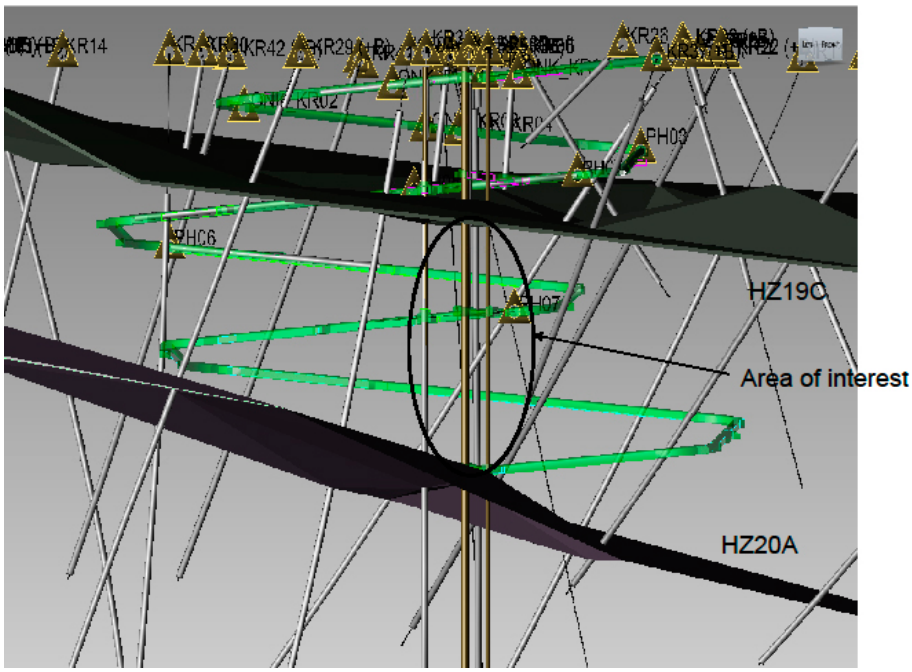

Figure 5-1. *Illustration of the setting of the Task 7C volume.*

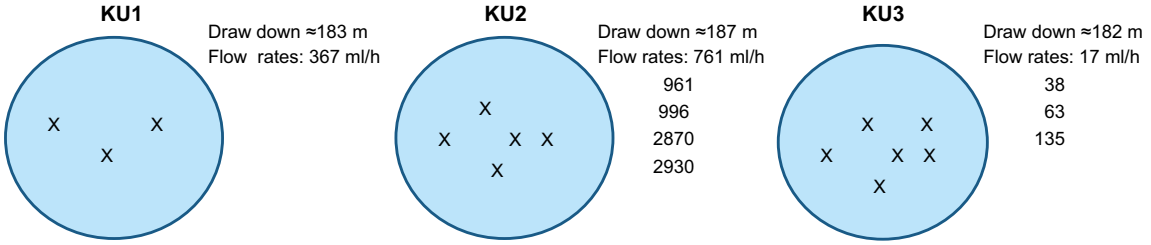

Figure 5-2. *A brief summary of the experimental data concerning the simple hole pump tests in KU1, KU2 and KU3.*

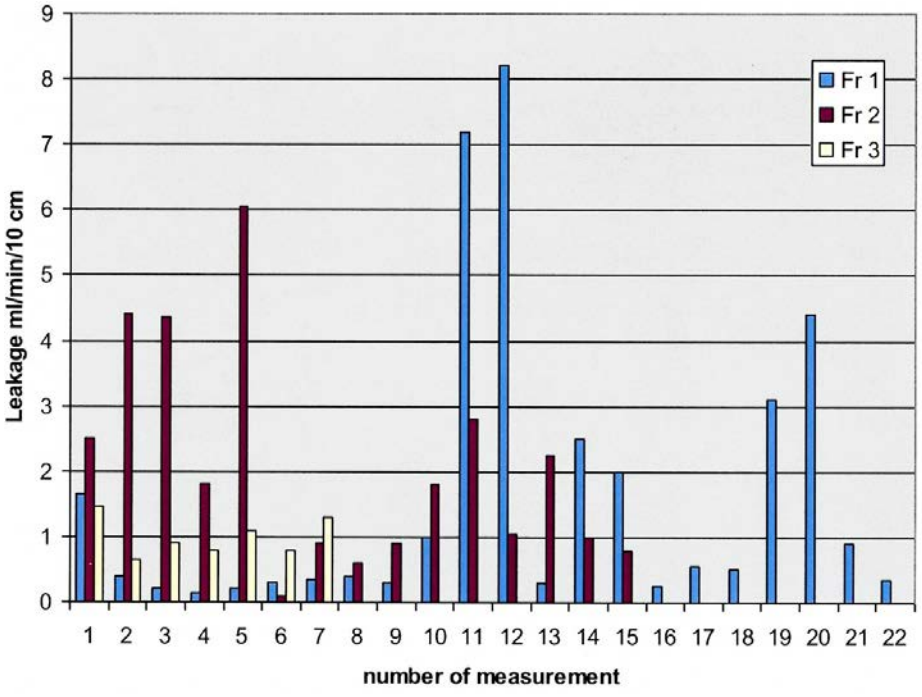

Figure 5-3. *A brief summary of the experimental data concerning the inflow distribution in KU2.*

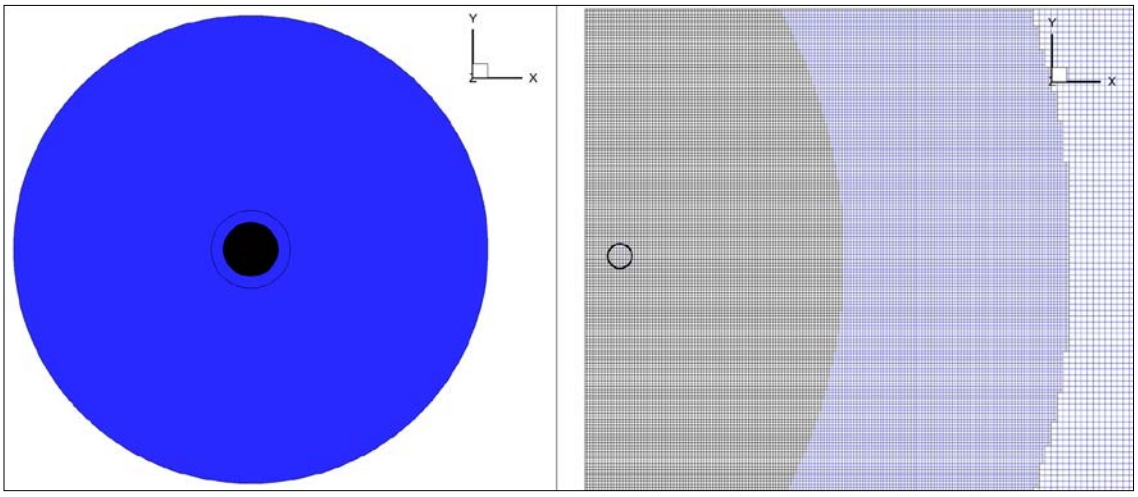

Figure 5-4. *The domain is a circle with radius 15 m. Inside a radius of 2.5 m a cell size of 0.01 m is used, outside this circle a cell size of 0.02 m is used. In total about 2 million cells. Black filled circle in the left figure indicates the shaft, while the small circle in the right figure indicates a borehole.*

5.3.2 Computational grid

A basic cell size of 0.02 m is used. Inside a radius of 2.5 m a cell size of 0.01 m is specified, see Figure 5-4. The total number of cells is about 2 million.

5.3.3 Boundary conditions

At the outer boundary a fixed pressure boundary condition is used. When simulating the pump tests, the measured heads in the boreholes were specified. When the inflow to shaft KU2 was simulated, a fixed pressure condition was used at the shaft boundary.

5.4 Results

5.4.1 Introduction

Two examples of the DFN in contact with the single fracture are shown in Figure 5-5. In realization two a fracture is seen to cross the whole shaft. This is also clearly illustrated in Figure 5-6, where the permeability in shaft KU1 is illustrated.

5.4.2 Single hole pump tests

The single hole pump tests were used to evaluate the mean transmissivity of the fractures crossing KU1, KU2 and KU3. The measured head was prescribed in the borehole and the inflow was calculated. Three realizations of the DFN were used. It was found that the transmissivities shown in Table 5-1 fitted the data quite well.

Table 5-1. Estimated transmissivities of the three fractures in shafts KU1, KU2 and KU3.

Shaft	T (m^2/s)
KU1	5×10^{-10}
KU2	2×10^{-9}
KU3	5×10^{-11}

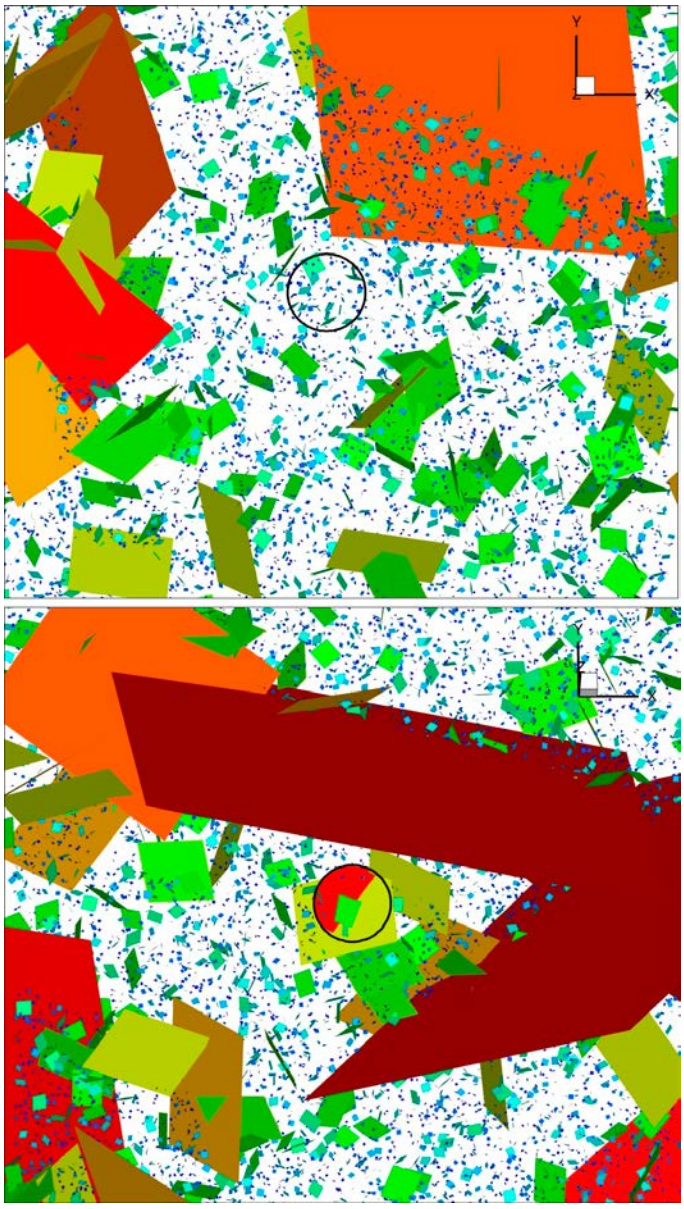

Figure 5-5. *Realization one (top) and two of the DFN. Black circle indicates a shaft. All DFN fractures in contact with the single fracture are shown.*

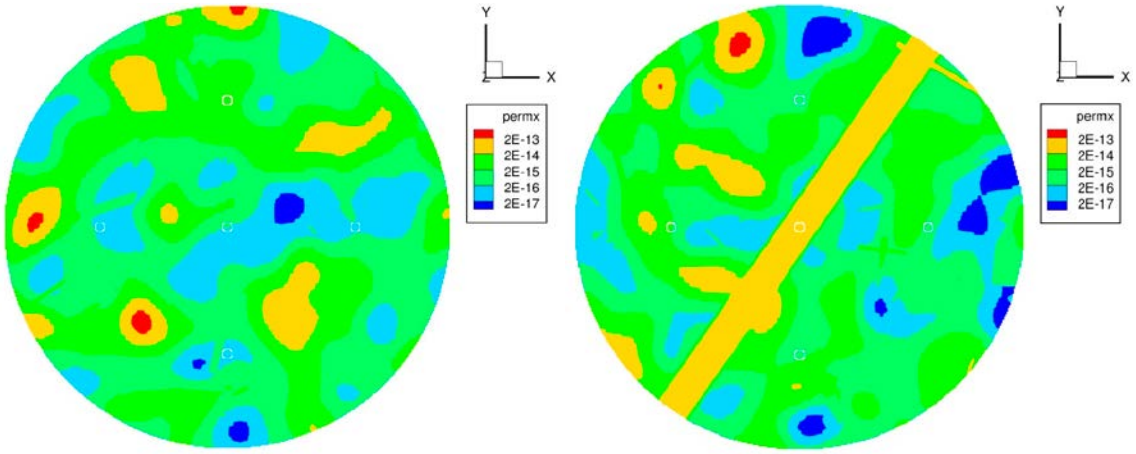

Figure 5-6. *Permeability distributions in shaft KU1. Conductivity is obtained by division with 2×10^{-7}. Thickness 0.1 m. Realization one (top) and two. The open white circles indicate the borehole positions in the simulations.*

The comparisons between measured and simulated flow rates are shown in Figure 5-7. It should be remembered (see Figure 5-2) that we have 5 observations for KU2, 4 for KU3 and only one observation for KU1. In the simulation model 5 boreholes were used for every shaft and three realizations of the DFN were evaluated. In Figure 5-7 the points are plotted with an increasing flow rate, along the horizontal axis. From the figure we may conclude that the calibrated mean transmissivities do generate a correct magnitude of the inflow. The spread in the data does further indicate that the heterogeneity of the fracture gives a variation of the flow rate that is in some agreement with data. Note that a homogeneous fracture should only give one point in each diagram.

Finally the simulated pressure fields in shaft KU1 are illustrated in Figure 5-8 and the corresponding flow fields in Figure 5-9. It is clear that the different realizations give very different solutions.

5.4.3 Inflow distribution to shaft KU2.

In the simulations shown a correlation length of 0.2 metre was assumed in the micro structural model.

After the excavation of the shaft the inflow distribution was measured for one crossing fracture (called Fracture 1) in shaft KU2. The measured distribution is shown in Figure 5-3. In this section we will investigate if the assumed correlation length can be supported by the measured inflow distribution.

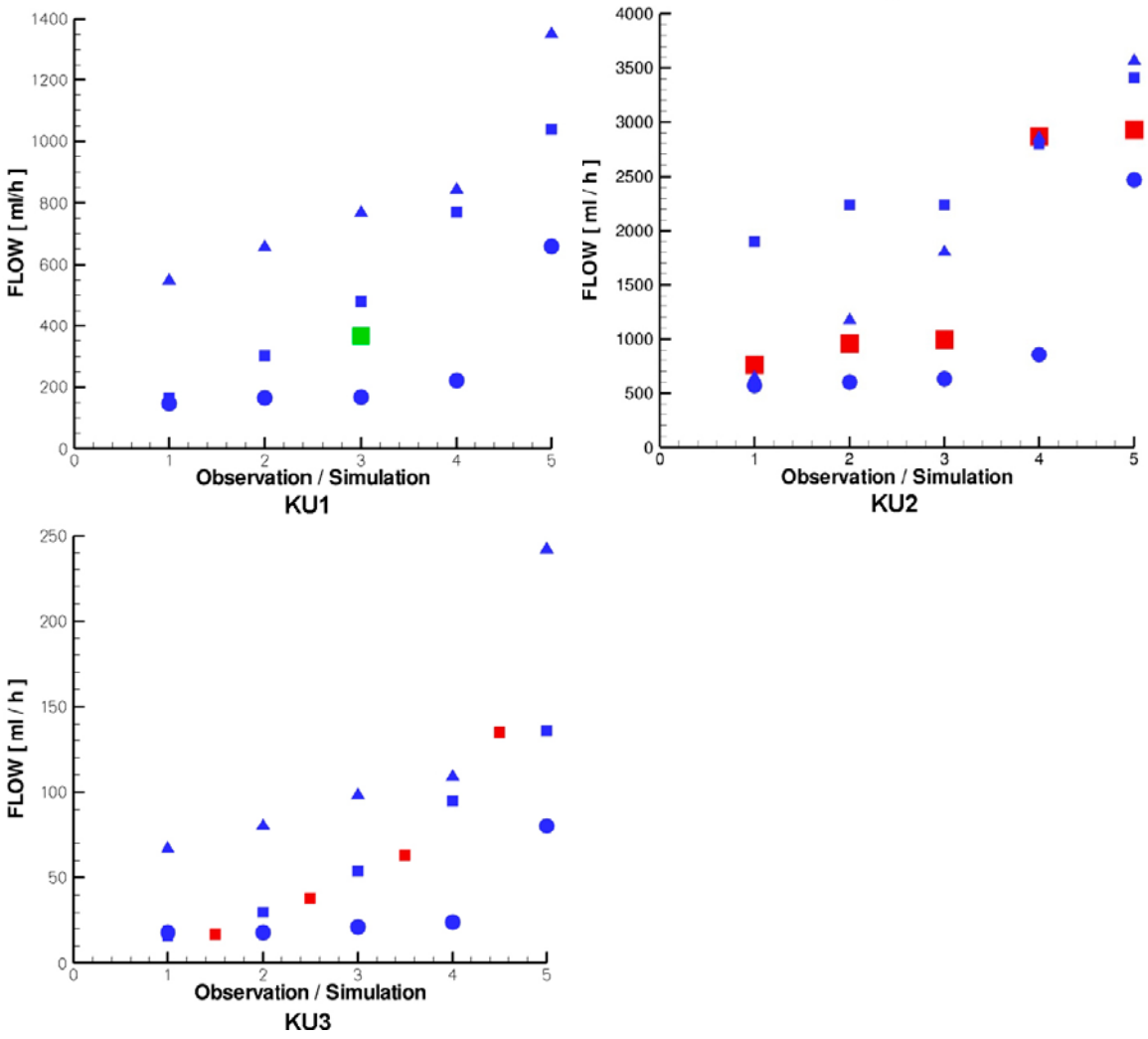

Figure 5-7. *Comparison with measured flow rates. Squares give field measurements and blue symbols give simulations (three realizations).*

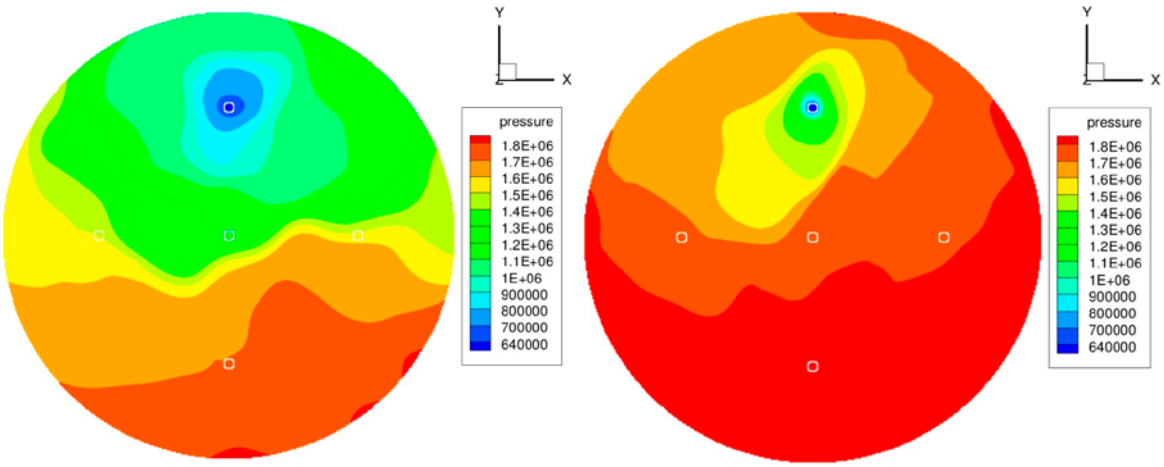

Figure 5-8. *Pressure fields. A flow rate of about 660 ml/h in KU1, for two realizations.*

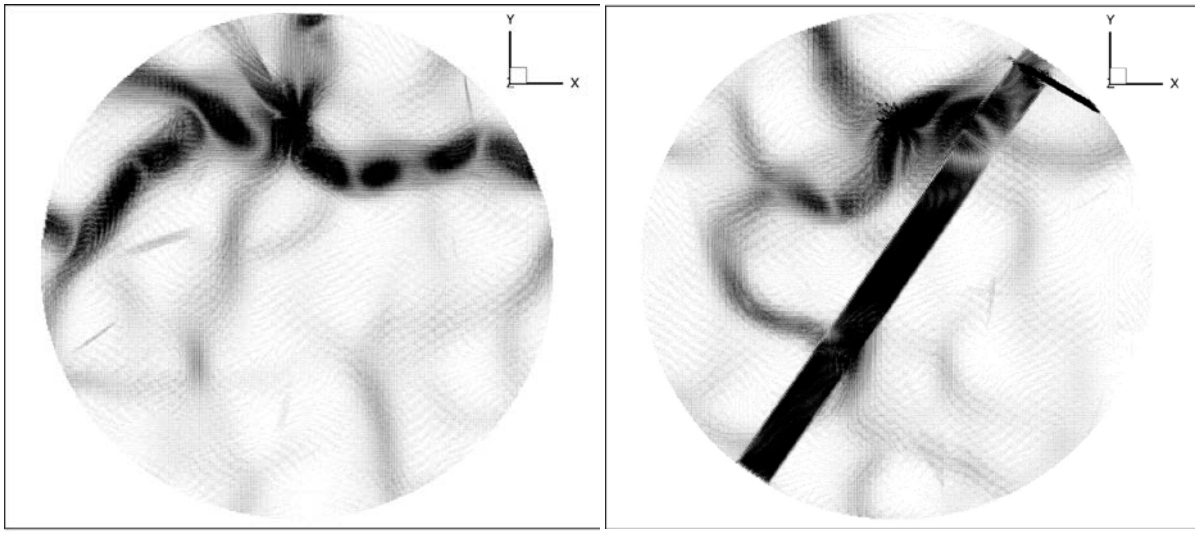

Figure 5-9. *Flow fields in shaft KU1, for two realizations.*

The pressure and flow in Fracture 1 are in Figure 5-10 shown for three correlation lengths. It is clear that the inflow distribution is strongly related to the correlation length.

A more detailed representation of the inflow distributions is given by Figure 5-11, where the number of peaks is related to the correlation length. Two realizations are shown for each correlation length; the number of peaks does not seem to be very sensitive to the chosen realization.

5.5 Concluding remarks

- The suggested 2D micro structural model rests on two basic assumptions; on the small scale a correlation length of 0.2 m exists, a DFN provides fracture crossings which in turn generate “easy flow paths”.
- Simulations demonstrate that this model can be calibrated to reproduce flow rates from single hole pump tests, carried out before the shafts were excavated.
- The inflow distribution in KU2 is found to be sensitive to the correlation length specified in the micro structural model. It is difficult to conclude which correlation length the inflow distribution implies, but the adopted value does not contradict measurements.

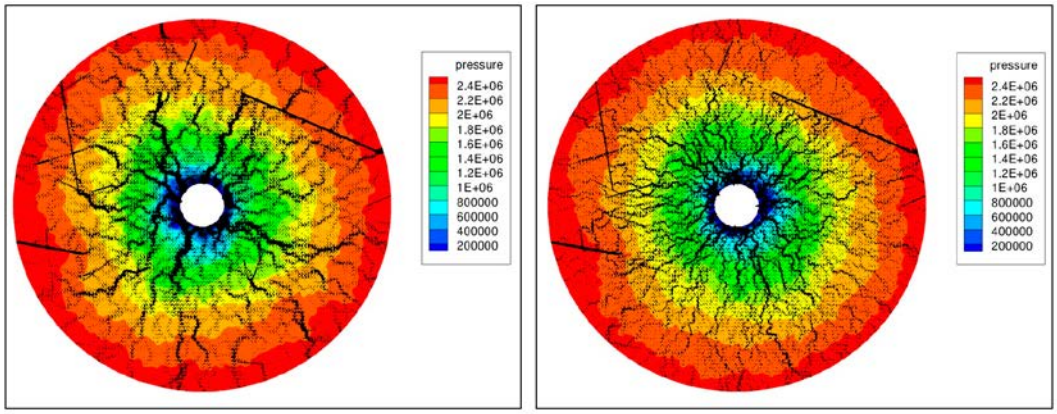

Correlation length 0.2 m (left) and 0.1 m.

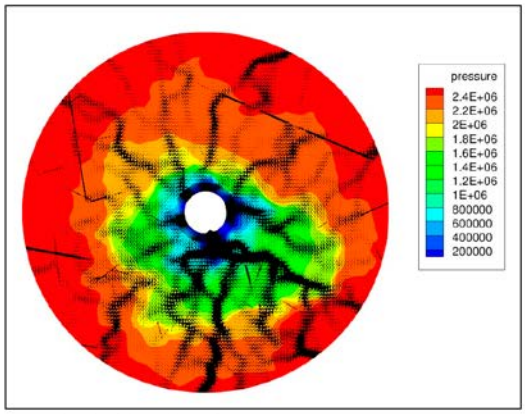

Correlation length 0.6 m.

Figure 5-10. *Flow and Pressure distribution. Atmospheric pressure in KU2. Three correlation lengths.*

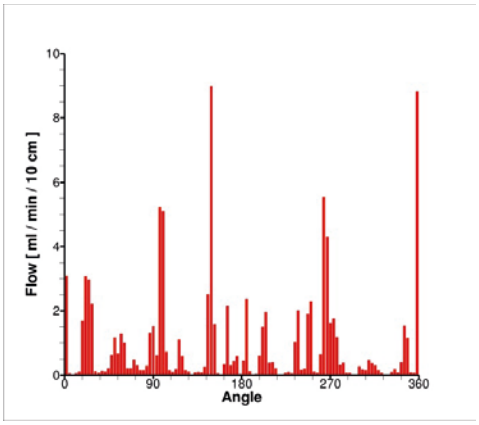

Realization 1: ∑Q = 103 ml/min
number of peaks = 17

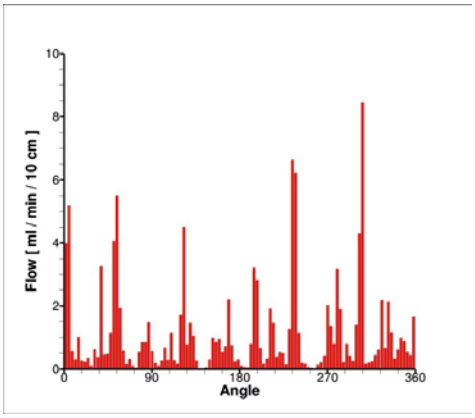

Realization 2: ∑Q = 125 ml/min
number of peaks = 21

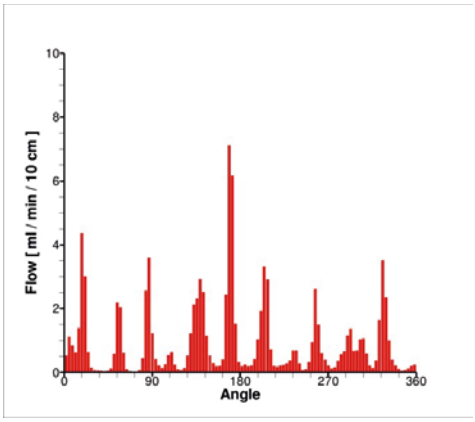

Realization 1: ∑Q = 102 ml/min
number of peaks = 12

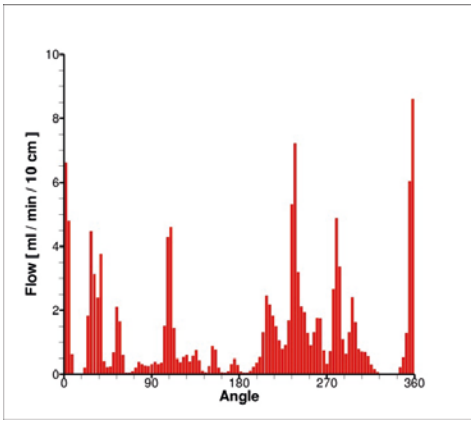

Realization 2: ∑Q = 139 ml/min
number of peaks = 12

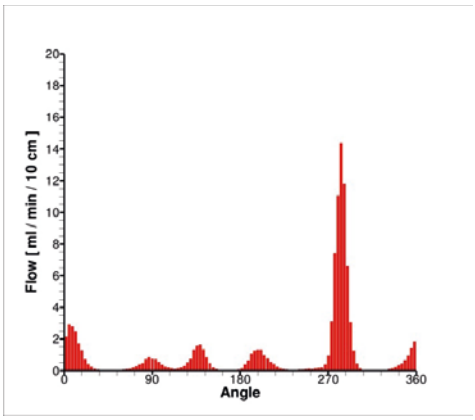

Realization 1: ∑Q = 110 ml/min
number of peaks = 5

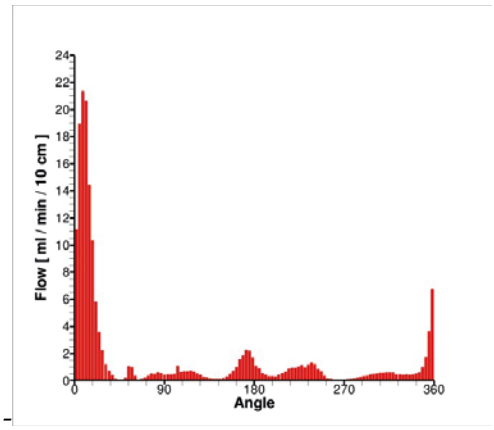

Realization 2: ∑Q = 179 ml/min
number of peaks = 6

Figure 5-11. *Inflow distribution for different correlation lengths; 0.1 m (top two), 0.2 m (middle two) and 0.6 m (bottom two).*

6 Task ABC

6.1 Introduction

6.1.1 Background

Three major tasks have been carried out in Task 7. Task 7A concerned the regional scale, 7B a pump test (KR14–18) in the block scale and 7C focused on the heterogeneity of a single fracture (micro structural model).

As a final step, it has been suggested that the micro structural model, as developed in 7C, should be applied to the pump test in 7B.

The DarcyTools model of 7B included the whole regional model, as developed in 7A. If the 7C model is introduced in 7B, this means that we have a single model covering all three tasks. We will call this model ABC, even if the label TS28 is used in the task description.

6.1.2 Objective

Develop a single model that covers all three subtasks of Task 7.

6.1.3 Outline

First some specific features of the ABC model will be discussed. As all other features of the model have been described in the subtasks, we can go directly to results. Finally, some concluding remarks are given.

6.2 Key features

The ABC model shares most features of the individual models and as these are described earlier we do not need to repeat these. Some specific features should however be listed:

- The local DFN that generates flow paths in the fracture planes will be the same as used in 7C.
- A much finer computational grid is needed to resolve the heterogeneous sheet joints. A local cell size of 0.12 m was used. This results in a model with about 8 million cells.
- The pump tests in the open boreholes KR14–18 were repeated with homogeneous sheet joints and with heterogeneous sheet joints; five realizations of the sheet joints were tested.

6.3 Results

6.3.1 Permeability fields

As the main feature of the ABC model is the introduction of heterogeneous sheet joints, we will start by some illustrations of the permeability fields, see Figure 6-1.

The lower sheet joint is located at a depth of 50 mbsl and all sections in Figure 6-1 are for this reason at this depth. The mean transmissivity of the lower sheet is 10^{-5} m^2/s and as the vertical cell size where the sheet joint is located is 0.12 m, the mean conductivities is around 10^{-4} m/s and the mean permeability 2×10^{-11} m^2.

6.3.2 The pump test KR14–18

The pump test in KR14–18, described in detail in Task 7B, will next be simulated using heterogeneous sheet joints. Five realizations of the sheet joints will be tested. The result can be studied in Table 6-1. In the table we include the measured draw downs and also the draw downs simulated with homogeneous sheet joints.

The main impression from the table is that the heterogeneous sheet joints will generate large variations in draw downs in pumped boreholes, while a smaller effect is found in observation boreholes.

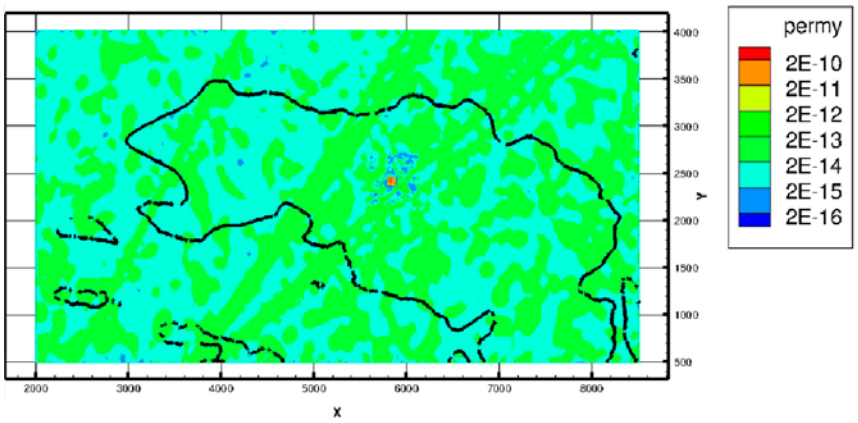

Regional scale. Outline of coastline shown for orientation.

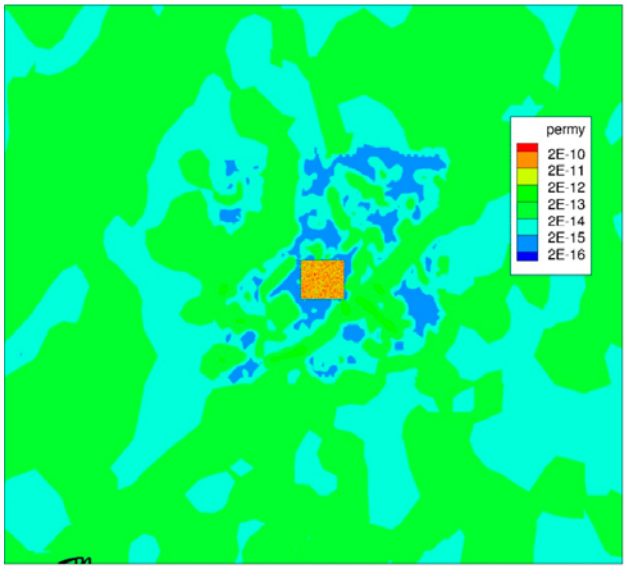

Block scale. Higher resolution in a square of 500 x 500 m. Small square is the sheet joint.

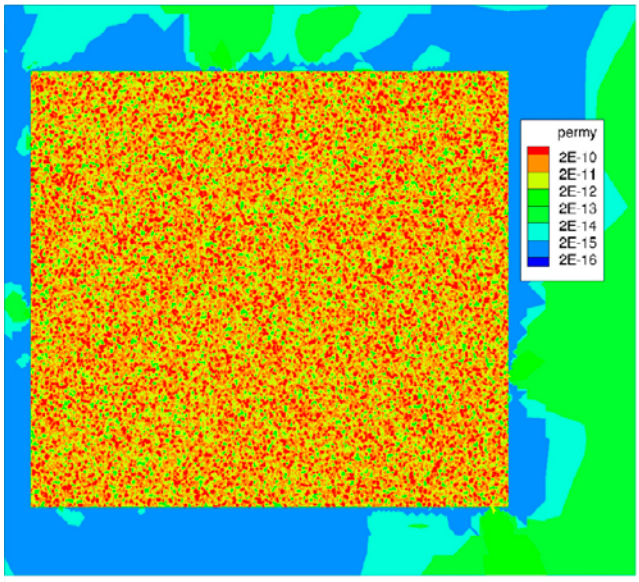

Sheet joint 100 x 100 m²

Figure 6-1. *Permeability at 50 mbsl.*

Table 6-1. Draw down in the pump test KR14–18, five realizations (black measured, red homogeneous and blue heterogeneous) . Left vertical column indicates the pumped borehole.

	KR14		KR15 A, B				KR16 A, B				KR17 A, B				KR18 A, B			
KR14	6.0	5.8	3.4	3.3	4.4	4.3	3.0	3.1	3.0	2.4	3.0	3.0	0.2	1.8	3.0	3.2	5.6	4.3
	6.3	6.3	3.4	3.4	4.3	4.4	3.2	3.3	4.2	4.3	3.3	3.1	1.8	1.9	3.3	3.3	4.4	4.5
		6.6		3.5		4.5		3.3		4.3		3.1		1.9		3.4		4.5
		6.6		3.5		4.5		3.3		4.3		3.2		1.9		3.4		4.5
		6.0		3.4		4.3		3.3		4.3		3.1		1.9		3.3		4.5
KR15 A	1.0	1.0	10.0	16.1	2.0	0.9	3.5	4.3	2.4	0.8	3.0	4.9	1.0	0.4	3.2	5.3	1.3	0.9
	1.1	1.0	14.1	11.8	0.9	0.9	4.1	4.2	0.9	0.8	4.9	4.8	0.4	0.4	5.3	5.1	0.9	0.9
		1.1		20.2		1.0		4.1		0.9		4.8		0.4		5.3		0.9
		1.1		19.6		0.9		3.9		0.9		4.8		0.4		5.2		0.9
		0.9		11.0		0.9		3.5		0.8		4.4		0.4		4.7		0.8
KR16 A	0.9	1.1	3.3	3.7	1.0	1.0	10.0	11.6	1.7	1.3	3.4	4.7	0.4	0.5	3.7	4.6	0.9	1.0
	1.2	1.1	3.8	3.8	1.1	1.0	13.8	10.5	1.1	0.9	4.8	4.9	0.5	0.5	4.7	4.6	1.1	1.0
		1.2		3.8		1.1		15.7		1.1		4.5		0.5		4.8		1.1
		1.2		3.7		1.1		17.5		1.1		4.8		0.5		4.7		1.1
		1.2		3.8		1.2		18.7		1.1		4.6		0.5		4.6		1.1
KR17 A	1.0	1.4	3.5	5.7	2.0	1.3	3.9	6.4	1.5	1.3	11.0	16.5	0.2	0.7	3.7	6.6	0.9	1.3
	1.5	1.4	5.9	5.7	1.4	1.3	6.3	6.3	1.4	1.3	17.3	14.3	0.7	0.6	6.8	6.4	1.4	1.3
		1.6		6.1		1.5		6.5		1.4		24.2		0.7		7.3		1.5
		1.8		5.3		1.3		5.5		1.2		16.1		0.6		6.1		1.2
		1.4		5.6		1.4		5.7		1.3		18.3		0.7		6.3		1.3
KR18 A	0.8	0.9	3.5	4.2	0.9	0.8	3.5	4.3	1.5	0.8	3.2	4.5	0.2	0.4	10.0	11.4	0.8	0.8
	1.0	1.0	4.3	4.4	0.9	0.9	4.2	4.3	0.8	0.8	4.6	4.6	0.4	0.4	10.6	11.8	0.9	0.9
		0.9		3.9		0.8		3.9		0.8		4.2		0.4		9.0		0.8
		0.9		4.0		0.8		3.9		0.8		4.4		0.4		9.5		0.8
		0.9		4.1		0.9		3.8		0.8		4.2		0.4		9.1		0.8

6.3.3 Flow and pressure fields

Finally we show some visualizations of the flow and pressure distributions near a pumped borehole, see Figure 6-2. The horizontal sections are still at 50 mbsl and hence in the lower sheet joints. It is clear that both the flow and pressure distributions are strongly affected by the heterogeneity.

6.4 Analysis

An inspection of the simulated draw downs gives:

- A large variation in drawdown in pumped boreholes is caused by the heterogeneity.
- In observation boreholes only minor variations are found.

In the pumped boreholes the drawdown can be 5–6 m larger, or 2–3 m smaller, as compared to the homogeneous fracture. It is suggested that this variation can be understood by looking at some analytical solutions.

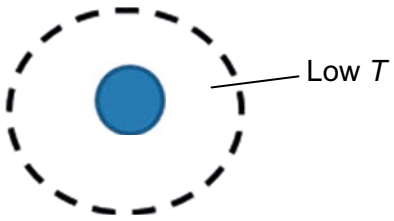

If the borehole is located in an area with low transmissivity this is analogue to a grouted layer around a tunnel. The inflow, or drawdown, is quite sensitive to the properties of the layer.

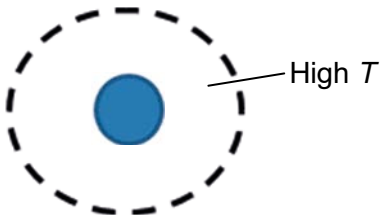

If the borehole is located in an area with high transmissivity we can approximate this case by an increased radius of the borehole. The inflow, or drawdown, is not very sensitive to a small increase of the radius.

We can hence expect that the increase of the drawdown is larger than the decrease, due to the heterogeneity.

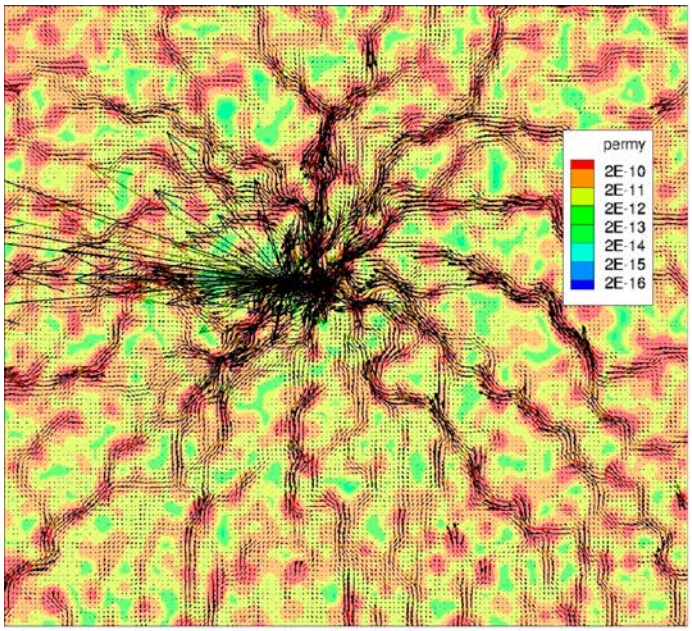

Flow due to pumping in KR15A. Permeability shown as transparent contour.

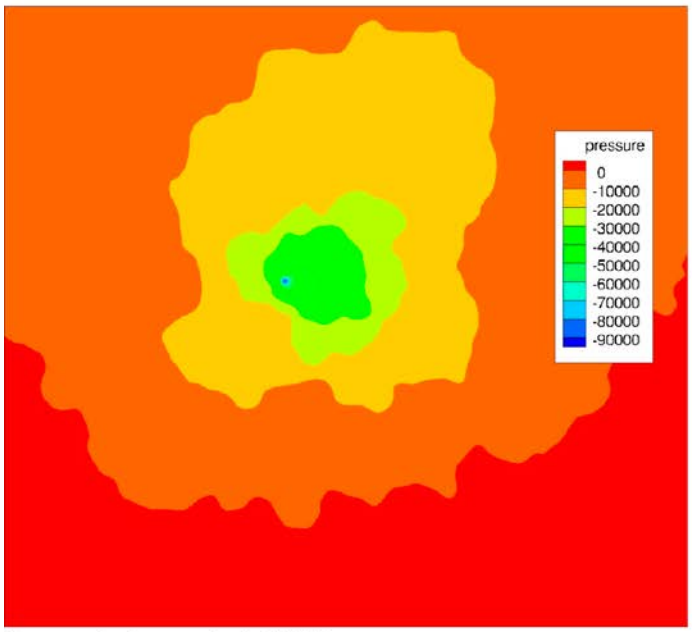

Pressure due to pumping in KR15A.

Figure 6-2. *Flow and pressure distribution 50 mbsl, shown for a square of 20×20 m^2. Pumping in KR15A.*

6.5 Concluding remarks

- The heterogeneous sheet joints will, as expected, result in a certain variation in drawdown when different realizations are used. The largest variation is found in the pumped boreholes, which is also expected.
- The micro structural model has some support from Task 7C, but it should be noted that the sheet joints have orders of magnitudes larger transmissivity, as compared to the fractures analyzed in Task 7C.
- The main achievement of the study is perhaps that a single model covering all three subtasks of Task 7 could be set up and used.

7 Conclusions

During the course of Task 7, the Performance Assessment (PA) aspects have been emphasized and discussed. The present report has focused more on numerical modelling techniques. However, Appendix B is devoted to PA issues and hence fills the gap to some degree.

The main achievements of the work reported can be summarized as follows:

- Task 7 has provided an opportunity to develop methods to simulate boreholes, in the code DarcyTools. Methods to analyze pumped, open and packed-off boreholes are now available in DarcyTools.
- The PFL data on flow along boreholes has provided a new, challenging way to test simulation models.
- The final Task ABC model illustrates a novel way to set up models; all scales from the heterogeneity of fractures to the regional scale are handled simultaneously. The unstructured grid technique made this development possible.
- Hopefully, all the simulations reported have contributed to the understanding of the hydrogeology of the Olkiluoto site.

References

SKB's (Svensk Kärnbränslehantering AB) publications can be found at www.skb.se/publications.

Black J H, Barker J A, Woodman N D, 2007. An investigation of 'sparse channel networks'. Characteristic behaviours and their causes. SKB R-07-35, Svensk Kärnbränslehantering AB.

Hakami E, Wang W, 2005. Äspö Hard Rock Laboratory. TRUE-1 Continuation Project. Fault rock zones characterisation. Characterisation and quantification of resin-impregnated fault rock pore space using image analysis. SKB IPR-05-40, Svensk Kärnbränslehantering AB.

Koskinen L, Rouhiainen P, 2007. Interconnected flow measurement between boreholes using a borehole flowmeter. In Krásný J, Sharp J M (eds). Groundwater in fractured rocks: selected papers from the Groundwater in Fractured Rocks International Conference, Prague, 2003. London: Taylor & Francis, 423–436.

Neretnieks I, 2006. Channelling with diffusion into stagnant water and into a matrix in series. Water Resources Research 42, W11418. doi:10.1029/2005WR004448

RETROCK, 2004. RETROCK Project. Treatment of geosphere retention phenomena in safety assessments. Scientific basis of retention processes and their implementation in safety assessment models (WP2). SKB R-04-48, Svensk Kärnbränslehantering AB.

RETROCK, 2005. RETROCK: Treatment of geosphere retention phenomena in safety assessments. Final report of the RETROCK Concerted Action. Work performed as part of the European Atomic Energy Community's (Euratom) framework of the specific research and training programme. Contract No FIKW-CT-2001-20201, EUR 21230 EN, European Commission.

Svensson U, 2006a. Äspö Hard Rock Laboratory. Äspö Task Force on modelling of groundwater flow and transport of solutes. Modelling of Task 6D, 6E, 6F and 6F2. Flow, transport and retention in a sparsely fractured granite. SKB IPR-06-21, Svensk Kärnbränslehantering AB.

Svensson U, 2006b. The Laxemar and Forsmark repositories. An analysis of the water inflow distribution. SKB R-06-102, Svensk Kärnbränslehantering AB.

Svensson U, Ferry M, Kuylenstierna H-O, 2010. DarcyTools version 3.4 - Concepts, Methods and Equations. SKB R-07-38, Svensk Kärnbränslehantering AB.

Vidstrand P, Ahokas H, Bockgård N, Dershowitz W, Holton D, Lanyon W, Poteri A, Koskinen L, 2012. Task Force GWFTS – Task 7 Descriptions for hydrogeological modelling of Olkiluoto, Finland. Compilation of all task descriptions assessed within the Task 7 of the SKB Task Force on Modelling of Groundwater Flow and Transport of Solutes. SKB P-12-21, Svensk Kärnbränslehantering AB.

Appendix A

Computational aspects of borehole simulations

A1 Introduction

A1.1 Background

Our knowledge about the transport properties of the "deep rock" is largely based on the information that we obtain from boreholes; for example, interference tests give transmissivities and water samples the chemical properties of the water.

The Äspö Task Force has decided to address the question how borehole measurements, and in particular long-term pumping tests, can be simulated and analysed by means of numerical models. The project is called Task #7 and focuses on an experiment carried out at Olkiluoto site in Finland.

Some introductory cases, called Task 7A, have been defined by Vidstrand et al. (2012) and the present report aims to "respond" to the suggestions presented by these authors.

A1.2 Situation considered

The first case presented by Vidstrand et al. (2012) deals with two boreholes that cross three fracture zones, see Figure A-1. The steady state pressures and flows along the boreholes are requested for natural (no pumping) and pumped conditions.

A2 Objective

The objective of the study is to suggest and analyse methods to simulate open and pumped boreholes.

A3 Methods

A3.1 Resolution of a borehole

The computational approach for the defined problem will depend on the discretization technique (Finite Elements, Finite Volumes, etc) and the software used. For the present simulations the code DarcyTools V3.0 will be used. This is a finite volume code that embodies an unstructured Cartesian grid. As will be shown, this technique is quite flexible and seems to be well suited for borehole simulations.

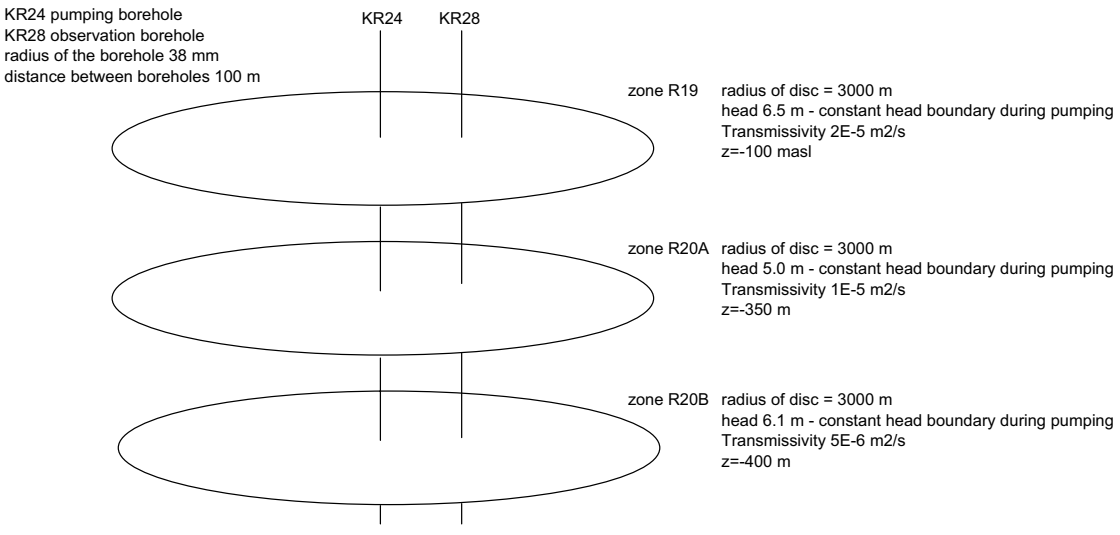

Figure A-1. *Situation considered, Case A, as given by Vidstrand et al. (2012).*

It is presently not clear what the final Task 7 specification will entail, and we will therefore investigate three different approaches to borehole simulations. The methods are outlined in Figure A-2 to Figure A-4, and will now be commented.

The first one, see Figure A-2, is called "Resolved borehole" as the actual geometry, i.e. the cylinder, is represented in the grid. In order to resolve the borehole, the grid cells in the borehole wall should be smaller than 0.01 m. The Task 7A cases specify a zone radius of 3,000 metres and it is immediately clear that the cell size ratio may be a problem in this method.

The second method is called "Single cell borehole" and is outlined in Figure A-3. The cell that represents the borehole should have roughly the same area as the borehole, but it is anyway clear that the radial inflow to the borehole can not be correctly described by the Cartesian cell system. One should also note that the calculated flow into the cell will be based on a gradient based on Δ (the cell size), while it should be based on a gradient from $\Delta/2$, as the pressure can be assumed to be uniform in the borehole. A correction to the conductivities in the borehole walls can be derived as follows:

Simulated inflow: $$Q_s = 4K_s\Delta\frac{\Delta H}{\Delta} \tag{A-1}$$

"Correct inflow": $$Q = 2\pi K\Delta\frac{\Delta H}{\ln \Delta / r} \tag{A-2}$$

Where ΔH is the head difference between the borehole and the neighbouring cells and index s indicates simulated. From these expressions we find that:

$$K_s = \frac{\pi}{2\ln \Delta / r}K \tag{A-3}$$

For $\Delta = 0.06$ and $r = 0.038$, (A-3) gives a correction factor of 3.4.

The third method is outlined in Figure A-4 and is called "Implicit borehole". Also for this case it is possible to correct conductivities for the borehole cell, along the procedure outlined above. In this method we need to calculate the pressure in the borehole cells in an iterative manner, as we are not calculating the flow along the borehole explicitly. The following procedure is used:

$$P_{bh}^{i+1} = P_{bh}^{i} + c\left(Q_{in}^{i} - Q_{pumped}\right) \tag{A-4}$$

where P_{bh}^{i} is the pressure in the borehole at iteration step i, Q_{in}^{i} the total inflow at step i, Q_{pumped} the prescribed pumping rate and c an under-relaxation factor. Obviously, in the converged solution $P_{bh}^{i+1} = P_{bh}^{i}$ and $Q_{in}^{i} = Q_{pumped}$ irrespective of the value of c. For the case of a prescribed head in a pumped borehole, one simply fixes the pressure in the borehole cells and calculates the inflow, using the corrected conductivities in the borehole walls.

A3.2 Grid generation

From Figure A-1 we note that the radius of the zones is 3,000 metres. As the radius of the borehole is 0.038 metres, it is concluded that grid generation is not a trivial task. In fact, for traditional finite volume codes methods A and B are not within scope. DarcyTools V3.0 embodies an unstructured grid, as mentioned above, and can handle all three methods.

It is not within the scope of the present report to describe this grid system. However, we may give some short hints:

- A number of objects (bricks, cylinders, lines, points, CAD-geometries) are first defined.
- The grid is generated with conditions related to these objects. We may for example state that "the border of the cylinder should be resolved with a cells size not larger than 0.01 m" or "all cells that are cut by this line should have a cell size not larger than 1 metre". We can use conditions as "inside", "outside", "border", etc.
- Cells that are of no interest can be removed. We can for example use a condition related to the porosity, and remove all cells that have a porosity smaller than a specified value.

In Figure A-5 the grid used for the situation outlined in Figure A-1, is illustrated. The single cell method is used to describe the borehole. When not needed cells have been removed, we have three 2D-slices of cells (the three zones) and two 1D lines of cells (the two boreholes). The smallest cell size is $0.0625 \times 0.0625 \times 1.0$ m^3 and the largest one $64 \times 64 \times 1$ m^3.

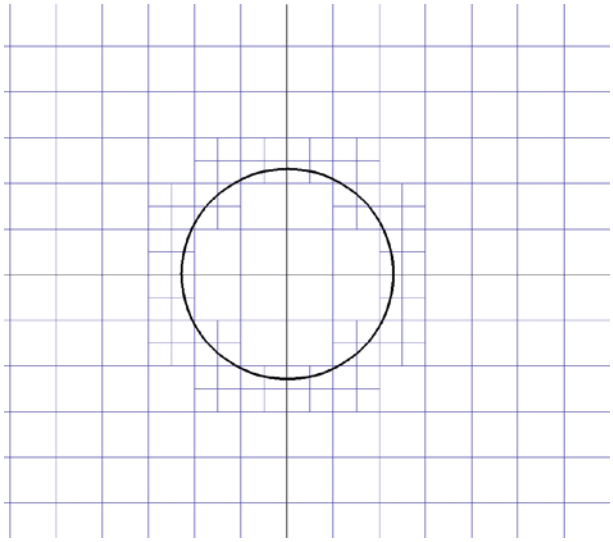

Characteristics

- Cell size in the borehole wall should be less than 0.01 m.
- "Direct" method in the sense that no corrections are needed (methods B and C do).
- Large ratio largest/smallest cell size may be a problem.

Figure A-2. *Resolved borehole, method A.*

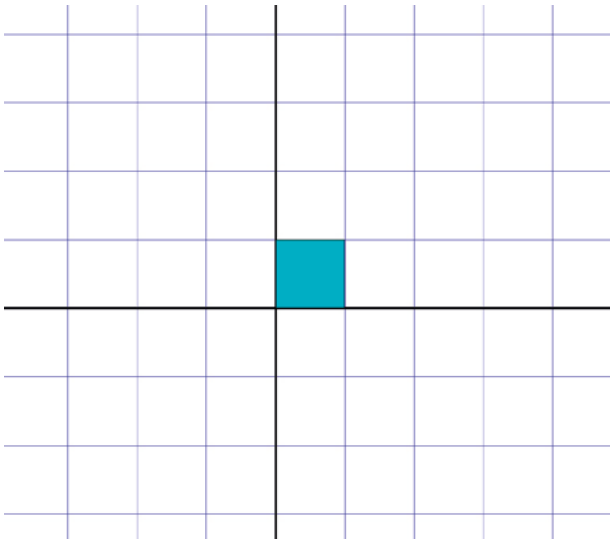

Characteristics

- One cell represents the borehole in a plane perpendicular to the borehole axis. The size of this cell should be chosen with some care.
- Conductivities of the borehole walls should be subject to corrections.
- Flow along borehole explicitly simulated.

Figure A-3. *Single cell borehole, method B.*

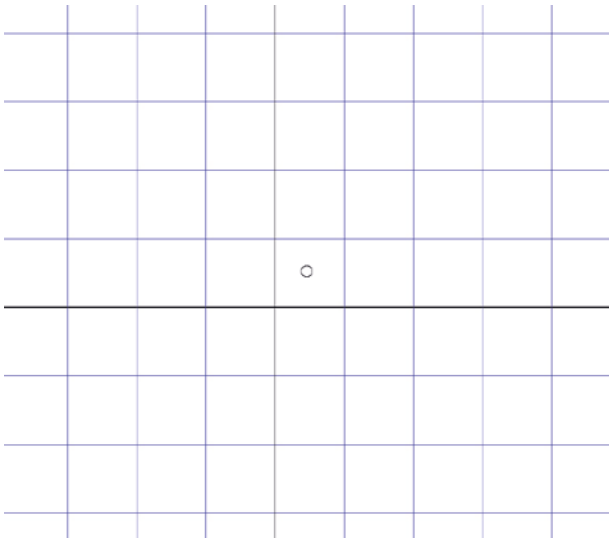

Characteristics

- Cell size can be significantly larger than borehole radius.
- Corrections to conductivities in borehole cell can be derived.
- Both pumping and no pumping conditions can be simulated.
- No explicit solution of flow along borehole.

Figure A-4. *Implicit borehole, method C.*

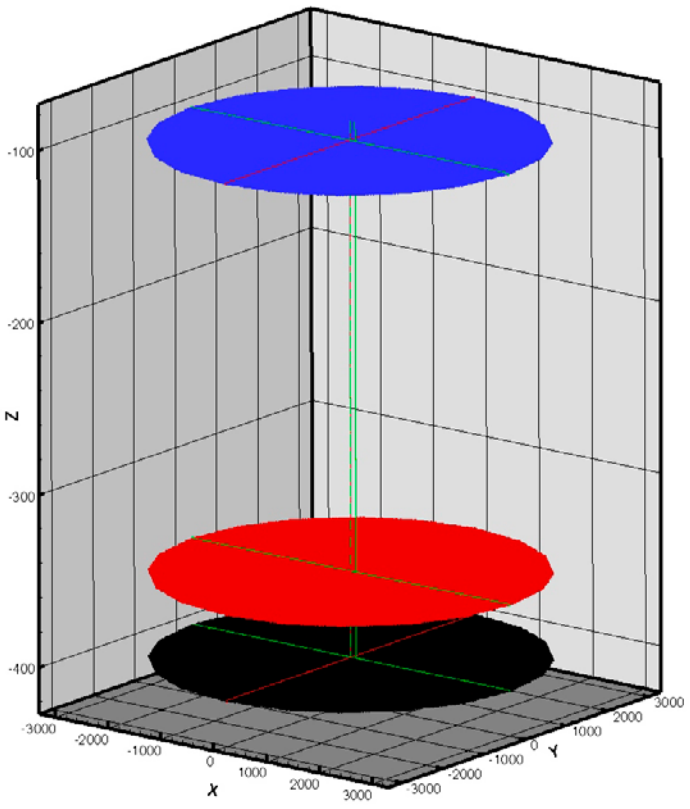

Figure A-5. *Illustration of the grid used for the situation outlined in Figure A-1.*

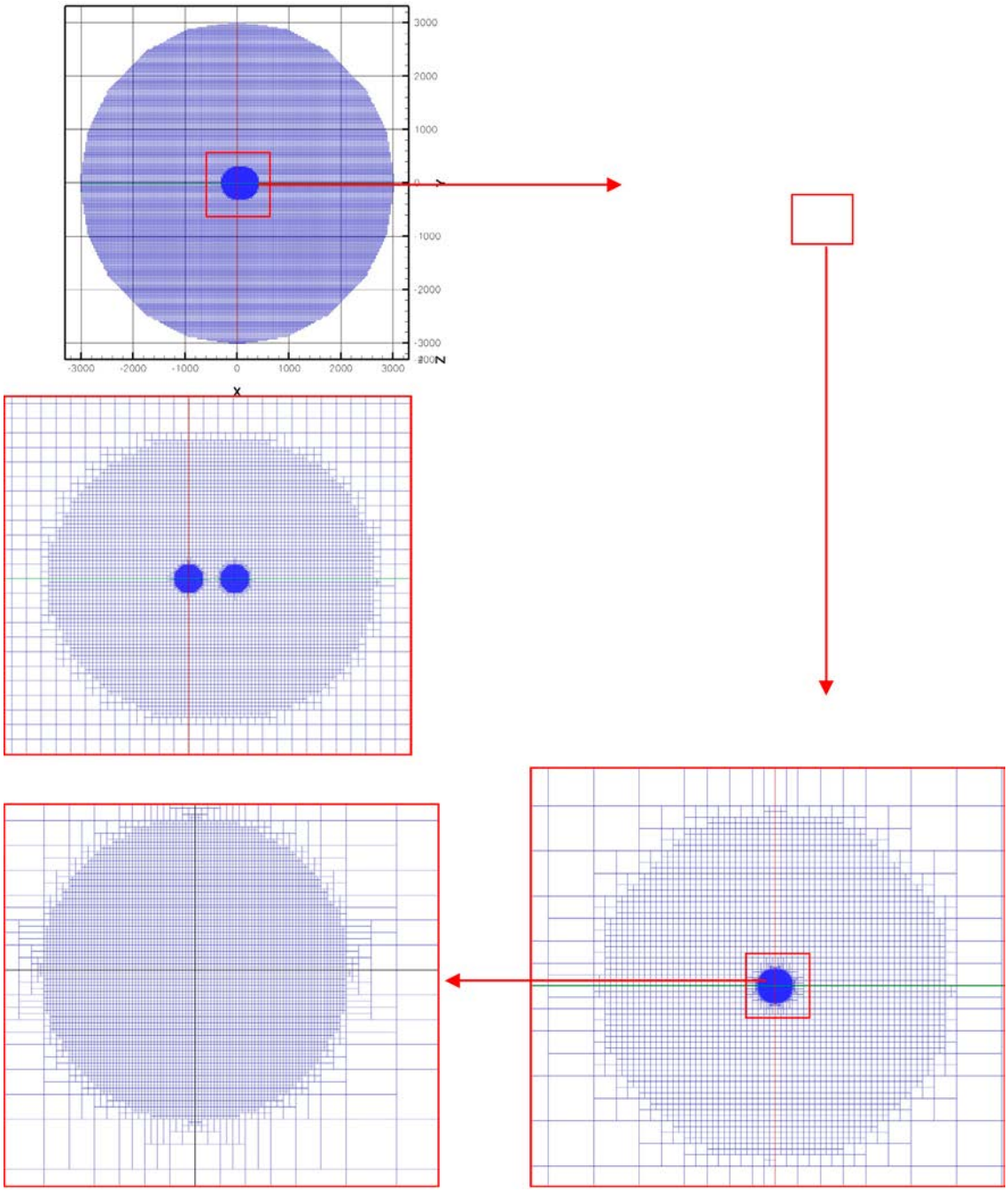

Figure A-5 Continued. *Resolution in a zone.*

A4 Results

A4.1 Borehole Conductivity

When discussed, boreholes are often described as " super-conductors" and the implications of a borehole that connects two fracture zones are often mentioned as an uncertainty.

The first thing to clarify is hence the conductivity of a borehole. The resistance of a laminar pipe flow is well known and we may directly establish the head gradient:

$$\frac{h_f}{L} = \frac{64\nu u}{2gD^2} \qquad \text{(A-5)}$$

where h_f is the head loss, L the length, ν viscosity, u velocity, g gravity and D the borehole diameter.

By a comparison with Darcy's law we find:

$$K = \frac{2gD^2}{64\nu} \tag{A-6}$$

where K is the conductivity. If some typical values are used ($D = 0.076$, $\nu = 10^{-6}$ m^2/s we find that K ≈ 2,000 m/s. A perspective on this number can be obtained by multiplying with the borehole area and compare this value with the width times the transmissivity of the fracture zone:

$$\frac{K\pi D^2}{4} = T_f W_f \tag{A-7}$$

It is found that the borehole "flow capacity" is comparable to a fracture zone with

$T_f = 10^{-2}$ m^2/s and $W_f = 10^3$ m, which indeed seems dramatic.

However, a borehole will never carry a flow comparable to the equivalent fracture zone. The reason for this is that *the flow in the borehole is governed by the resistance associated with in-and outflows to the borehole and not by the flow resistance in the borehole*. This is important to establish.

A4.2 Flow in a borehole connecting two zones

If the resistance is dominated by in and outflow resistance, equations from well-pumping can be used. Let us consider the case shown in Figure A-6; a borehole connects two zones with heads H_1, H_2 and transmissivities T_1 and T_2. If $H_1 > H_2$ the flow into the borehole from zone 1, Q_1, and the flow from the borehole to zone 2, Q_2, can be written as:

$$Q_1 = 2\pi T_1 \frac{H_1 - H_{bh}}{\ln R / r} \tag{A-8}$$

$$Q_2 = 2\pi T_2 \frac{H_{bh} - H_2}{\ln R / r} \tag{A-9}$$

where R is the zone radius and r the borehole radius. As $Q_1 = Q_2$ we can derive an expression for H_{bh}, the head in the borehole, which is assumed to be a constant as the resistance in the borehole is neglected.

$$H_{bh} = \frac{H_1 T_1 + H_2 T_2}{T_2 + T_1} \tag{A-10}$$

and the flow through the borehole is given Equation (A-8).

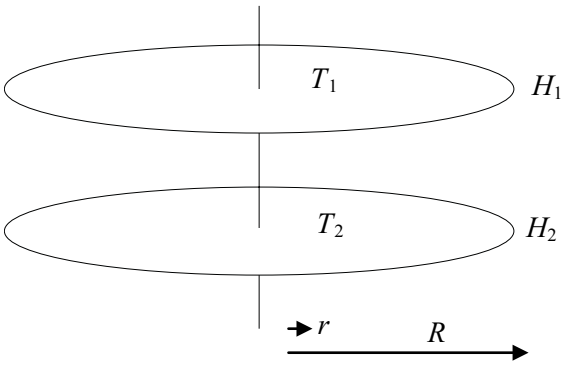

Figure A-6. *A borehole connecting two zones.*

The equations derived will next be compared with numerical simulations of the case outlined in Figure A-6. Without loss of generality we may put $H_2 = 0$ and rewrite Equation (A-11) as:

$$\frac{H_{bh}}{H_1} = \frac{1}{1 + T_2 / T_1} \tag{A-11}$$

A4.3 Evaluation of methods

The situation shown in Figure A-6 will be used for an evaluation of the three methods. The following specification applies:

- H_1 is put to 1.0 and $H_2 = 0$.
- T_1 is put to 10^{-5} m^2/s, T_2 is varied.
- Distance between zones is 100 metres and the radius of the zones is also 100 metres.
- The borehole radius is 0.038 metres.

The results are summarized in Table A-1. Analytical results are from Equations (A-8) and (A-10) above, and these are used to normalize the numerical results.

The general impression is that all three methods give accurate results; the error is in most cases less than 1%.

Table A-1. Evaluation of the three suggested methods. For the analytical results the flow is in kg/s and the head in m. The numerical results are normalized with the analytical ones.

	T_1/T_2					
	0.5		1.0		2.0	
Case	Q	H	Q	H	Q	H
Analytical	5.32×10^{-3}	0.333	3.99×10^{-3}	0.500	2.66×10^{-3}	0.667
Resolved borehole	0.996	1.000	1.000	1.000	0.989	1.000
Single cell borehole	0.989	1.003	0.992	1.000	0.989	1.000
Implicit borehole	0.993	1.000	0.992	0.998	0.992	1.000

A4.4 Task 7A Cases

Next we consider Case A in the paper by Vidstrand et al. (2012), see also Figure A-1. However, in the spirit of "method evaluation" we will approach this case in a stepwise manner, starting with a single unpumped borehole and finish with pumping in KR24 and observing in KR28.

The single unpumped borehole can be analysed in a similar manner as the two-zone system above, with the following results:

$$H_{bh} = \frac{H_1 T_1 + H_2 T_2 + H_3 T_3}{T_1 + T_2 + T_3} \tag{A-12}$$

which with the present data give $H_{bh} = 6.014$ m. It is then straight forward to calculate inflows/outflows to the three zones.

The analytical and numerical results are given in Table A-2.

Table A-2. The single unpumped borehole.

Case	Flow [kg/s]×10^3			H_{bh} [m]
	R19	R20A	R20B	
Analytical	5.42 (in)	5.66 (out)	0.24 (in)	6.014
Numerical	5.5 (in)	5.68 (out)	0.28 (in)	5.99

The next situation considers two (KR24 and KR28) boreholes without any pumping. The boreholes are 100 metres apart, with KR24 at the centre of the zones. KR28 is hence somewhat closer to the prescribed head at the boundaries; however considering that the fixed head boundary is about 3,000 metres away we expect similar conditions to develop in the two boreholes.

The inflows/outflows to KR24 are given in Table A-3. It is found that the flow rates in KR24 are now reduced, as compared to the single borehole case.

Table A-3. Two unpumped boreholes. Inflows/outflows to KR24 (same for KR28).

Flow [kg/s]×10^3			H_{bh} [m]
R19	R20A	R20B	
4.2 (in)	4.4 (out)	0.20 (in)	5.98

Finally pumped conditions are simulated. The head in KR24 is reduced by 1.1 metre, as compared to the unpumped case above (hence fixed to 4.88 metres).

The result is summarized in Table A-4. A tentative analyses indicates that “the inflow to KR24 through R20A is supported by the outflow to this zone in KR28”.

Table A-4. Pumped conditions in KR24, as given by a specified head.

Borehole	Flow [kg/s]×10^3			H_{bh} [m]
	R19	R20A	R20B	
KR24	16.8 (in)	1.96 (in)	3.33 (in)	4.88, specified
KR28	4.1 (in)	4.33 (out)	0.23 (in)	5.67

A5 Discussion

Three methods to simulate open and pumped boreholes have been suggested and evaluated. The methods should not be considered as competing, but may all be valuable depending on the application at hand. Methods A and B give the possibility to map conditions (like fracture traces) at the very borehole wall, while this is not within scope for method C. This method may on the other hand be the right choice if only the effect of the borehole is requested.

If the flow along the borehole is explicitly calculated, i.e. methods A and B, a borehole conductivity needs to be specified. In Section A4.1 it was stated that a value of about 2,000 m/s would give the correct resistance. However, from a computational point of view we need to calculate a pressure drop along the borehole that can be resolved numerically. In the simulations presented it was found that a total head difference along the borehole of about 5–10 mm is a good choice. A borehole conductivity in the range 10–25 m/s was found to produce such a gradient.

A6 Concluding remarks

the following points summarize the work presented:

- Three methods to simulate open and pumped boreholes have been suggested and analyzed.
- Case A in the paper by Vidstrand et al. (2012) has been analyzed in a stepwise manner.
- The unstructured grid, embodied in DarcyTools V3.0, seems to be suitable for the task.

Appendix B

An approach to pa transport simulations

Abstract

An approach to PA transport simulations is discussed. A brief review of some recent papers and reports reveals that the groundwater flow distribution is one of the major uncertainties in such simulations. For this reason the focus will be on this issue. Transport simulations do however need to consider exchange with the rock matrix. A novel micro scale model, which includes the matrix, is introduced and sample results are discussed.

Abstract (Swedish)

En metodik för att simulera transport under PA förhållanden diskuteras. En snabb översikt av aktuell litteratur visar att grundvattenflödets fördelning i tid och rum är av central betydelse för denna typ av simuleringar. Rapporten har därför fokus på denna fråga. Transportberäkningar inkluderar dock med nödvändighet utbyte med omgivande berg (matrisen). En modell som behandlar processer på mikro-skalan introduceras för detta ändamål.

B1 Introduction

B1.1 Background

As a general background to Task7 we quote the following paragraphs from Vidstrand et al. (2012):

Task 7 aims at providing a bridge between the site characterisation (SC) and performance assessment (PA) approaches to long-term pumping tests and measurement from borehole flow logging. Open boreholes are nowadays a feature at many sites and Task 7 aims to develop an understanding of the effects of open boreholes on the groundwater system and the use of data from such boreholes in site characterisation and performance assessment.

The strategy of Task 7 is to proceed from the largest scale (site scale with focus on fracture zones) to smaller scales (rock block). Task 7 may finish with exercises at the scale of the engineered barrier. At each scale, specific goals will be defined within the context of the overall Task 7 goal, and modelling tasks will be defined to support those goals.

Task 7A considers an approximately 10 km^2 region surrounding borehole KR24 at the Olkiluoto site in Finland. KR24 was used for a long-term pumping test. The test setup included pumping from two borehole sections. The lower part of KR24 was partially isolated by a by-pass packer (throttle valve) so that the deeper sections of the borehole experienced a smaller drawdown than the upper section during the pumping.

Task 7A has been split up into several sub-tasks. Results from Task 7A 1-2 have been reported (Appendix A). Tasks 7A 3-5 are more loosely defined and it is expected that different modelling groups will choose to carry out one or perhaps two of these tasks. This report concerns Task 7A3, for which the following outline is given in Vidstrand et al. (2012):

(7A3) Ideas for calculation of PA relevant parameters from open borehole information:

Here, each modelling group will consider how the PFL and open hole long-term pumping experiments database of Task 7 might be used to derive transport parameters.

- *Beta (hydrodynamic control of retention – see Cheng et al. 2003)*
- *Tau (water residence time – see Cheng op cit)*
- *"Q/W" (flow rate per fracture width)*
- *Flow wetted surface (FWS)*
- *Transport aperture*
- *Transport width*

- *Q (water flow m^3/s) through designated volumes (e.g. around a repository) or structures (e.g. flow through a fracture zone or a single fracture); or*
- *v (flow velocity m/s) within fractures (relevant to buffer erosion)*

To the extent possible, the derivation of PA relevant measures from PFL measurements should be compared to the derivation using traditional packer testing.

The results will be defined through discussion points and example calculations based on the results of Task 7A1 and 7A2. It will also be useful to identify the importance of additional information (e.g. micro-structural model) required for transport calculations.

It is clear that it is to a large extent left to each modelling group to define the content and approach of the Task. For this reason the present contribution will focus on the groundwater flow distribution, which has been identified as one of the critical issues in PA transport simulations.

B1.2 Objective

The main objective of the report is to discuss an approach to PA transport modelling which focuses on the groundwater flow distribution. It should perhaps be clarified that this approach concerns a "process-oriented research model" and not a PA model of the kind currently in use.

B1.3 Problem considered

As we are dealing with PA transport simulations, it will be assumed that it is "transport from a leaking canister under closed repository conditions" that defines our starting point, see Figure B-1. Strictly we need to consider also the partly open phase, as well as the resaturation phase, but for simplicity we will here focus on the quasi-steady period after the repository has been fully resaturated. It will be assumed that the flow field is then the same as before the repository was excavated.

The flow path illustrated in Figure B-1, is assumed to be a flow path in a sparsely fractured granite. As the repository will be located at a certain distance from major fracture zones, it is expected that a number of smaller fractures make up the flow path. It is often argued that this part of the natural barrier, say the first 50–100 metres from the deposition hole, is the most critical as the flow rates in the major fracture zones are much larger.

B1.4 Outline

The report should be considered as a discussion of how PA transport simulation should be carried out. The next section then starts by a brief review of some recent relevant papers and reports. Guided by the conclusions of these, an approach based on three steps is discussed. The first step, Section B2.2, discusses site scale information. Next, Section B2.3, the flow path in a fracture is considered and finally, Section B2.4, a micro scale model is presented. The report ends with a discussion section followed by some concluding remarks.

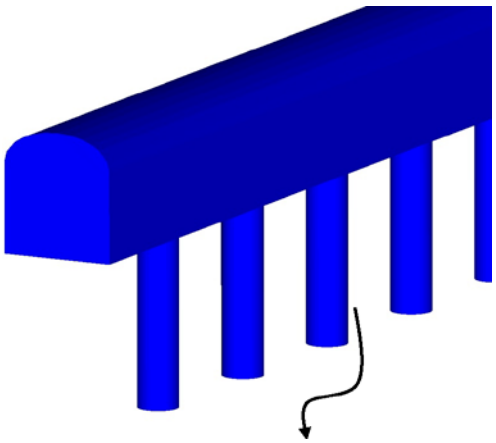

Figure B-1. *Transport along a flow path from a leaking canister.*

B2 Suggested approach

B2.1 Introduction

A number of recent papers and reports have emphasized the role of the groundwater flow distribution (spatial and temporal) in transport simulations. Let us quote a few:

- *The RETROCK Project (2004, 2005) has examined the retention and transport of radio nuclides and also how these processes are dealt with in PA models. The project concludes that the groundwater flow distribution is an important process and that further research is needed. Figure B-2 is a good illustration of this conclusion.*
- *Neretnieks (2006) summarizes a number of field studies and concludes that "most water flow in fractured rocks takes place in only a small part of the fractures". The flow channels form a sparse network with an unevenly distributed flow. A typical width of a flow channel may be 0.05–0.3 m and the aperture is less than 1 mm.*
- *In a report by Black et al. (2007) the following is concluded:*

In summary, the weight of evidence suggests that groundwater flow systems in fractured crystalline rocks have the following characteristics:

– *Groundwater flows within a sparse network of channels just above the percolation limit.*

– *The frequency of intersections is low in that individual channels extend considerable distances between significant junctions. Ten metres or more may be common.*

– *Individual channels often extend over many fracture surfaces and the resulting flow system is only weakly related to the density or size of mappable fractures*

– *The system is so sparse that it is controlled by a few 'chokes' that give rise to compartments of head, and probably, groundwater chemistry.*

– *Channels occur on all fracture planes, including those within fracture zones, and although the characteristics of the fracture zone channel networks may differ from those in surrounding rocks, they should still be regarded as channel networks.*

– *The actively flowing sparse channel network, occurring within any particular rock, is a naturally selected, small sub-set of the available channels. Hence, there are many conductive channels that do not participate within the active network but are connected to it, however tortuously.*

The present work will start by accepting these statements about sparse channel networks. It will also consider the present conceptual SKB view of the fracture, as given in Figure B-3, as a realistic representation. The modelling challenge is hence to accommodate these concepts and statements.

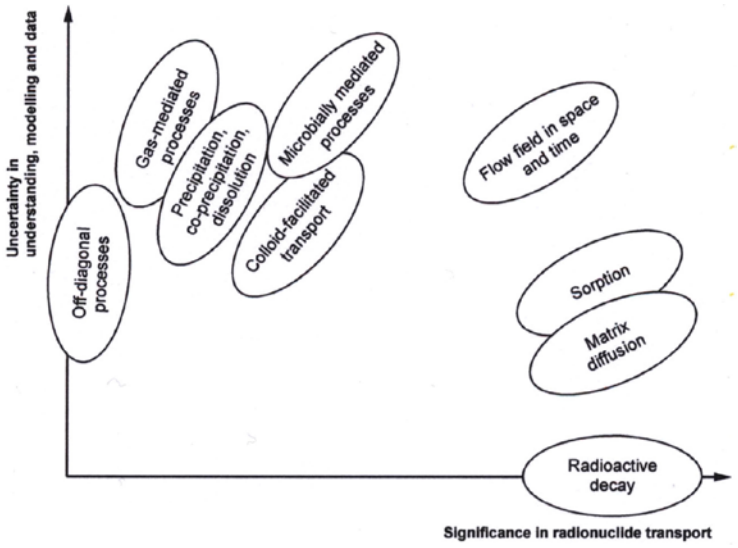

Figure B-2. *The uncertainties in the treatment of retention and transport processes versus their PA relevance were assesses early in the project with this kind of graph. The participants' opinions on the sketch were not fully coherent, but the graph was found to be useful tool in communicating the views. A difficulty in placing many of these processes in a simple graph stems from their site- and concept-specificity. (from RETROCK 2005)*

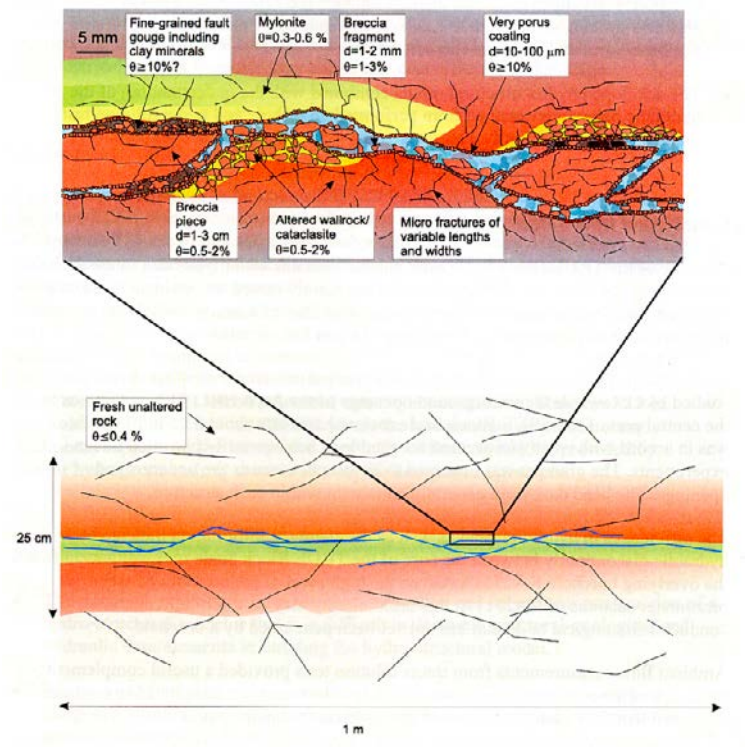

Figure B-3. *Illustration of the present conceptual model as given by the TRUE project.*

B2.2 Information from site scale models

The strategy of Task 7 is to proceed from large scale analysis and models towards smaller scales. We will follow this strategy and first evaluate what input site scale models can provide.

The distribution of inflows to deposition holes for an open repository has been analyzed in Svensson (2006b). The main objective of that work was to find the number of deposition holes that could be expected to get an inflow exceeding a certain critical inflow. It was however also analyzed what the flow at these high inflow points would be under closed (or undisturbed) conditions. Illustrations of these results are given in Figures B-4, B-5 and B-6.

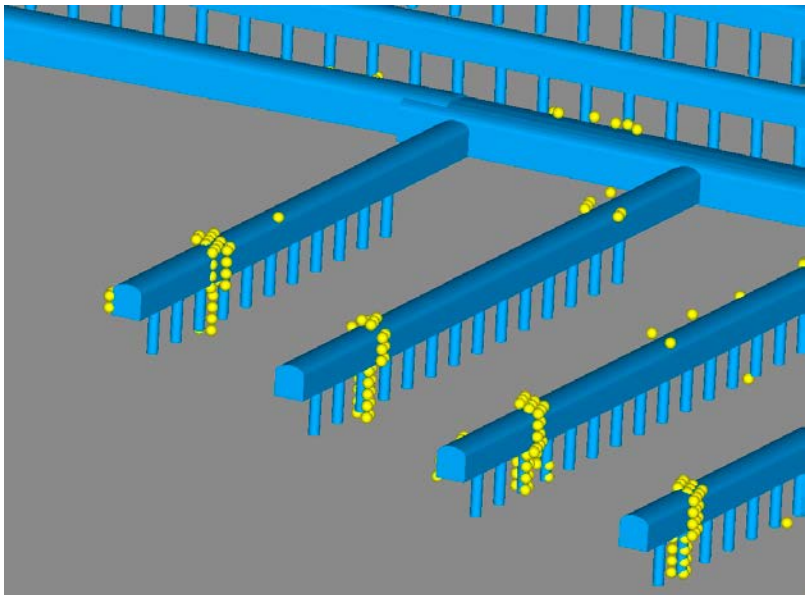

Figure B-4. *Close up view of South-West part of the Laxemar repository. Cells with an inflow larger than 0.05 l/min are marked.*

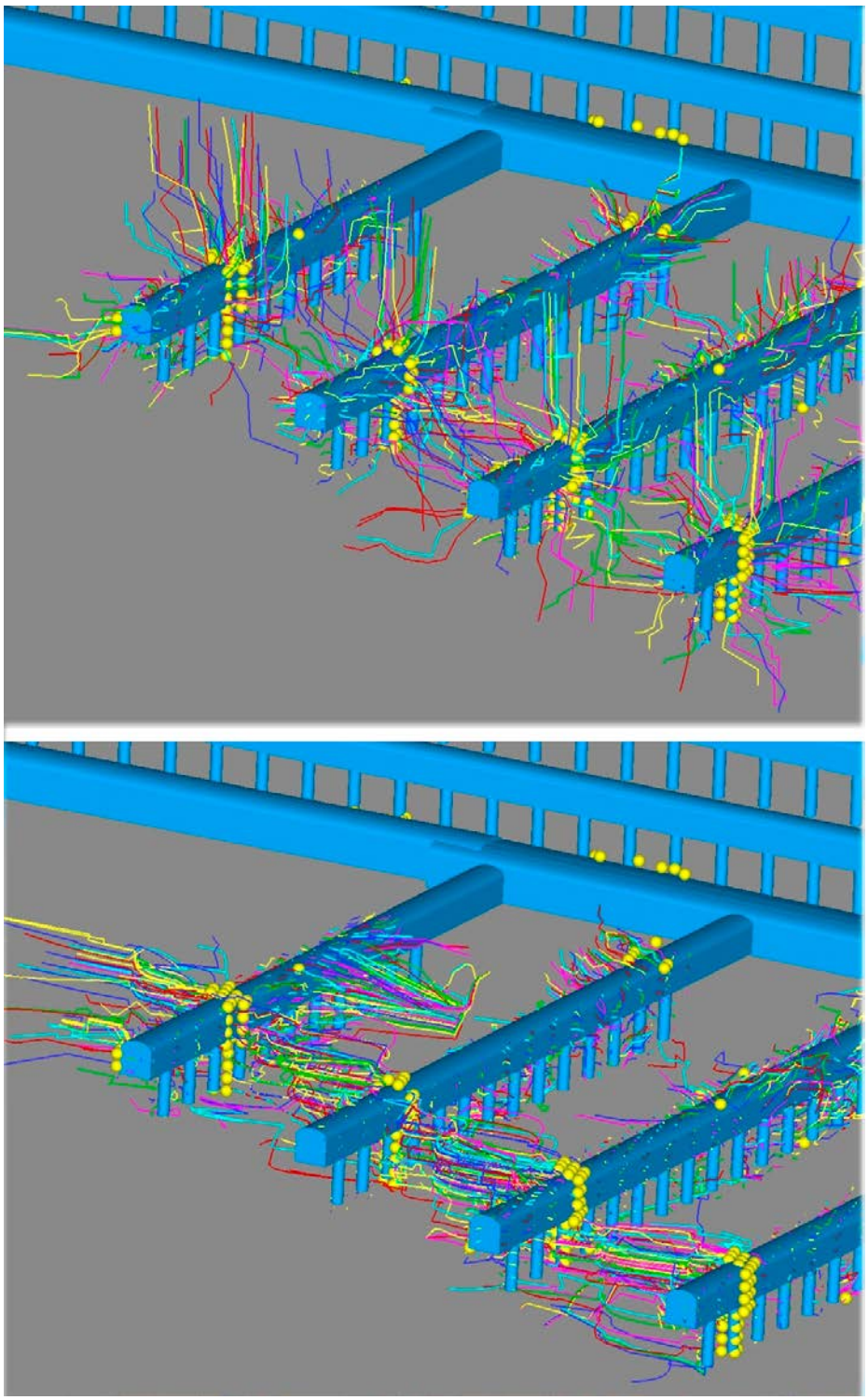

Figure B-5. *Backtracking of particles for open repository (top) and without a repository. Integration time is one hour for the open repository (top) and 100 days for undisturbed conditions.*

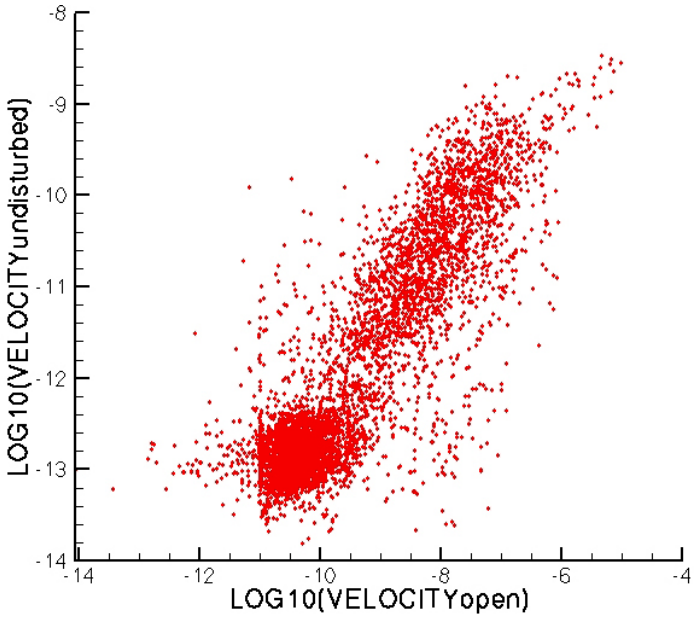

Figure B-6. *Cross-correlation between Darcy velocities (in m/s) at the same location for open repository and undisturbed conditions.*

By placing a box around a deposition hole and calculate the flux through the faces of the box, we can obtain the flow that passes the deposition hole. It is straight forward to do this for all deposition holes and get the statistical distribution of the flux. This is of course valuable information for our problem, as defined in Figure B-1.

Our main concern in this report is the groundwater flow distribution and it is then natural to question if the inflow distribution to the deposition holes can be trusted. Do we have the right channelling in the model? As discussed above, recent evidence suggests that the network of flow channels is sparse with very unevenly distributed flow rates. Site scale models are, as known to the author, never or seldom analyzed with respect to the distribution of flow channels. For PA transport simulations, as defined in Figure B-1, it seems essential to improve our current understanding of this problem.

In order to illustrate this point, some results from Task 6E (Svensson 2006a) are re-examined, see Figures B-7 and B-8. A brief description of the case is "the flow through a box, 200×200×200 m^3, driven by a pressure difference between the low and high x-faces". The fracture network is built up of 30 large fractures and about 5,000 smaller background fractures. In Figure B-7 a contour plot of the velocity in the x-direction (note that the flow is in the negative x-direction) is shown and also the flow vectors through this plane. All fractures were given a uniform transmissivity, i.e. no variation in the fracture plane. We find that five spots have a Darcy velocity magnitude above 10^{-10} m/s. In Figure B-8 the corresponding results for a variable fracture transmissivity (details are left out) for the 30 largest fractures are shown. Now we find that about fifteen spots have a Darcy velocity magnitude above 10^{-10} m/s, even if the flow through the box is about the same. The maximum velocity in the plane is also about ten times larger. Is this a more realistic picture? It is tempting to try to answer this question by making reference to the Stripa experiments or the inflow distribution to the Äspö Hard Rock Laboratory. However, we should note that for the PA problem we need to consider flow under natural condition (head gradients), while all observations from tunnels and boreholes concern strongly forced conditions.

We will conclude this section by rephrasing the above question in a slightly more general form: "If a plane, 100×100 m^2, is placed at repository level and the spots that make up 90% of the total flow through the plane are marked, how many spots do we need to mark?" This for natural conditions.

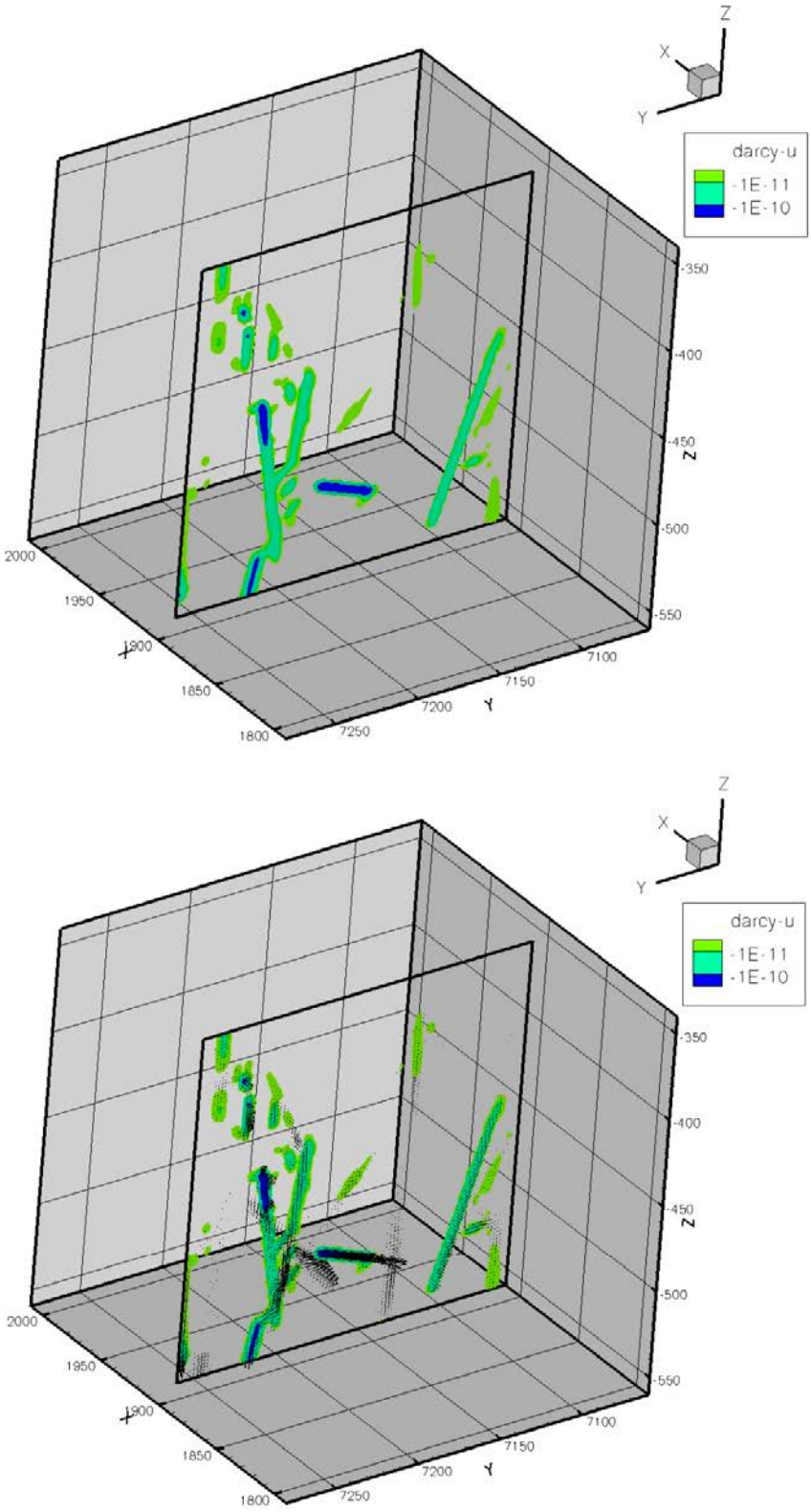

Figure B-7. *Contour plots (top) of x-component of the Darcy velocity. Contours above 10^{-12} m/s are blanked out. Corresponding flow vectors (bottom). No transmissivity variation in fracture planes.*

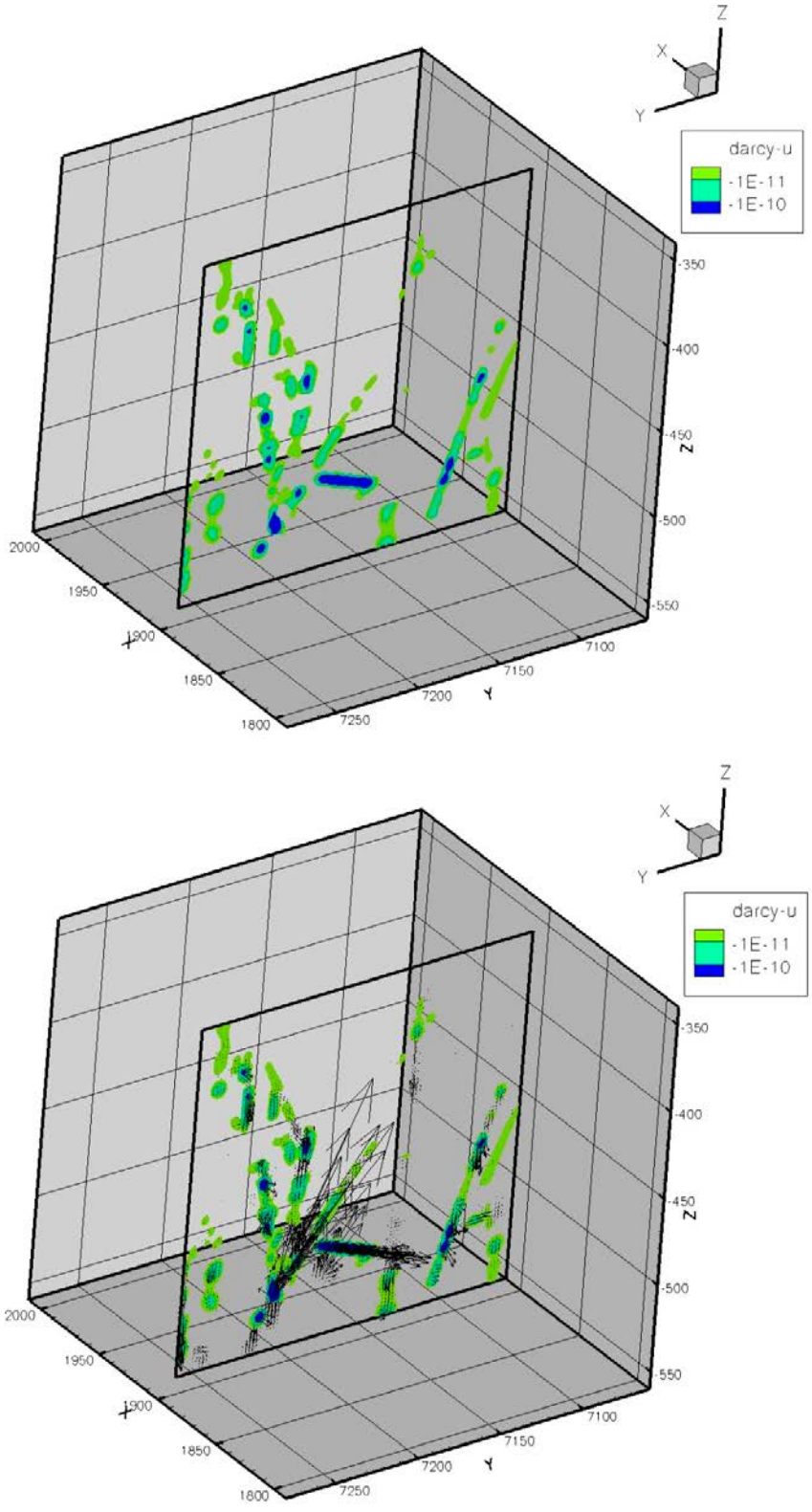

Figure B-8. *Contour plots (top) of x-component of the Darcy velocity. Contours above 10^{-12} m/s are blanked out. Corresponding flow vectors (bottom). Variable transmissivity in the fracture plane for the 30 largest fractures.*

B2.3 Flow paths in a fracture

For the sake of the arguments we will now assume that the site model can provide the flux that passes a certain deposition hole. We then find that we are faced with the same problem again "How is this flux distributed?".

For the case shown in Figure B-5 it was found that the flux is about 10^{-9} m^3/s and the head gradient about 10^{-3} m/m. Let us see the implication for the quantity "flow wetted surface divided by the flow", or transport resistance, for two very different assumptions.

A cylinder

A pipe flow analysis gives the diameter of the pipe as 1.6 mm. For a 1 m long pipe we then get $\pi \times 1.6 \times 10^{-3} / 10^{-9} \approx 5 \times 10^6$ s/m.

Ten channels with rectangular cross section

If we instead assume that the flux is carried by ten flow channels of a rectangular cross-section we get the following numbers. The width is assumed to be 0.1 m (see above) and the aperture will be small enough not to influence the flow wetted surface. Hence $2 \times 0.1 \times 1 / 0.1 \times 10^{-9} \approx 2 \times 10^9$ s/m.

It is generally agreed that the transport resistance is a key parameter in PA transport simulations and our simple examples then well illustrate how important the flow path geometry is.

In order to proceed we will assume that the flux passing one deposition hole is due to one channel with a rectangular cross-section. If the flux is 10^{-9} m^3/s, the head gradient 10^{-3} and the width 0.1 m the cubic law gives an aperture of 0.3 mm.

Fracture surface roughness is an additional complexity that needs to be considered. It has been well established that the roughness affects the transmissivity of a fracture. It will certainly also affects the flow path within the fracture plane, as the flow will seek out the path with the lowest resistance. For transport simulations it is essential to consider the variation in aperture as it will result in regions of slowly moving or stagnant water in the fracture plane. According to Neretnieks (2006) these stagnant volumes are important, as they can add to the exchange between the flowing water and the matrix.

B2.4 Transport simulations

So far we have been concerned with the groundwater flow distribution. In this section we will assume that a relevant flow channel has been established, i.e. we now consider the flow rate, head gradient and typical cross-section size as known. It is then time to focus on the transport problem. The common way to consider the rock surrounding the flow path, i.e. the matrix, is to assume homogeneous conditions for a layer of a certain extent. The exchange between this layer and the flow channel is due to diffusion. In our key references (Section B2.1) it is however argued that this is a too simple view. We need, for example, to consider the stagnant water in the fracture plane and also the distribution of the connected porosity in the matrix.

For these reasons we will introduce a novel micro scale model that has the potential to accommodate a detailed description of both the flow channel and the matrix. The main features of this model are:

- The flow channel can be given any basic cross sectional shape (rectangular, circular, ellipse, diamond, etc). The fracture walls are given a "topography" in order to simulate roughness. The roughness model is based on a self similar fractal approach with the fractal dimension (or Hurst exponent) as an input parameter.
- The matrix is generated as a fracture network with fracture lengths down to the mm scale. Fractures are given transmissivity, porosity and diffusion coefficients and advection in the matrix is hence possible.
- Flow in the open fracture is solved by a direct application of the Navier-Stokes equation. In the matrix a linear resistance term is added.
- Transport is simulated by an advection/diffusion equation. The flow channel and the matrix is considered as a single computational domain with variable advection and diffusion properties.

By such an approach, it is clear that we do not need to explicitly specify many of the commonly used parameters (LW/Q, hydraulic and transport apertures, etc). However, other parameters are needed but it is argued that these are "more physical" and can be measured. A drawback of the approach is that it is computationally heavy as we attempt to resolve a number of small scale features explicitly.

The computational tool is DarcyTools (Svensson et al. 2010), which includes a Navier-Stokes solver. Here a few sample results will be discussed.

A two dimensional fracture

Our first case concerns a two-dimensional fracture with rather complex geometry, see Figure B-9. The total length of the fracture is about 1 metre and the largest aperture about 0.5 mm. The fracture is embedded in a matrix where we specify a fracture network with fracture sizes from 5 mm to 0.25 metre; these fractures have an aperture of 0.1 mm and a constant transmissivity of 10^{-6} m^2/s.

With this case we want to demonstrate the coupling between the channel (where the Navier-Stokes equation is solved) and the matrix. First the steady flow problem is solved, after that the transport of a conservative tracer is discussed.

Results

The computational grid is illustrated in Figure B-10. The fracture walls are resolved with grid cells of dimension 0.03 mm (in aperture direction) by 0.5 mm. An explicit resolution of the fracture coating is hence within reach.

Streamlines and vector plots are shown in Figure B-11. The streamlines show that temporary excursions into the matrix occur and that the two branches of the fracture are connected by the fracture network. In the top figure the velocity vectors in the channel have been blanked out in order to see the flow pattern in the matrix. The contour in the figure represents the permeability with blue colour giving the lowest values (the solid rock). In the lower figure the flow field in a cavity is shown; the fracture network connects the cavity to the main channel.

Finally the transport problem is addressed. A Dirac pulse is introduced at the inlet of the steady flow field. The tracer distribution at three times is found in Figure B-12 and the break through curve in Figure B-13. The main thing to note is that the tracer interacts with the matrix, as is suggested by our present conceptual view.

Figure B-9. *A two dimensional fracture.*

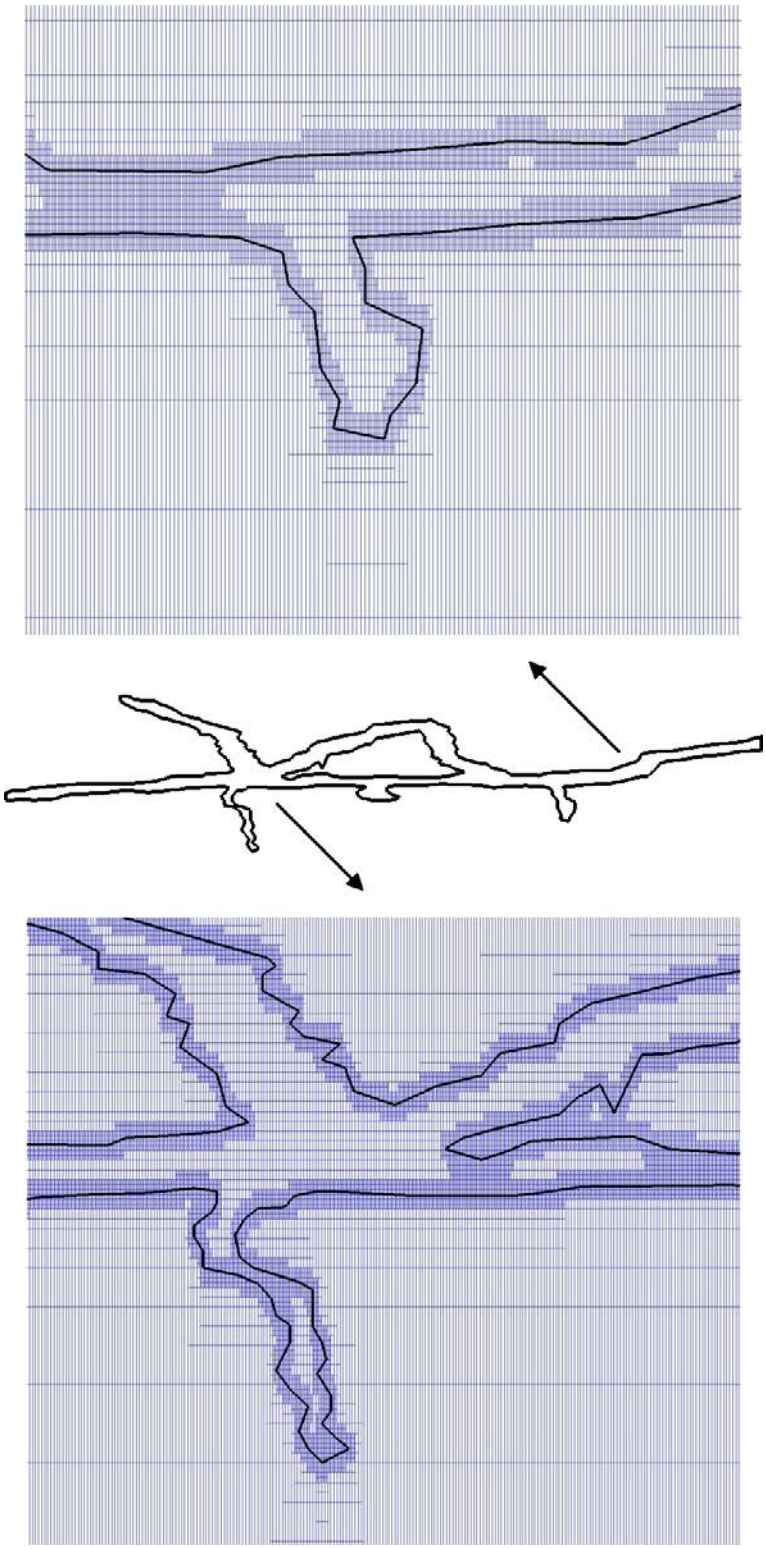

Figure B-10. *Computational grid for a two-dimensional fracture.*

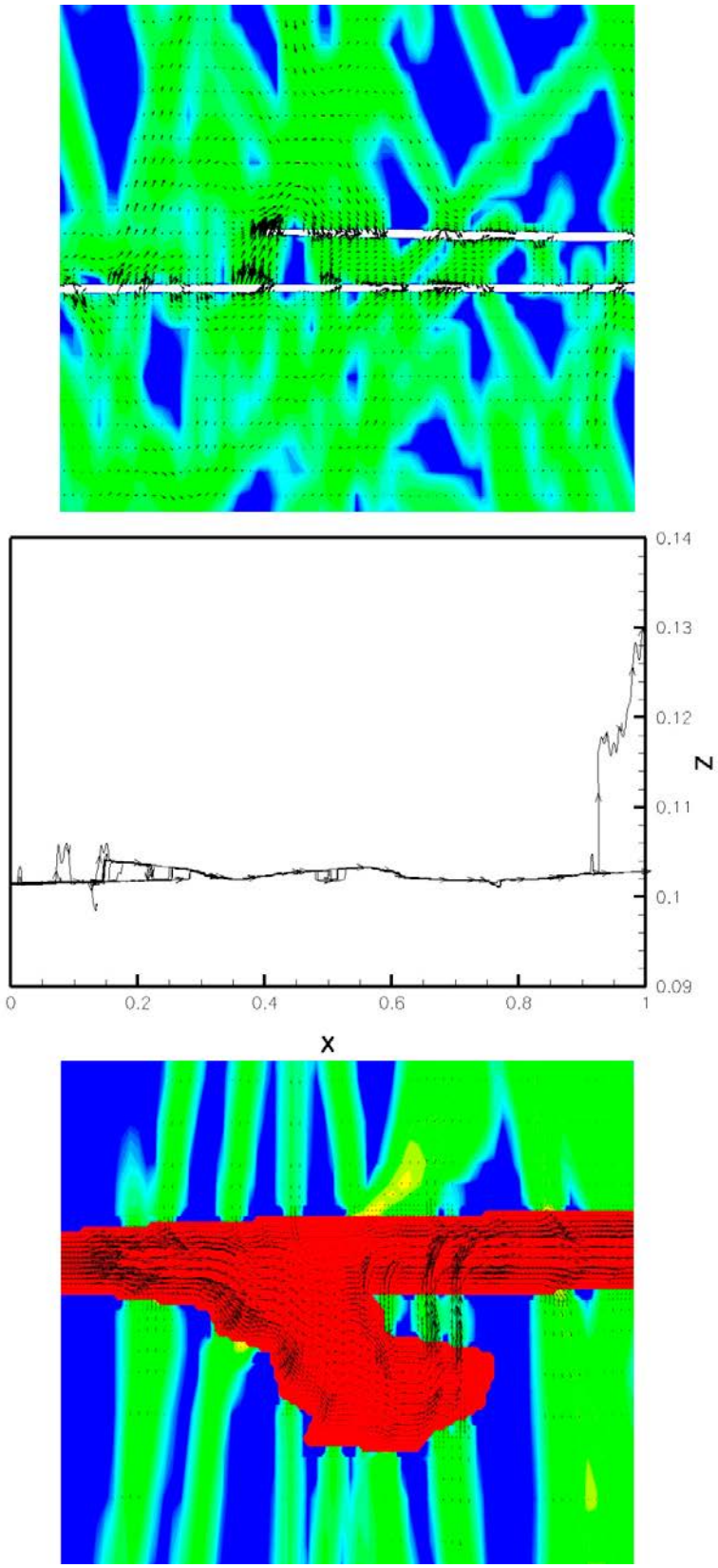

Figure B-11. *Streamlines (middle), flow in the matrix (top) and flow in the fracture. The top figure is at x = 0.15 m and the bottom at x = 0.75 m.*

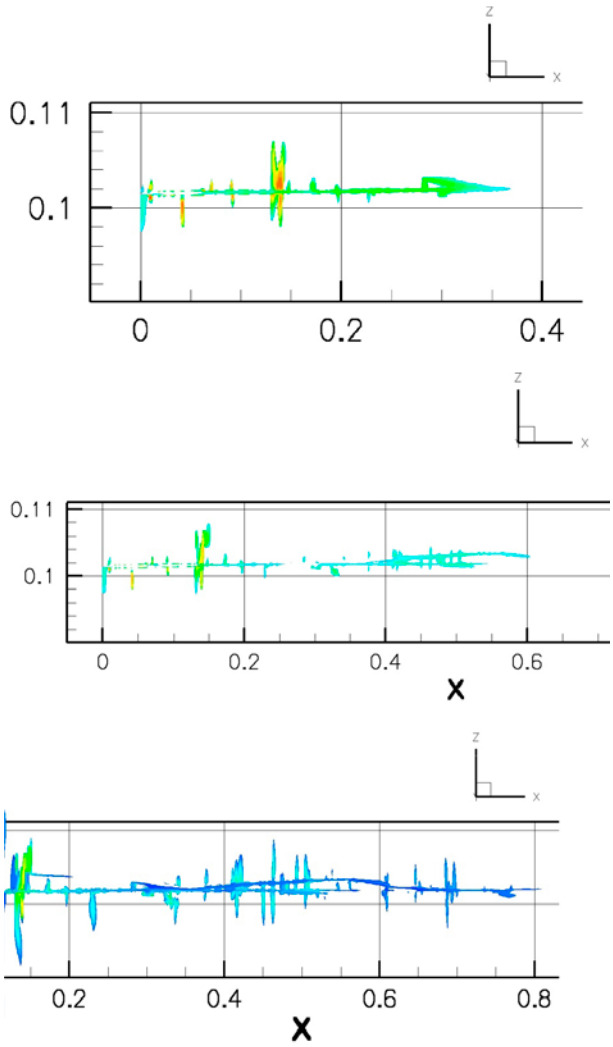

Figure B-12. *Tracer distribution at 10 h (top), 20 h (middle) and 30 h (bottom).*

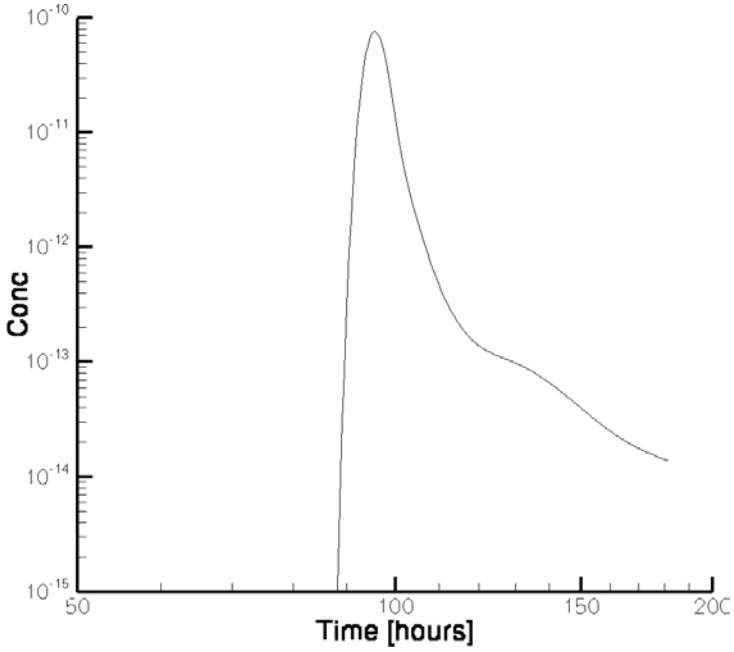

Figure B-13. *Break-through-curve.*

A three-dimensional fracture

The next case to be discussed deals with a three dimensional fracture with wall roughness, embedded in a matrix with a fracture network (with length scales from 5 to 250 mm). The basic cross section of the fracture is diamond shaped with a maximum aperture of 0.4 mm and a width of 100 mm. The application of wall roughness will however modify this basic shape significantly. The matrix will extend 0.1 m out from the channel and as the length of the channel is 1 metre, the computational domain is $1.0\times0.3\times0.2$ m^3.

The purpose of this case is to introduce a cross sectional fracture shape and to demonstrate that a fully three dimensional simulation can be carried out.

Streamlines and a contour plot of the main velocity component in a mid-plane can be found in Figure B-14. The maximum velocity is about 10^{-5} m/s.

Finally the transport of a conservative tracer will be studied. The tracer is inserted as a Dirac pulse and the distribution in the midplane at four times can be studied in Figure B-15.

B3 Discussion

The report emphasizes two aspects of PA transport simulations; the groundwater flow distribution and the micro-scale model. Let us use the discussion section to elaborate these issues further.

It is the present writer's opinion that the groundwater flow distribution is a topic that needs much further consideration, from the km down to the mm scale. When the inflow distribution to an open repository is evaluated it is obvious that the number of flow channels per unit area (see Figures B-7 and B2-7) will influence this distribution. Many of these flow channels will be the active flow channels also for PA conditions and the large scale distribution is hence relevant for PA. On the mm scale we need to understand the role of stagnant water volumes, wall roughness, etc in order to be able to determine the access to the matrix. In this work it is suggested that a fracture geometry should be generated and the flow inside the fracture should be calculated explicitly by solving the Navier-Stokes equation. This approach eliminates the need to specify many semi-empirical parameters, but does on the other hand require realistic fracture geometries. Recent work see Figure B-16, may however provide this input.

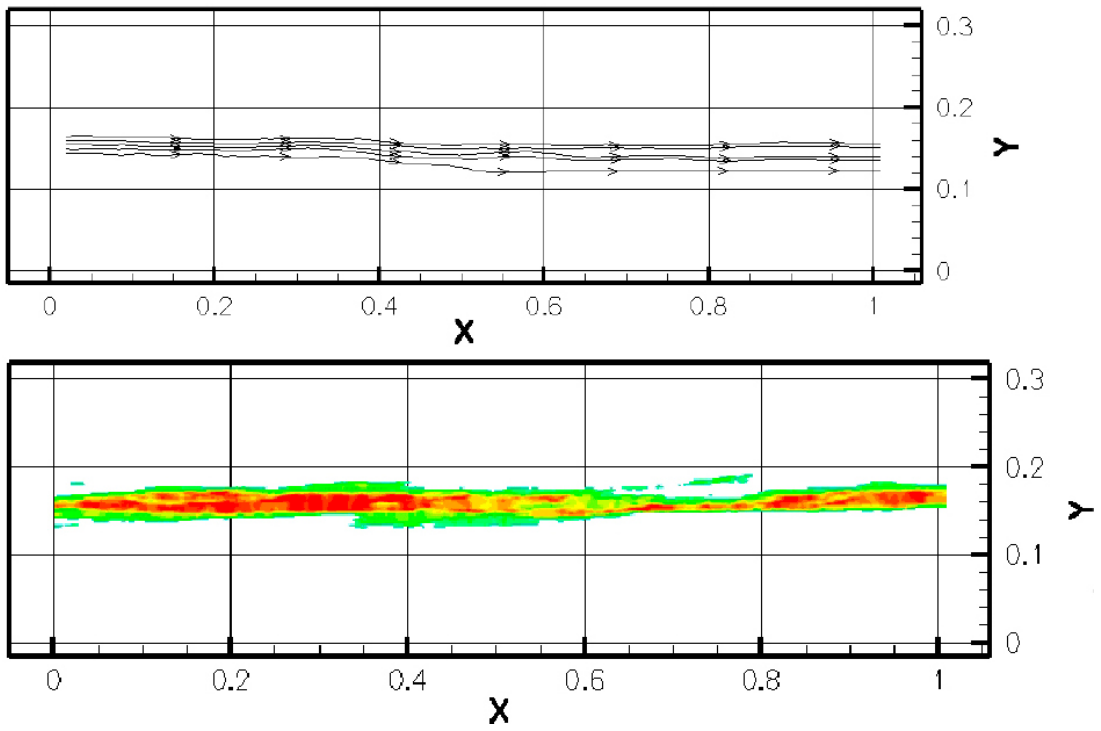

Figure B-14. *Streamlines (top) and x-velocity contours at the fracture mid-plane.*

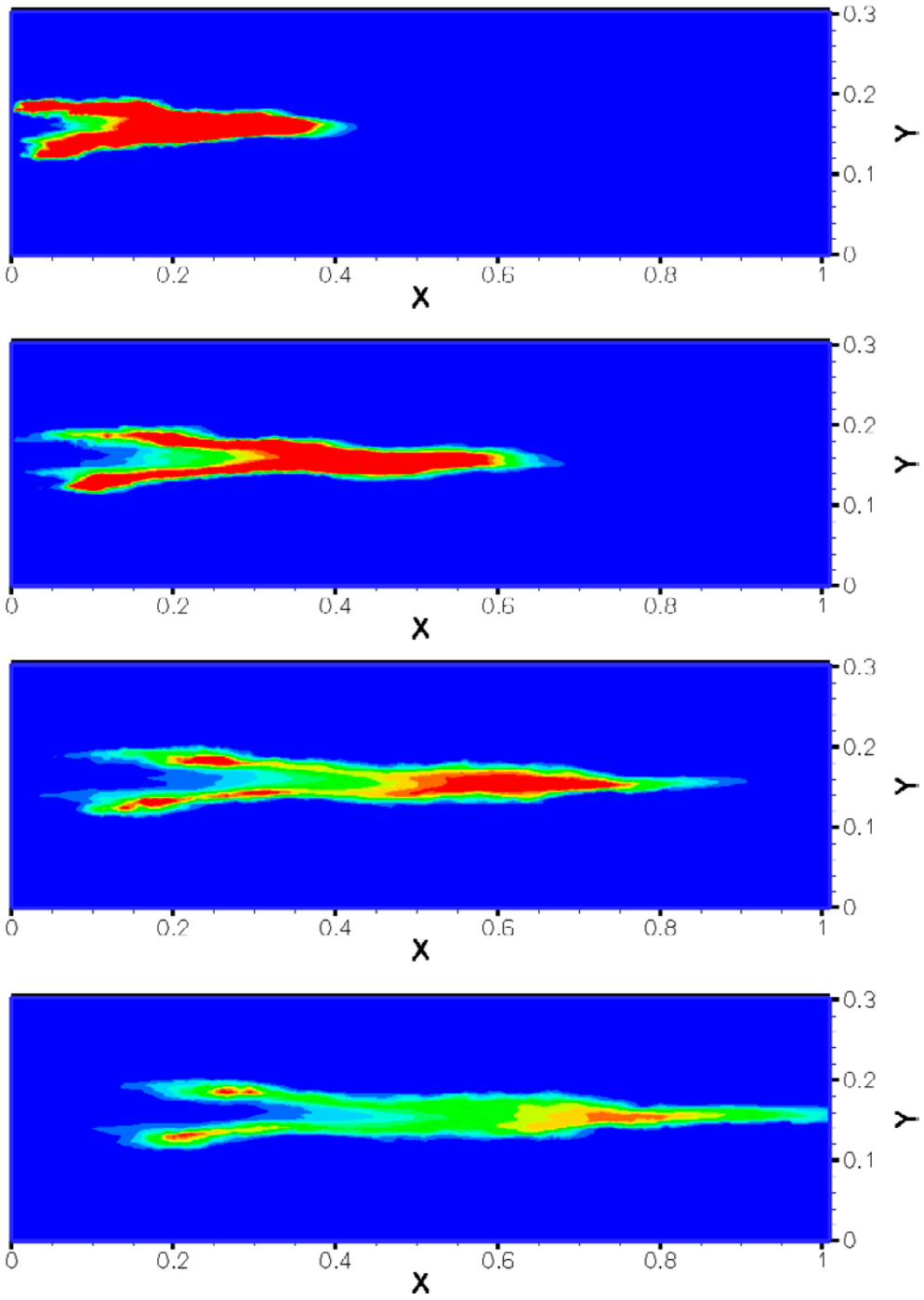

Figure B-15. *Tracer distribution at 10, 20, 30 and 40 hours.*

A micro scale model has been introduced in this report. This model deals with both the flow channel, as discussed above, and the matrix. It attempts to mimic the present conceptual view as given in Figure B-3; this conceptual view seems to be supported by the photo shown in Figure B-16. The matrix of the micro scale model is accordingly built up of a 3D fracture network with fractures down to the mm scale. It is argued that this allows for a comparison with measurements in a fairly direct way; one may for example compare how the connected porosity decreases with distance from the flow channel. It would also be interesting to see how the matrix properties relate to the break through curve (like late time slope). However, the micro scale model has only recently been suggested and only demo-style simulations have so far been carried out.

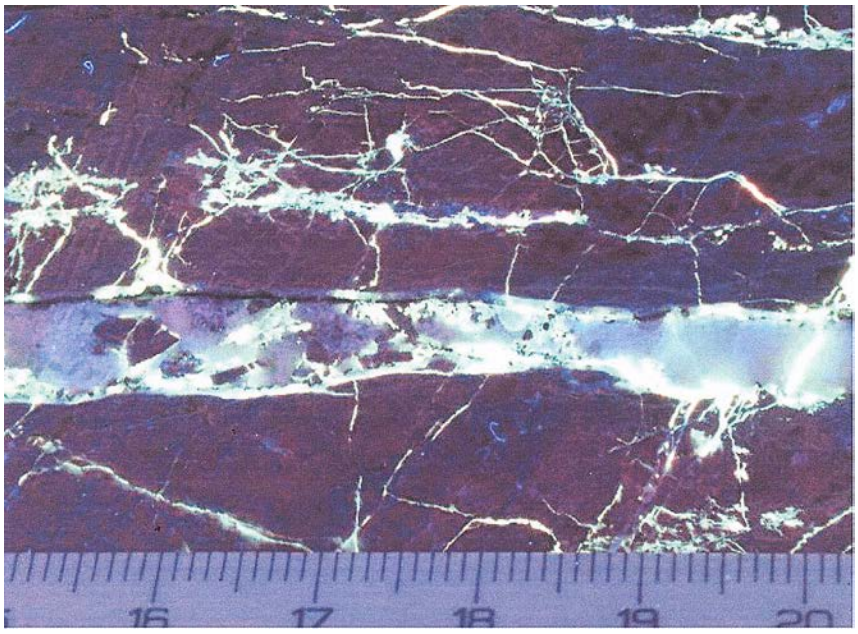

Figure B-16. *A photo (Hakami and Wang 2005) of a fracture (note the scale).*

B4 Concluding remarks

Looking back on the Task 7A3 description one may question if the content of the report is in line with the intentions of the task. At a first glance this can perhaps be difficult to motivate, but it should be noted that:

- The information from a pumped borehole, like KR24, is here replaced with the information from a site scale model, as we can then directly obtain the flow passing a deposition hole. However, if this information is not available we could perhaps use the information from the pump test, although it is not clear how this should be done.
- The list of transport parameters that should be derived is considered by the present work in two ways; either we can obtain the parameter or we do not need it in the present formulation.
- We have followed the recommendation that "results will be defined through discussion points and example calculations" as well as a discussion of a micro-structural model.

In conclusion one may say that the report does not link PA relevant parameters to borehole information, but suggests anyway an approach to obtain relevant PA parameters. This approach puts focus on weaknesses that have been identified in recent papers and reports.

Basic concepts of the Task 7b model

(Presented at a project meeting in Oxford 2008-05-13)

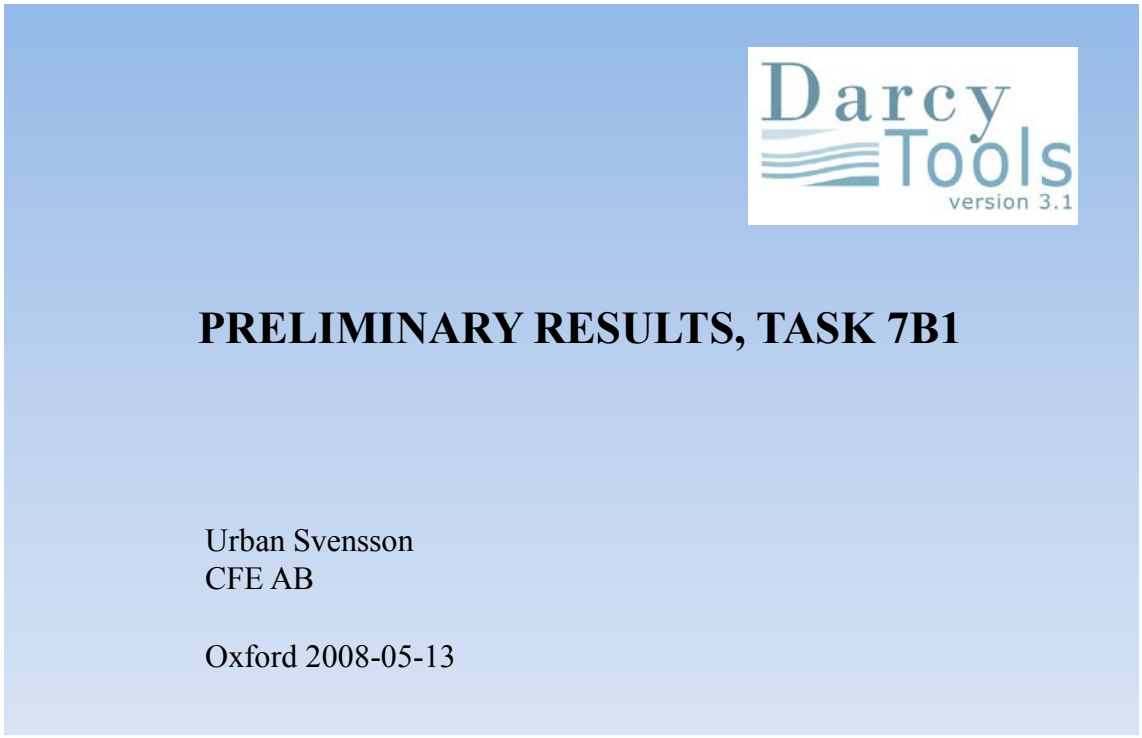

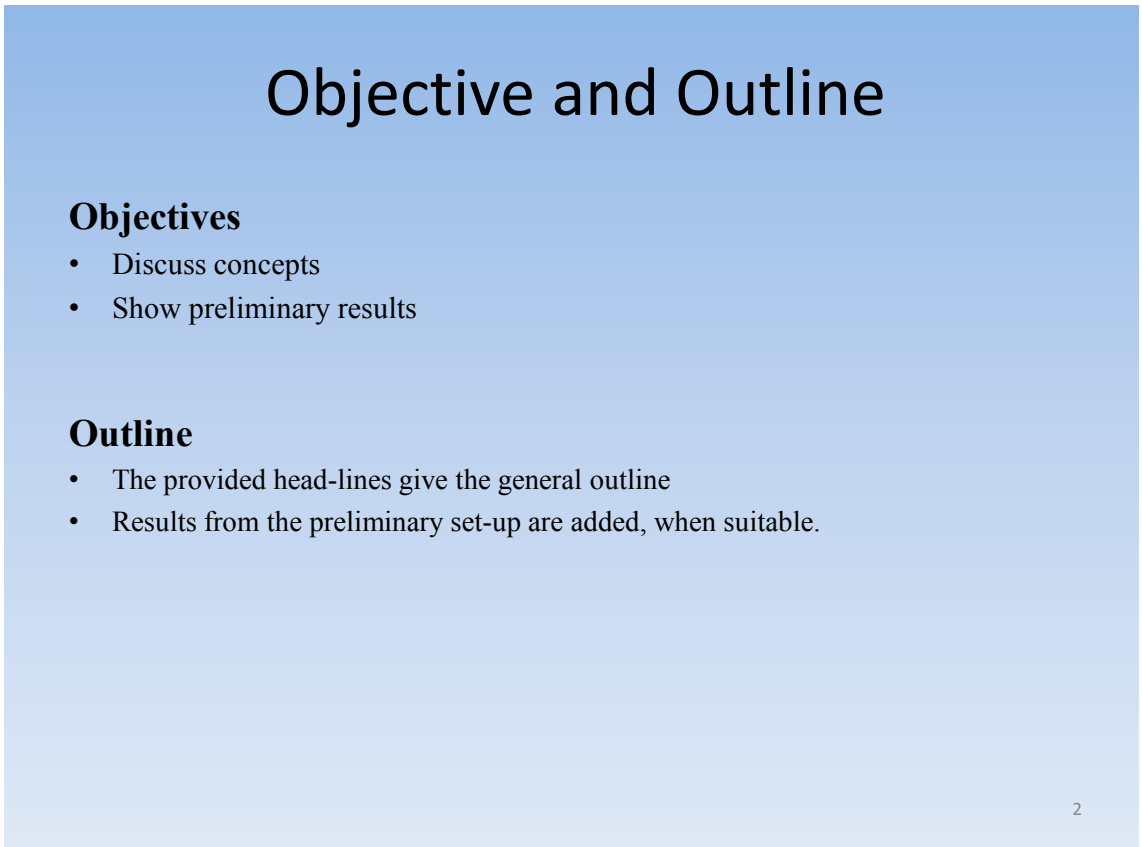

Model Boundary Conditions

Task: Derive and justify boundary conditions and treatment of boreholes.

Approach: Include the whole regional domain and refine the grid successively down to the borehole size. Use a ”free groundwater table method”, with P-E specified.

Arguments

- For undisturbed conditions (and PA) pressure gradients result from large scale topography.
- Boundary conditions are far away and “natural”.
- Generality; basically the same model as for KR24 test.
- The approach fits the grid system in DarcyTools.

3

Computational Grid

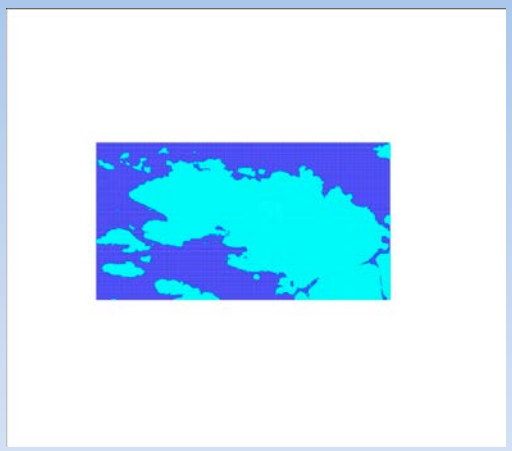

Regional scale

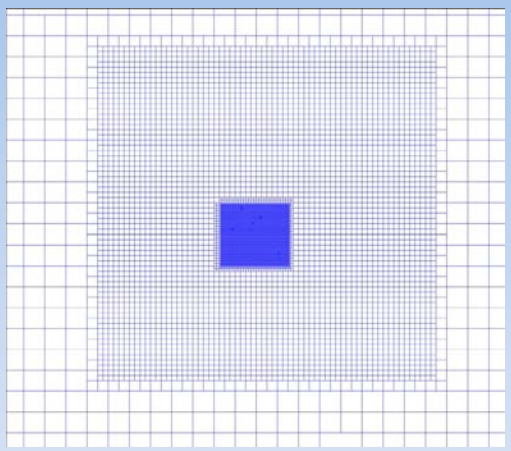

500 m scale

4

Computational Grid

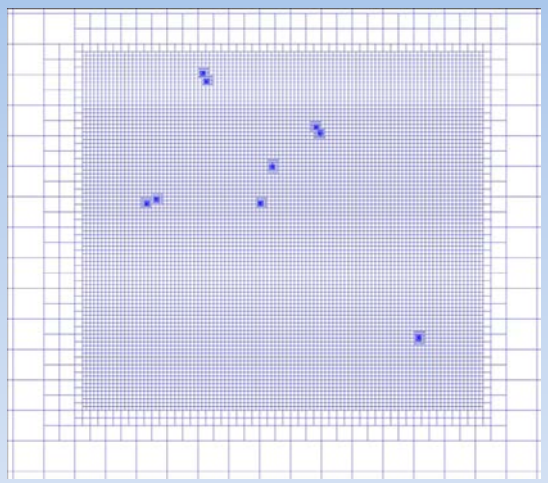

100 m scale

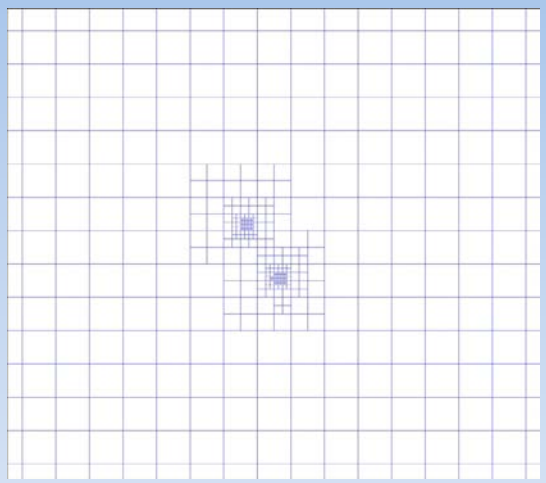

borehole scale

5

Computational Grid

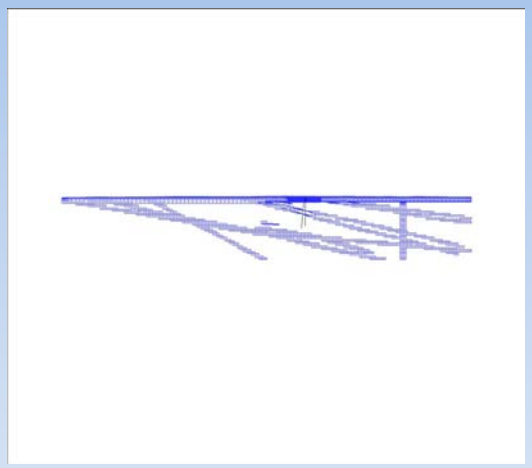

Regional scale

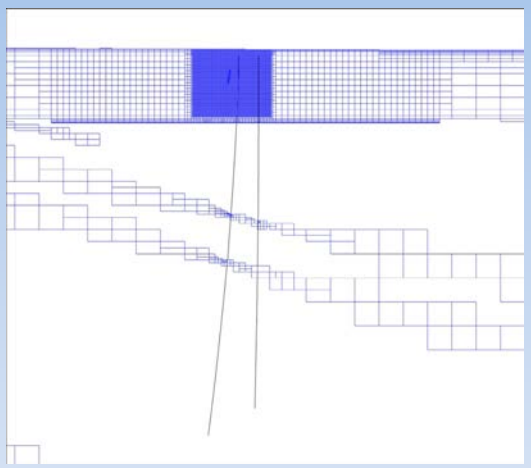

500 m scale

6

Background Fracture Population

Task: Develope and describe a methodology for representing the background fractures in the model region.

Approach: In DarcyTools deterministic and random fractures are represented in a finite-volume grid by the "intersecting volume technique".

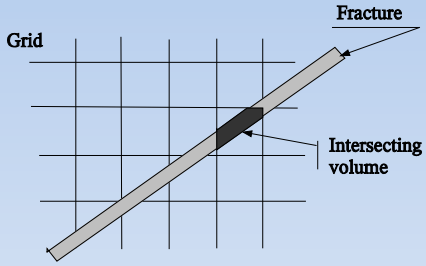

Arguments

- Accurate for both flow, transport and particle tracking.
- Efficient, "millions of fractures represented on millions of cells can easily be handled".

Representation of permeability

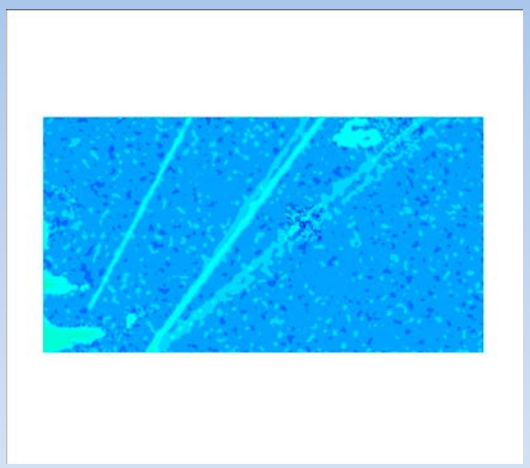

Regional scale

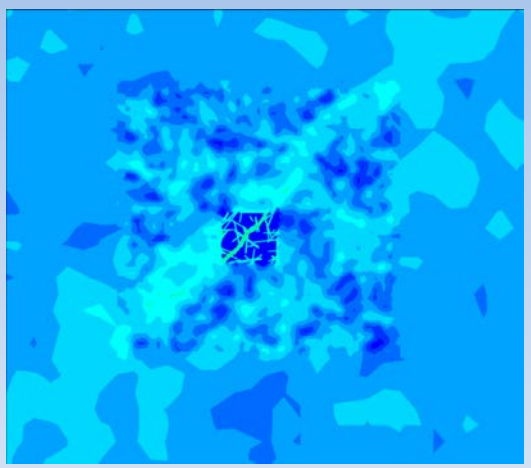

500 and 100 m scale

8

Sequential Model Development

Task: Define approaches for estimation of fracture geometries and properties from a modelling sequence.

Approach:

Case: Äspö			
Input	Performance Measures		
Deterministic zones - Coordinates - Properties (T, n, s, CF, GST,..) Stochastic network - Intensity - Power-law exponent - l_{min}, l_{max} - $T - l$ - $e_2 - T$ - Thickness-l - Fisher-orientation - FWS - CF and GST - Storativity Subgrid network - β_c (total immobile vol.) - α_{min}, α_{max}, k	GEOMETRY	Measured data	1. HPF-frequency [2] 2. P_{32}, P_{10}, etc. 3. Fractal dimension
		Expert judgement	1. Porosities n_{im}, $n_{transmissive}$ [3] 2. α_w-statistics 3. Scale of critical connectivity
	FLOW	Measured data	1. Drawdown data (tunnel, LPT2, etc.). [1] 2. Inflow distribution to tunnel, time dependent.
		Expert judgement	1. Block-conductivities for different scales. 2. Number of flow channels/m^2.
	TRANSPORT	Measured data	1. $\alpha_L / L - 0.05 \rightarrow 0.10$ 2. Water types (Glacial, etc.). 3. Salinity data 4. Tracer experiments, BTC:s.
		Expert judgment	1. F-factor. $F - t$ 2. Trajectory visualisation. 3. Water Residence time.

Compartmentalisation Analysis

Task: Evaluate possible conceptual models and boundary conditions to explain observed phenomena.

Approach: Not needed as this is an property of a sparsely fractured rock.

Arguments

- A high transmissive feature embedded in a media with lower conductivity must have a uniform pressure.
- Glacial water, as an example, can “rest peacefully” for 10 000 years in a dead-end fracture system. This is in agreement with the 1D-diffusion equation.

10

From Äspö-model

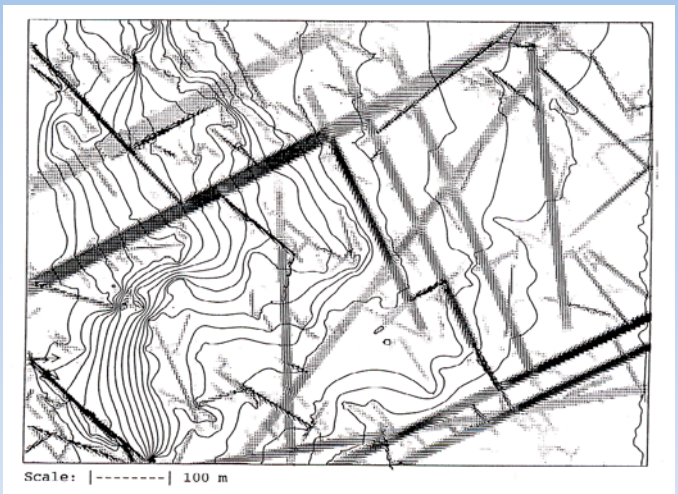

Flow vectors (flow from left to right) and 20 pressure lines.

11

Flow distribution

Task: Evaluate possible generic approaches for utilising the flow distributions measured in single and multiple boreholes. Also cross-flow.

Approach: Explicit resolution of boreholes (cells 0.125 x 0.0625 x 0.0625). Open, packed off and pumped boreholes can be simulated.

Arguments

- Explicit resolution allows a direct evaluation of the flow both along and cross the borehole.

12

Resolution of borehole KR15

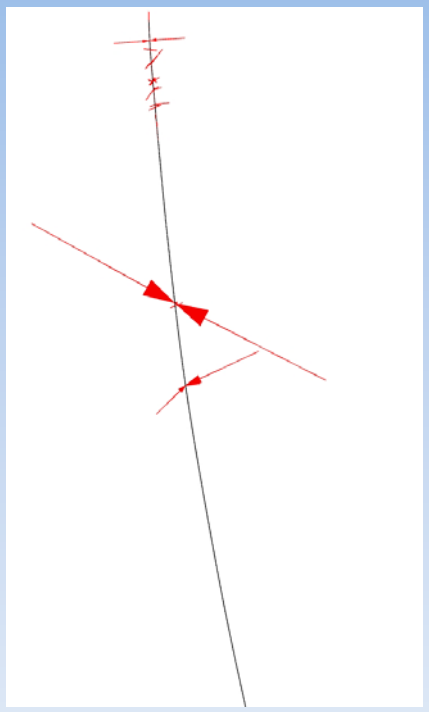

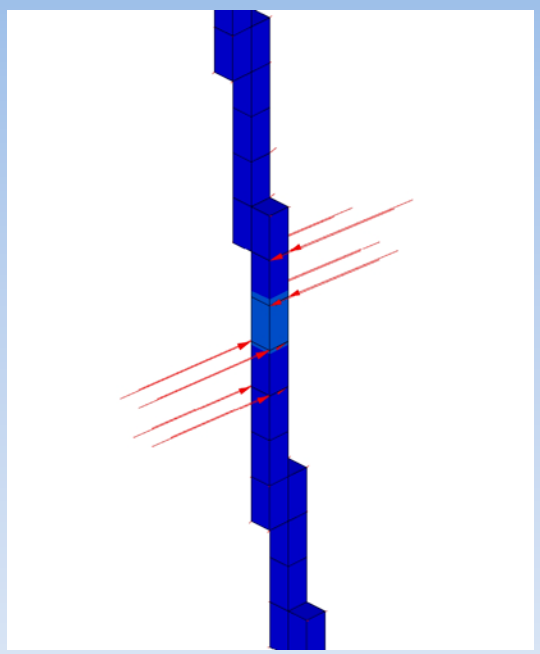

13

Resolution of borehole KR14

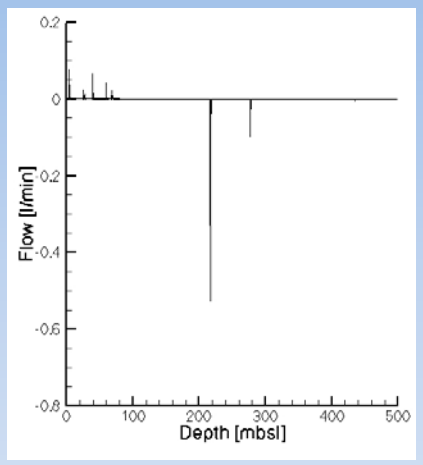

Inflows

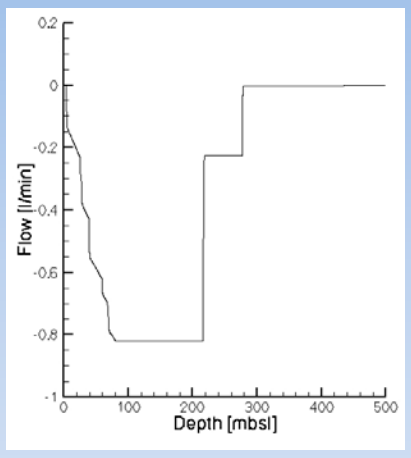

Flow along

14

Concluding remarks

- The PFL data is an interesting challenge for numerical models. We should however look for flow directions and magnitudes of flow, rather than direct comparisons of numbers. This because of fracture heterogeneity.

- Task 7B1 suggests several demanding subtasks often stated by "Develop and describe .....". Probably most modelling groups will use what they have available. Perhaps it should be emphasized that flow along and cross boreholes should be in focus.

15

Appendix D

Various methods to generate heterogeneous fractures in DarcyTools

(Presented at Task Force meeting number 25, Mizunami 2009-10-15).

Task 7C1 & C2

- Preliminary results

Urban Svensson

CFE AB

Mizunami 2009-10-15

Introduction

From the Task Description

Task 7C aims at understanding the near-field scale in regards of flow and responses. Task 7C will consider small sub-volumes surrounding three ventilation shafts of Onkalo at the Olkiluoto site in Finland.

Task 7C1 – Parameterized and Justified Microstructural Model for Three Fractures
The three fractures identified as the focus of Task 7C1 are characterized by borehole, PFL, and hydraulic testing, and draft/shaft mapping. This data includes information that can be processed in a number of different ways to build a microstructural model for fracture roughness and aperture distributions.

Task 7C1 is intended to provide advances in the characterisation and understanding of flow in of low transmissivity single fractures, with particular emphasis on patterns of aperture, including fracture minerals and infillings, channelling, and fracture intersection effects

Task 7C2 – SIMULATION OF FLOW PATTERNS IN LOW TRANSMISSIVITY FRACTURES
Task 7C2 is primarily a simulation task for evaluation of the quantitative fracture microstructural descriptions developed in Task 7C1. The task also attempts to assess the implication of these models for safety assessment and reduction of uncertainty.

2

Objectives of presentation

- Discuss three different methods to generate heterogeneous fractures. The methods are part of DarcyTools V3.3.
- Summarize experiences and questions about the Task.

3

The three methods

A. Multivariate normal distributions. A random number with a specified correlation length is the basis. Anisotropic fields can be generated. All variables (*T, n fws,* etc.) are considered by individual std, but the same correlation structure.

B. Random fractures. The fracture is composed of a fracture network. The fracture network can be specified with respect to fracture lengths, transmissivities, orientation, etc.

C. Fractal surface. A self affine procedure generates a surface with a specified fractal dimension. A basic correlation length can be introduced. Fine scale roughness can be generated.

4

Some details

- All fractures are 30 x 30 metres.
- Transmissivity = 10^{-10} m^2/s.
- Correlation length of *T*-field about 3-5 metres.
- Flow simulation based on a $\Delta h = 1$ m.

5

Method A. Multivariate normal distributions

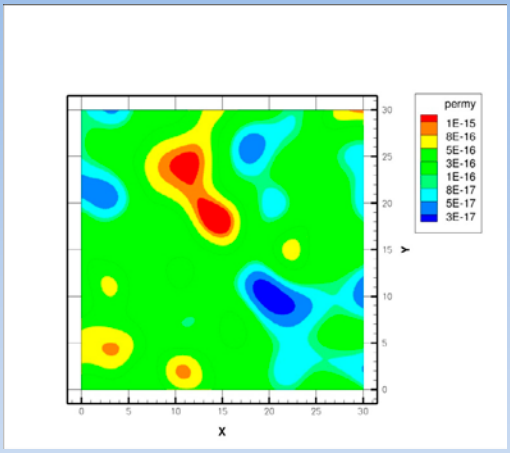

Permeability

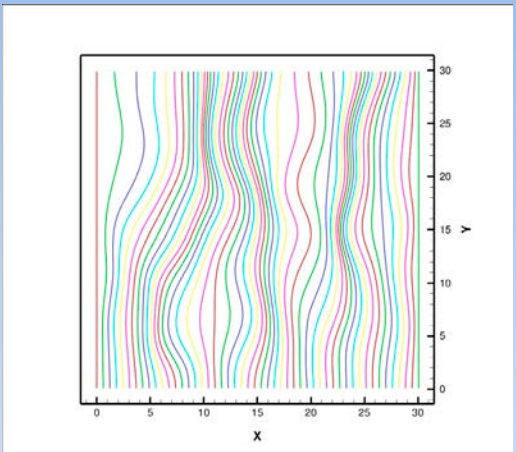

Trajectories

6

Method A. Flow vectors

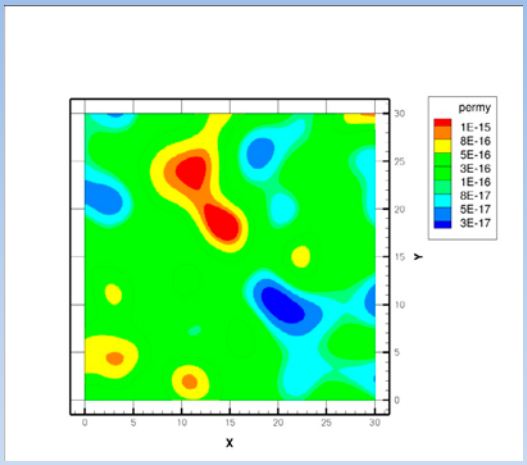

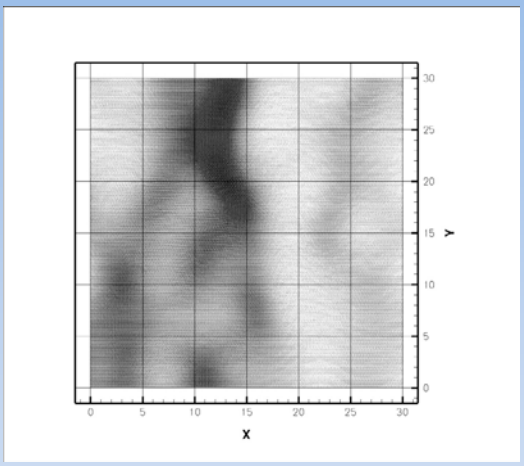

Permeability

Flow vectors

7

Method A. The correlation structure

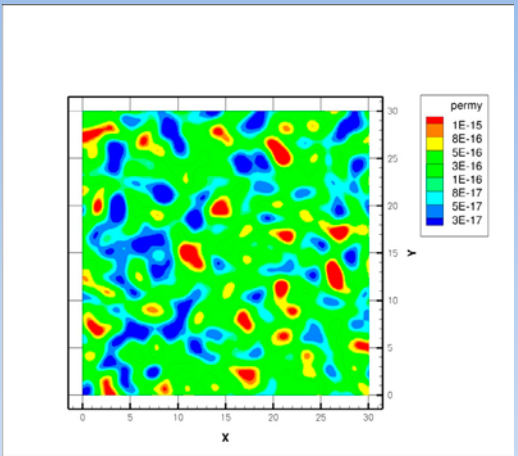

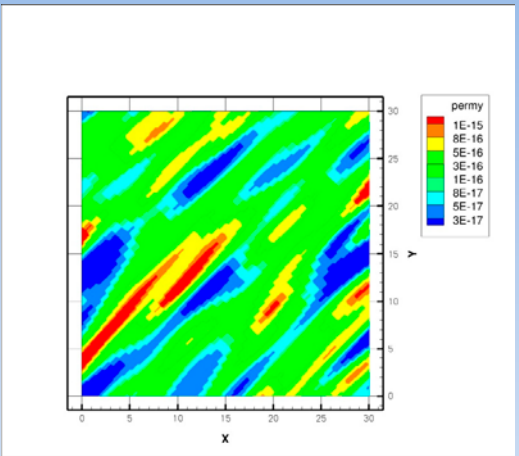

Smaller correlation length

Anisotropic field

8

Method B. Random fractures

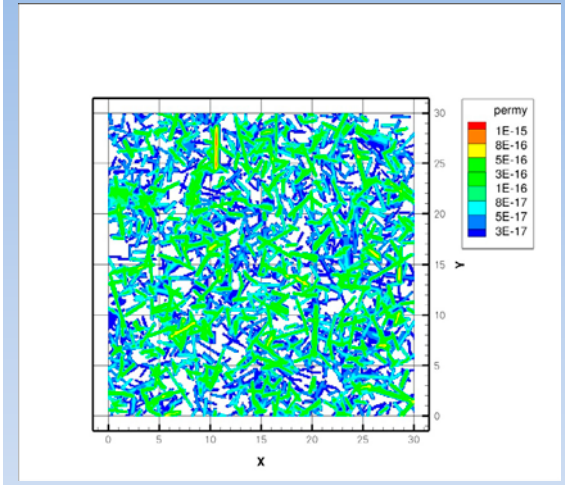

Permeability

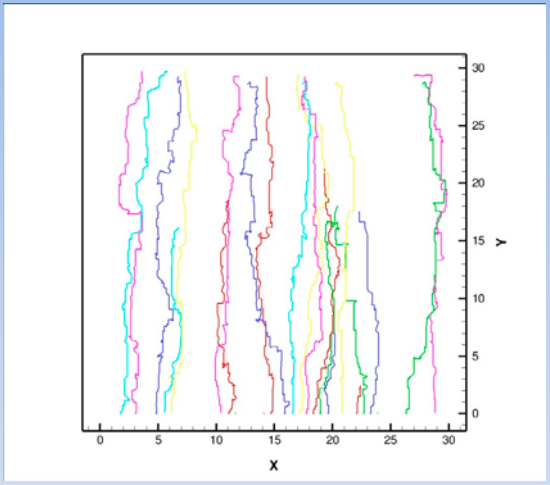

Trajectories

9

Method B. The fracture network

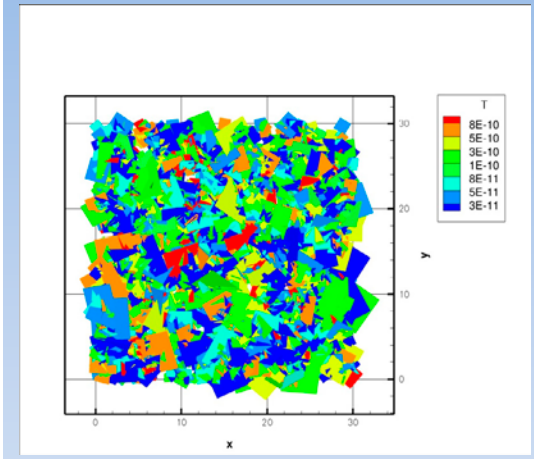

In fracture plane

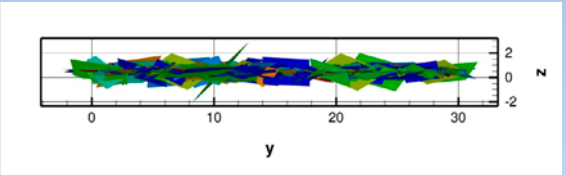

Section

10

Method B. Flow vectors

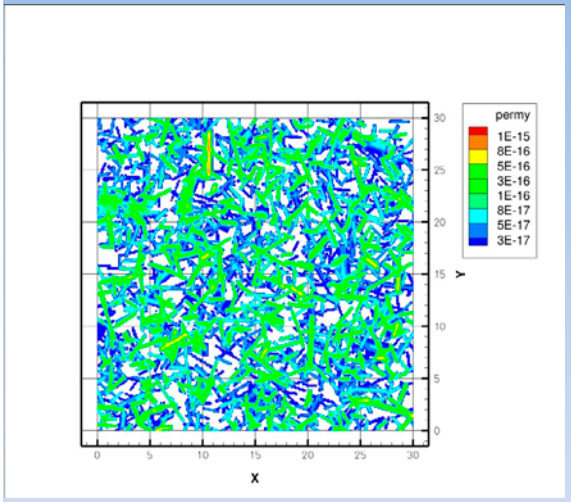

Permeability

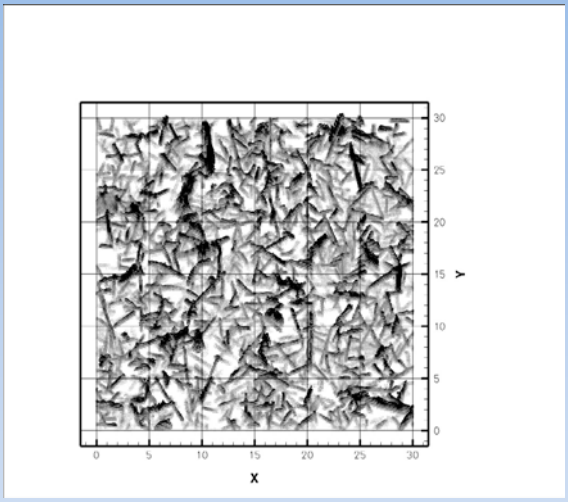

Flow vectors

11

Method B. Another network

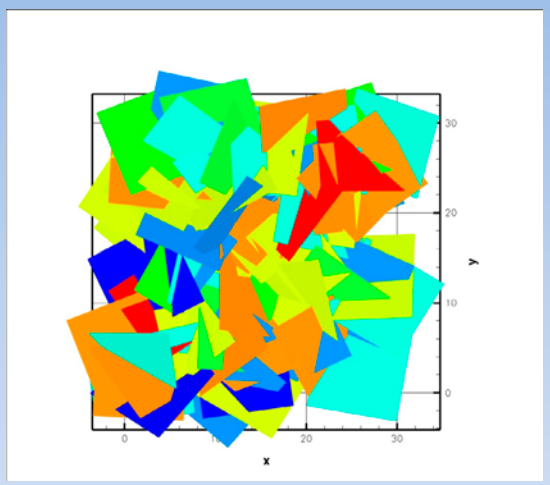

In fracture plane

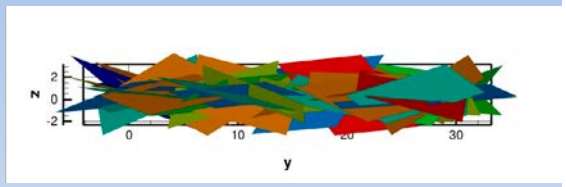

Section

12

Method C. Fractal surface

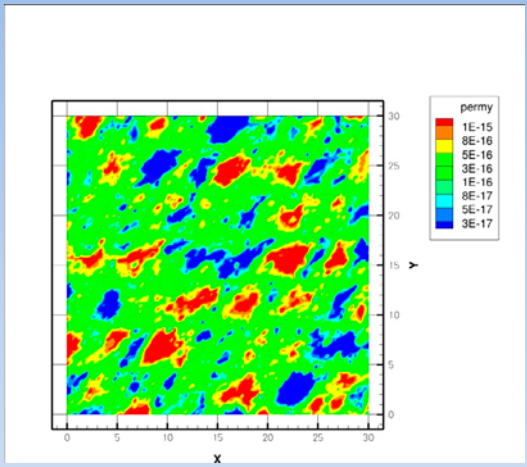

Permeability

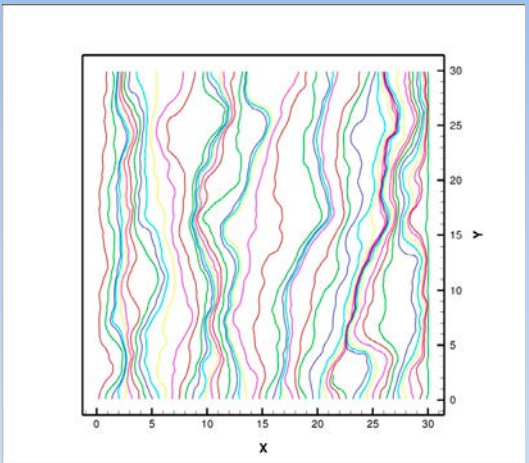

Trajectories

13

Method C. Flow vectors

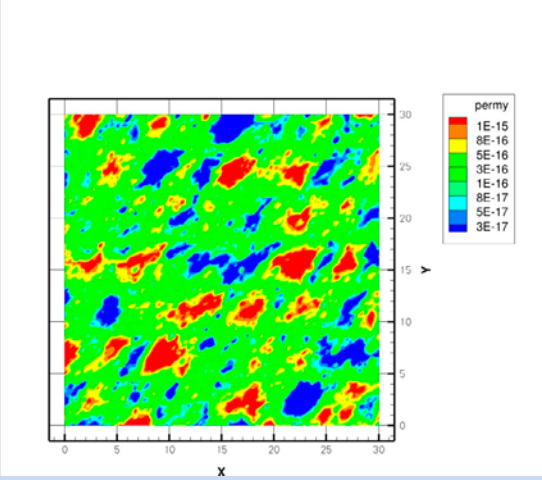

Permeability

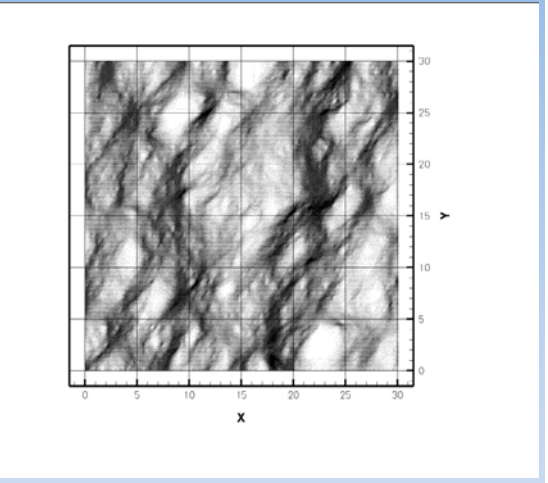

Flow vectors

14

Method C. The fractal surface

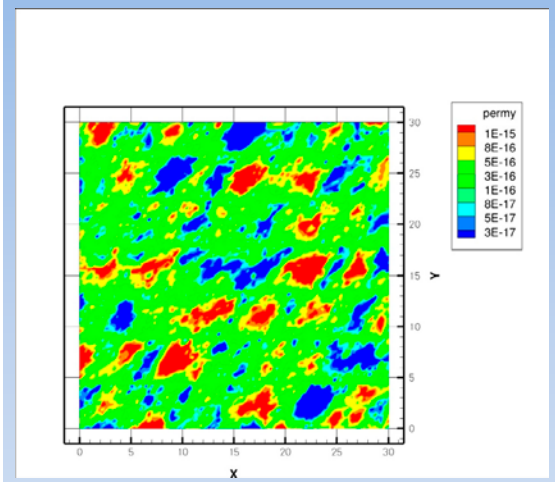

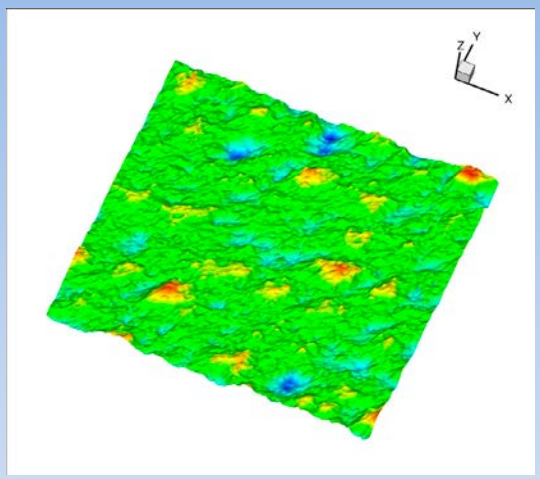

Permeability

The fractal surface

15

Method C. Variations

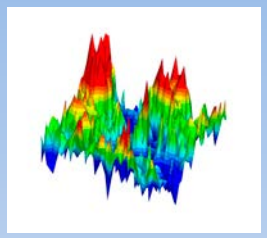

Level=5 Hurst=0.3

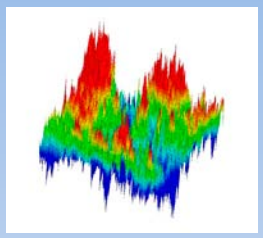

Level=8 Hurst=0.3

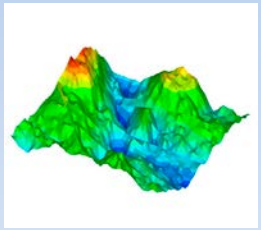

Level=5 Hurst=0.9

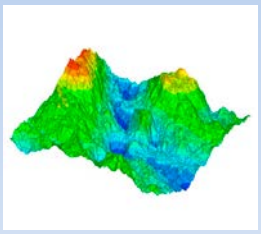

Level=8 Hurst=0.9

Concluding remarks

- Three methods to generate heterogeneous fractures, with a $T = 10^{-10}$ m^2/s, have been discussed.
- Although the three methods differ in complexity and required computational resources, it is expected that all methods can be applied to the real geometry.
- It is expected that applications to the real geometry and comparisons with measurements will bring out the merits and drawbacks of the three methods.